A STUDY OF THE ELECTRICAL DOUBLE LAYER.

A Thesis

submitted to the

University of Glasgow

for the

Degree of Doctor of Philosophy

by

James M. Peacock, B.Sc.

October, 1953.

ProQuest Number: 13838837

All rights reserved

INFORMATION TO ALL USERS
The quality of this reproduction is dependent upon the quality of the copy submitted.

In the unlikely event that the author did not send a complete manuscript
and there are missing pages, these will be noted. Also, if material had to be removed,
a note will indicate the deletion.

ProQuest 13838837

Published by ProQuest LLC (2019). Copyright of the Dissertation is held by the Author.

All rights reserved.
This work is protected against unauthorized copying under Title 17, United States Code
Microform Edition © ProQuest LLC.

ProQuest LLC.
789 East Eisenhower Parkway
P.O. Box 1346
Ann Arbor, MI 48106 – 1346

Preface.

The work described in this thesis was carried out at Glasgow University in the Physical Chemistry Department which is under the direction of Professor J. Monteath Robertson.

The writer wishes to record his sincere appreciation of the help and encouragement he received from the late Dr. J.C. James, who suggested the topic and under whose guidance most of the work was carried out.

Sincere thanks are also due to Dr. J.C. Speakman for valuable advice and assistance, and to the Department of Scientific and Industrial Research for the provision of a maintenance allowance.

Summary

The thesis is divided into four sections.

A. The introduction traces the development of electrical double layer theory and outlines the essentials of the Helmholtz, Gouy-Chapman, and Stern concepts. The ideal polarised electrode is then considered, and the application of electrocapillarity techniques to the structural elucidation of the metal-solution interface is discussed. Modifications and extensions of the Stern theory described by Grahame are then introduced, and finally the principal experimental methods of double layer investigation are summarised.

B. This is the main section of the work. It describes first an accurate alternating current bridge system designed to measure the differential capacity of the interface at a dropping mercury cathode in contact with a solution of some indifferent electrolyte. Thereafter the results obtained by this method are presented. Capacity data for aqueous N/10 potassium chloride are reported. The minimum value of 16.7 $\mu F/cm^2$. is in good agreement with 16.1 $\mu F/cm^2$. determined by Grahame. The effects on capacity of the addition of trace concentrations of a number of surface active substances, i.e., gelatin, eosin,

methyl red, and pyridine were then investigated, and finally, pseudo capacities obtained in the presence of small concentrations of salts such as cadmium chloride, were used to determine the effects of the reagents already mentioned, on reversible reduction of the cation.

The remaining part of this section is concerned with a systematic examination of capacity phenomena in some non aqueous solvents. Electrocapillarity measurements, using a capillary electrometer method were also made. Minimum capacities of 6.84 and 11.46 $\mu F/cm^2$. were found for anhydrous acetic and formic acids respectively. The supporting electrolytes were 1 molal ammonium acetate and 1 molal ammonium formate. Although the high decomposition potential of sulphuric acid restricted capacity determinations, a value of 17.75 $\mu F/cm^2$. for 98% (w/w) acid is reported at -0.6 volt v. a mercury pool reference electrode. Surface charge densities have been derived both from electrocapillarity differentiation and capacity integration, and electrocapillarity curves have been determined by a further integration.

Capacity and electrocapillarity data for water, anhydrous methanol, ethanol, n-propanol and pyridine with 1 molal lithium chloride as supporting electrolyte are presented. Some of the experimental work was carried out by the late Dr. J.C. James just prior to his death and so

it was thought to be appropriate to complete the work and to extend it to other systems. Thus, surface charge densities and electrocapillarity curves for the non aqueous solvents above have been derived from capacity integration. The minimum capacity values for water, methanol, ethanol, n-propanol, and pyridine were found to be 16.25, 9.50, 8.00, 8.00, and 5.75 $\mu F/cm^2$.

The effects of cation variation for a given anion in methanol were determined by comparison of cathodic capacities for 1 molal lithium, sodium, potassium, and ammonium iodides. The same trends as in aqueous solution were found, but the effects were much more pronounced.

C. A double layer capacity investigation of the system Cu/Cu^{++} was carried out by two different methods. The electrolyte was 0.5 M copper sulphate - 1 N sulphuric acid. An alternating current bridge system similar to that already mentioned was first used. The results were found to be frequency dependent, but a minimum capacity of 55 $\mu F/cm^2$. at 10,000 cycles per second is reported. The second method employed an oscillographic technique designed to present cathodic double layer charging curves, the slope of which measures capacity. The oscillograms obtained were initially linear prior to electrolysis, but the slopes were highly susceptible to current density variations.

The effects on the capacity of the copper system of trace concentrations of gelatin and thiourea were also investigated.

D. The last section reports work of a different nature, viz., the ion association which occurs between cations and dicarboxylate anions in aqueous solution. This was studied by potentiometric, conductometric, and spectrophotometric methods. Equilibrium constants are given, and the significance of these results is discussed.

Index

Introduction.

At the interface between two phases containing electrons or ions, a potential difference exists. Familiar examples of such boundary potentials are those developed

a) by a metal dipping into a solution of its ions,

b) at liquid junctions, and

c) at the interface between two metals.

Of particular importance are metal-solution interfaces at which the potential difference is due to an uneven distribution of ions with the consequent production of an array of oppositely charged particles in juxtaposition at the boundary. These closely aligned electrical entities constitute what is customarily referred to as "the electrical double layer". The thermodynamic properties of the layer are intimately related to the various electro kinetic phenomena including the electrokinetic zeta potential. A knowledge, therefore, of its structure and behaviour is of much interest and importance. The nature of the double layer is such that one of its chief properties is electrical capacitance. This is thermodynamically related to the surface charge density and to the surface tension of the metal when the latter constitutes the solid or non solution phase. Furthermore, because of their low electrical resistance and the ease with which an applied potential may be varied, metal-

solution interfaces lend themselves to an exact study of the layer. Although therefore a number of approaches to the problem can be made, perhaps the main experimental methods are concerned with

a) the direct measurement of double layer capacity at a metal-solution interface, and

b) the indirect determination of capacity, of surface charge density, and of other properties from electrocapillarity data.

Mercury is pre-eminently suitable as a metal, and the most important information relating to the double layer has been derived from the study of a mercury-indifferent electrolyte interface.

The original concept of the double layer was due to Quincke (1), although he did not refer to it as such, but the first quantitative approach was that of Helmholtz (2), who regarded the layer as a simple parallel plate condenser.

$$c = \frac{e}{V} = \frac{D}{4\pi d} \qquad \text{.....(1)}$$

where c = capacitance, e = charge, V = potential difference, and D = the dielectric constant of the medium between the plates, the distance apart of which = d. Gouy's value of minimum capacitance however required

$$d = 0.3 \times 10^{-8} \text{cm.}$$

which was regarded as unreasonably small. This is the

usual criticism of the application of this expression. Craxford (3) points out that a more fundamental criticism is that of Gouy (4), who objected to the neglect of thermal agitation effects. It is also evident that this simple theory does not take into account the variation of capacity with applied potential found experimentally

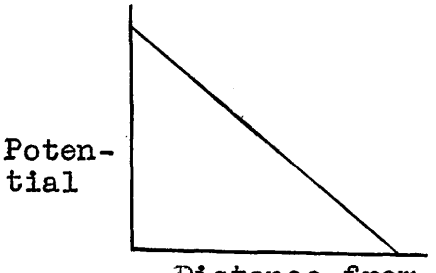

The Helmholtz rigid layer interpretation

Gouy (4) and Chapman (5) independently considered the double layer to be diffuse in character and by calculations similar to those employed by Debye and Huckel in the ion atmosphere theory, developed a quantitative treatment of a diffuse layer. Thus, if n_{oi} be the number of ions of a given type per unit volume in the bulk of the solution, then the number of ions n_i per unit volume of the same species at a point where the work required to bring an ion of this type from the bulk of solution to the point in question is w_i, will be given by

$$n_i = n_{oi} e^{-w_i/kT} \qquad \ldots\ldots\ldots\ldots\ldots (2)$$

where k is the Boltzmann constant and T is the temperature

absolute. Furthermore, if ψ be the potential of the point relative to the interior of the solution and Z_i be the ion valency, then

$$w_i = Z_i \varepsilon \psi \qquad \ldots\ldots\ldots (3)$$

Combination of equations (2) and (3) gives

$$n_i = n_{oi} e^{-Z_i \varepsilon \psi / kT} \qquad \ldots\ldots\ldots (4)$$

Also, the charge density in a lamina parallel to the electrode at a distance such that the potential is ψ is given by $\rho = \sum n_i z_i \varepsilon = \sum z_i n_{oi} \varepsilon e^{-z_i \varepsilon \psi / kT}$ ..... (5)

Introduction of the Poisson equation for a system, the potential of which varies in one direction only, gives

$$\frac{d^2\psi}{dx^2} = \frac{4\pi\rho}{D} = \frac{4\pi\varepsilon}{D} \sum n_{oi} z_i e^{-z_i \varepsilon \psi / kT} \qquad \ldots\ldots (6)$$

The identity

$$\frac{d^2\psi}{dx^2} = \frac{1}{2} \frac{d}{d\psi} \left(\frac{d\psi}{dx}\right)^2$$

enables equation (6) to be integrated noting that in the solution interior $\frac{d\psi}{dx} = 0$ and $\psi = 0$. This results in

$$\left(\frac{d\psi}{dx}\right)^2 = \frac{8\pi kT}{D} \sum n_{oi} \left(e^{-z_i \varepsilon \psi / kT} - 1\right) \qquad \ldots\ldots (7).$$

From Gauss' theorem, the field $\frac{d\psi}{dx}$ in a region of dielectric constant D just outside a plane of uniform charge density η is given by

$$\frac{d\psi}{dx} = \frac{4\pi\eta}{D} \qquad \ldots\ldots (8).$$

Hence, from equations (7) and (8), the total charge density on the diffuse layer will be

$$\eta^d = \left[\frac{DkT}{2\pi}\sum n_{oi}\left(e^{-z_i\varepsilon\varphi^d/kT} - 1\right)\right]^{\frac{1}{2}} \qquad \ldots\ldots (9)$$

For a Z - Z electrolyte n_{oi} will be the same for both ions and if $A^2 \equiv \frac{DkTn_{oi}}{2}$ equation (9) may be simplified to

$$\eta^d = \frac{2A \sinh Z\varepsilon\varphi^d}{2kT} \qquad \ldots\ldots (10)$$

Two types of diffuse layer capacity may be considered. These are, the differential capacity C^d and the integral capacity K^d which may be defined as follows

$$K^d = \eta^d/\varphi^d \quad \text{and} \quad C^d = \frac{d\eta^d}{d\varphi^d} \qquad \ldots\ldots (11)$$

$$\text{Then } K^d = \frac{2A}{\varphi^d} \sinh Z\varepsilon\varphi^d/2kT \qquad \ldots\ldots\ldots\ldots (12)$$

$$\text{and } C^d = \frac{Z\varepsilon A}{kT} \cosh Z\varepsilon\varphi^d/2kT \qquad \ldots\ldots\ldots\ldots (13)$$

In equation (3) ω_1 is an electrostatic work term, and no account has been taken of the work required a) to displace polar solvent molecules from a region of high field strength, b) to remove or displace the solvent sheath on close approach to the metal, or c) to crowd the ions in the region closer together. Quantitative corrections for this last effect have been made by Bikerman (6). The diffuse layer treatment alone, predicts values of capacity of the order of 250μF/cm^2. which are in general much too large at the potentials concerned. It leads to an exponential fall in potential from interface to solution interior.

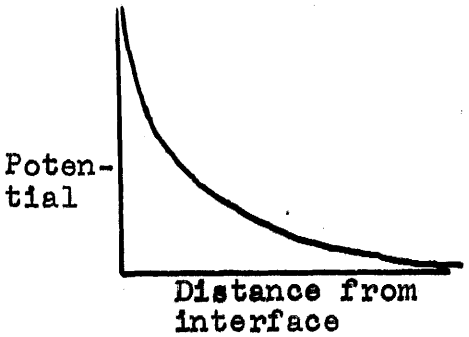

Gouy-Chapman diffuse layer interpretation.

The Stern theory (7), the model upon which modern ideas are based, combines the Helmholtz rigid layer interpretation with that of the Gouy-Chapman diffuse layer. Thus, the potential difference between interface and solution is assumed to fall linearly across the rigid layer, and thereafter to decay exponentially across the diffuse layer to zero in the solution interior. It is the first theory to take specific adsorption into account. Thus, if n_1 be the number of adsorbed ions per unit area of electrode surface, and n_{o1} be the number of ions per unit volume of the same type in the bulk of the solution, and if Z_1 and Z_{o1} be the corresponding maximum number of ions, then the time spent by an ion on the surface, t_1, or in the solution t_{o1} will be given by

$$\frac{t_i}{t_{oi}} = \frac{Z_i - n_i}{Z_{oi} - n_{oi}} e^{-\omega_i / kT} \qquad \ldots\ldots (14)$$

But, if all ions of a given type are considered for a short time instead of one ion for a long time, then

$$\frac{n_i}{n_{oi}} = \frac{t_i}{t_{oi}} = \frac{Z_i - n_i}{Z_{oi} - n_{oi}} e^{-\omega_i / kT} \qquad \ldots\ldots (15)$$

Solving for n_i,

$$n_i = \frac{Z_i}{1 + \frac{Z_{oi}}{n_{oi}} e^{-\omega_i / kT}} \qquad \ldots\ldots\ldots (16)$$

Stern approximates $\frac{Z_{oi}}{n_{oi}}$ to the mole fraction of the solute and doubles the unity in the denominator so that at large negative values of ω_i, $n_i \longrightarrow Z_i/2$, i.e., equal numbers of anions and cations are adsorbed. The term ω_i is divided into electrostatic and chemical work thus

$$\omega_i = Z_+ \varepsilon (\psi^d + \varphi_+) \qquad \ldots\ldots\ldots\ldots (17)$$

where Z_+ is the cation charge, φ_+ the adsorption potential of any cation, and ψ^d the potential across the diffuse layer or that of the boundary between diffuse and rigid layers. Similarly for anions

$$\omega_i = Z_- \varepsilon (\psi^d - \varphi_-) \qquad \ldots\ldots\ldots\ldots (18)$$

The charge on the Helmholz layer is now therefore given by

$$\eta^h = zF\left[\frac{1}{2 + \frac{1}{c} e^{z_- \varepsilon (\psi^d - \varphi_-)}} - \frac{1}{2 + \frac{1}{c} e^{z_+ \varepsilon (\psi^d + \varphi_+)}}\right] \qquad \ldots (19)$$

where $c = n_{oi}/Z_{oi}$, and in consequence, the total charge on the double layer which is the sum of the charges on the diffuse and rigid layer will be

$$\eta = \eta^d + \eta^h \qquad \ldots\ldots\ldots (20)$$

The final Stern expression then becomes

$$\eta = \eta^d + \eta^h = \frac{D}{4\pi d}(\psi - \psi^d) =$$

$$\left[\frac{DkT}{2\pi}\sum n_{oi}\left(e^{\frac{-z_i\varepsilon\psi}{kT}} - 1\right)\right] + zF\left[\frac{1}{2 + \frac{1}{c}e^{z_-\varepsilon(\psi^d - \phi_-)}} - \frac{1}{2 + \frac{1}{c}e^{z_+\varepsilon(\psi^d + \phi_+)}}\right] \quad \ldots\ (21)$$

where ψ is the potential difference between the phases

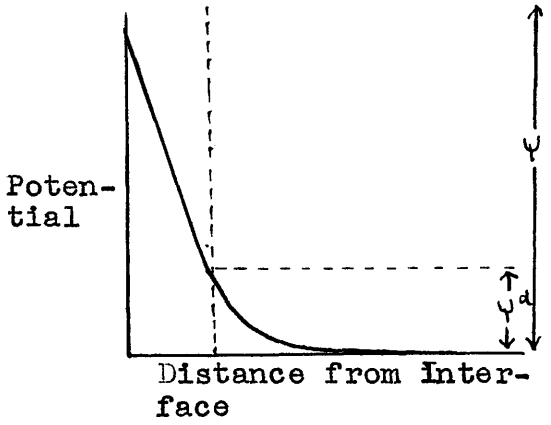

The Stern combined rigid and diffuse layer interpretation

Grahame (8) has pointed out that Stern's doubling of the unity in the denominator of equation (16) to make equal adsorption of anions and cations is not a compelling argument. He finds experimentally that the maximum adsorption on the Helmholtz layer represents 25% of a monolayer and that under these circumstances therefore the equation may be written

$$n_i = \frac{z_i}{z_{oi}} n_{oi} e^{-w_i/kT} \quad \ldots\ (22)$$

$$= 2rn_{oi} e^{-w_i/kT} \quad \ldots\ (23)$$

where r is the radius of a non solvated ion. Furthermore, in the Grahame concept (8) of the double layer only one type of ion will populate the Helmholtz layer. Again, in the final Stern expression (equation (21)), the total charge on the double layer is associated with

the potential difference $\psi - \psi^d$, i.e., with the potential across the fixed layer. Stern assumed that the difference between this potential and the potential of the solution interior was small, but Grahame (9) has observed violent disagreement between experimental values and those calculated from the Stern theory.

Electrocapillarity.

An ideally polarised electrode may be defined as an interface which has no charged or uncharged component common to both sides. Although therefore there is no thermodynamic equilibrium, a hydrostatic, thermal, and electrostatic equilibrium nevertheless exists between phases. It can however be treated by exact thermodynamic means, and herein lies its importance. The practical implication is that, if the potential difference between phases be altered, no charged component must cross the interface. Electrically, this is equivalent to an ideal condenser in which charge may approach or recede from either plate as a result of electrostatic attraction or repulsion, but no current must cross the intervening space. In practice, these conditions are never fully realised, but a clean mercury surface in contact with an indifferent electrolyte constitutes a reasonable approximation. Electrocapillarity is the study of such

electrodes.

Polarisation of this type of electrode causes the surface tension of the mercury to alter. Making use of the electrometer which bears his name, Lippmann (10) was the first to investigate the relationship between these variables. In general, as the mercury is made more negative, the surface tension rises to a maximum, and thereafter decreases. Thermodynamic investigation of the effect was made by both Lippmann (11) and Gibbs (12). They arrived at the same expression

$$\frac{d\sigma}{dE} = -q \qquad \ldots\ldots (24)$$

where σ is the surface tension of the mercury, E is the potential difference between phases, and q is the charge per unit area of mercury surface. Hence, the slope of the electrocapillarity curve at any potential is equal to the surface charge density. Furthermore, when $\frac{d\sigma}{dE} = 0$ $q = 0$, i.e., the charge on the mercury surface is zero. The potential at which this occurs is referred to as the electrocapillarity maximum potential. Again, since $q = CE$ and therefore $dq = CdE$, it follows from equation (24) that

$$\frac{d^2\sigma}{dE^2} = -\frac{dq}{dE} = C \qquad \ldots\ldots (25)$$

where C is the differential capacity of the double layer. If the latter behaved as a pure capacitance, electro-

capillarity curves would in general be simple parabolae. Although such curves are obtained almost exactly in the case of nitrates and fluorides, most electrolytes cause a lowering and shifting of the E.Cap.Max., and a steepening of one or other of the curve branches. This may be due to two factors,

a) a potential gradient in the neighbourhood although not in the immediate vicinity of the electrode at the E.Cap.Max., and

b) adsorption of an ionic species referred to as being capillary active. Although therefore the charge on the mercury surface at the E.Cap.Max. potential is zero, it does not follow that the potential difference across the double layer is zero. Oriented dipoles are sufficient to cause such a potential, and herein lies the difficulty in obtaining absolute single electrode potentials.

Since in practice the double layer does not behave like a static condenser, and a non linear relationship between q and E therefore exists, it is desirable to distinguish between differential capacity defined by equation (25), and that value obtained by dividing total charge by total applied potential and which may be called the integral or static capacity. Hence, if K be the integral capacity, as already indicated in equation (11),

$$K = \frac{-q}{E} \qquad \ldots\ldots\ldots \quad (26)$$

From equation (25),

$$q = -\int_{o}^{E} C.dE \qquad \ldots\ldots\ldots\ldots \quad (27)$$

If, therefore, the relationship between differential capacity and applied potential be known, it is possible, by a single graphical integration, to obtain a graph of surface charge density as a function of potential. For this it is necessary to know the potential at which $q = 0$, i.e., the E.Cap.Max. potential. A further integration yields surface tension as a function of potential, i.e., it gives the shape of the electrocapillarity curve, but the constant of integration necessary for its absolute determination must be obtained from a surface tension measurement at a particular potential.

A general thermodynamic treatment of electrocapillarity and the ideal polarised electrode has been made by both Grahame (8) and by Parsons and Devanathan (13). From the Gibbs adsorption equation

$$d\sigma + \Gamma_1 d\mu_1 + \Gamma_2 d\mu_2 + \ldots\ldots\ldots = 0 \qquad \ldots\ldots \quad (28)$$

expressions of the type

$$\left(\frac{d\sigma}{d\mu}\right)_{E_-} = \Gamma_+ \qquad \ldots\ldots \quad (29)$$

and

$$\left(\frac{d\sigma}{d\mu}\right)_{E_+} = \Gamma_- \qquad \ldots\ldots \quad (30)$$

have been derived. T_+ and T_- are the surface concentrations of cations and anions respectively. μ is the chemical potential and σ the mercury surface tension. Thus from equation (29), from a knowledge of the variation of surface tension with ionic activity at a fixed potential, it is possible to obtain the surface concentration of the cation. This is contingent upon the reference electrode being reversible to the anion. From equation (30), if the reference electrode be reversible to the cation, similar data for the anion may be evaluated. The contributions to the total double layer charge by each type of ion may be calculated, and hence a clearer picture of the behaviour and constitution of the layer at different potentials may be obtained. As a result of such measurements taken in conjunction with differential capacity data, a theory of the double layer, differing in some important respects from the Stern conception, has been presented by Grahame (8). He postulates

a) the metallic phase upon the surface at which there is an excess or deficit of electrons,

b) a region in the immediate vicinity of the metallic phase into which the electrical centres of no ionic species may move because of physical size,

c) a region accessible to the electrical centres of anions

but not of cations,

d) an outer diffuse layer region of the Gouy - Chapman type.

The boundary between regions (b) and (c), which corresponds to the closest approach to the metal surface of the electrical centres of anions is called the inner Helmholtz plane. The outer Helmholtz plane is the boundary between regions (c) and (d) and represents the closest approach to the metal of cation electrical centres. When anions are present at the inner Helmholtz plane, i.e., on positive polarisation, they are held to the metallic phase by short range covalent type forces. This is referred to as specific adsorption. Since cations show no tendency to exhibit this phenomenon, they occupy a three dimensional region in which the closest approach to the metal of their electrical centres is the outer Helmholtz plane. This is in contrast to the situation in the innermost region where the anions are held in a rigid layer.

The main differences between this theory and that of Stern are:

a) the Stern theory makes no distinction between inner and outer Helmholtz planes,

b) the Stern formulation leads to the adsorption of positive

and negative ions. Grahame recognises only a rigid anionic layer held by short range forces,

c) Stern's specific adsorption potentials φ_+ and φ_- are assumed to be independent of applied potential. Accurate capacity data contradict this assumption.

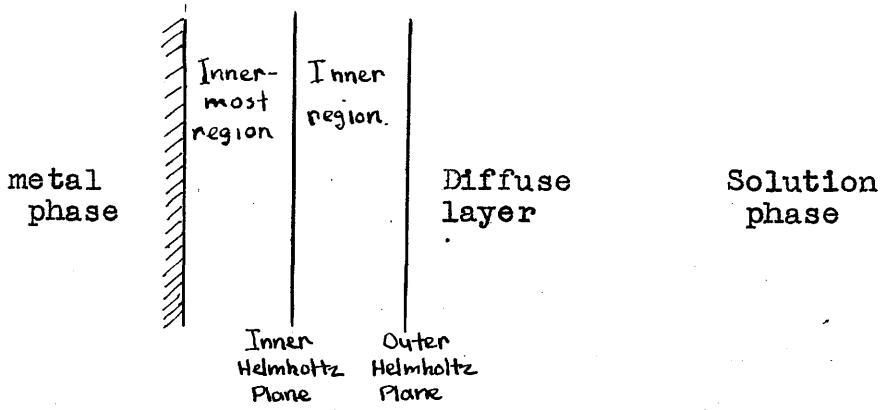

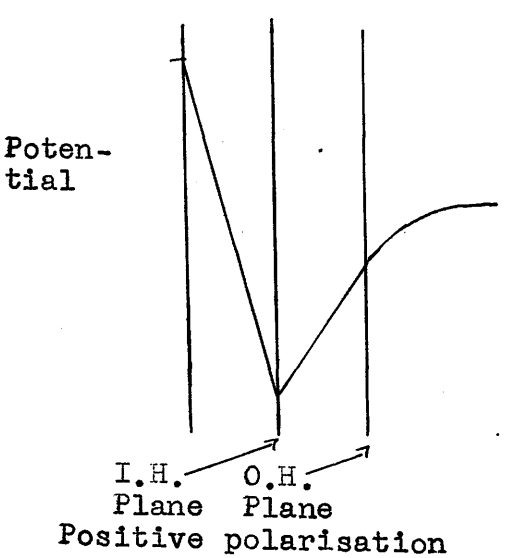

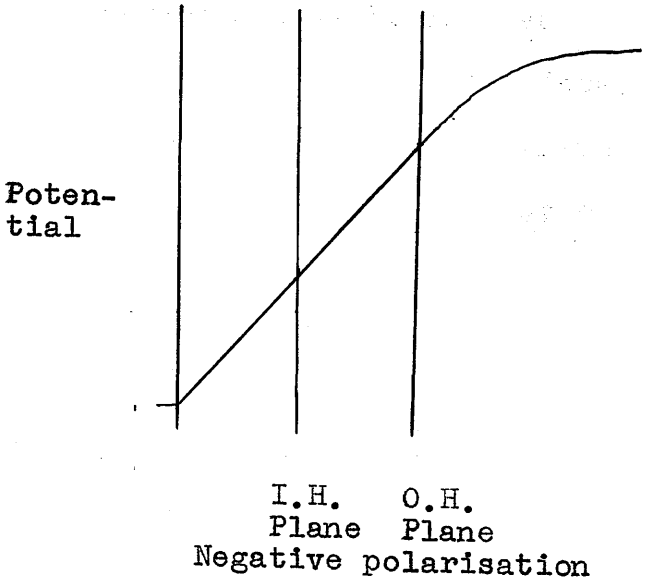

Grahame interpretation of the double layer.

Experimental methods for the investigation of the electrical double layer.

1). Electro capillarity techniques.

As already indicated, much information about the state of the interface may be obtained from surface tension - potential curves. To acquire such data, the Lippmann capillary electrometer is frequently used. This consists essentially of a narrow glass capillary in which the interface between mercury and solution is formed. Variation of the mercury potential causes the surface tension of the latter to alter, and hence the position of the mercury meniscus also changes. This may be restored by adjusting the mercury head, the alteration measuring the change of surface tension. The classical researches of Gouy (14) were carried out using such an arrangement, and the data thus provided are still of interest and importance. The Lippmann electrometer in various forms has since been used by a number of workers, many of whom have made modifications and improvements (15,16). The drop weight method for the determination of the surface tension of mercury at various potentials has also been used (17). It is said to be particularly suitable for non aqueous solvents, since, if the liquid does not wet the glass properly, the accuracy of the capillary method

is reduced.

Although pure mercury is pre-eminently suitable for these techniques, other metals have also been investigated. The electro capillarity curves for gallium, and for metallic amalgams have been studied by Frumkin and collaborators (18), whilst Karpachov and Strombergi (19) have investigated molten electrolyte and metal melt systems. Frumkin (20) has also developed a technique for determining the capillary curves of solid metals. This is based on the variations of the angle of contact of a gas bubble and the metal with the polarisation of the latter. Variations of the hardness of a metal with applied potential have been measured by observing the damping effect on the oscillations of a pendulum resting on the metal surface (21,22). Curves of hardness against potential are found to be similar to the electro capillarity curves, and agreement has been obtained between the maxima determined by this method and by the methods mentioned above.

2). Dropping mercury systems of estimating the charge on the double layer.

When mercury is allowed to drop through an electrolytic solution into a mercury reservoir, a current will

flow along a wire connecting the two mercury masses. If the droplet area be known, it is possible to evaluate the charge per unit area of mercury surface. The dropping electrode may be polarised from an external circuit, and such a system was used by L.St.J. Philpot (23) who evaluated capacities in hydrochloric acid and in sodium chloride solutions. He obtained values of 53.7 and 23.3 $\mu F/cm^2$. on positive and negative polarisations respectively for the former, and 57.3 and 23.6 $\mu F/cm^2$. for the latter. Similar measurements have also been made by Frumkin (24) and by Ilkovic (25). The latter, in potassium chloride solution, recorded corresponding values of 42.2 and 22.3 $\mu F/cm^2$.

3). The direct measurement of double layer capacity.

a). Charging curve method.

At a suitable metal cathode, prior to the liberation of an ion, current flow will be restricted to the build up and charging of the double layer. By photographing the movements of the fibre of an Einthoven string galvanometer, Bowden and Rideal (26) determined the rate of growth of potential at a mercury cathode prior to electrolysis. A charging curve was thus obtained.

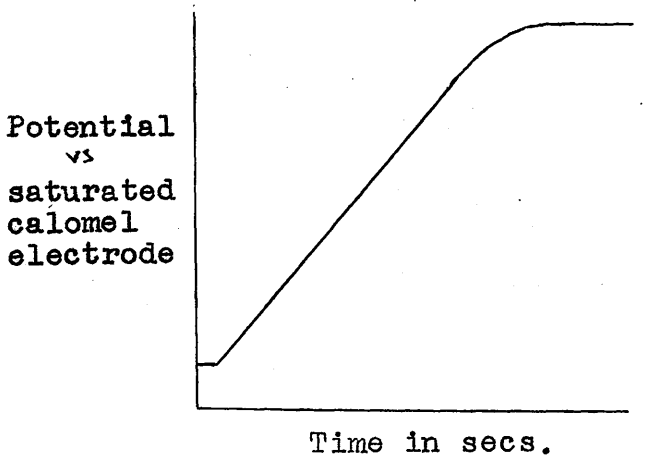

Since $C = \frac{idt}{dV}$, the capacity of the layer was evaluated from the slope of the initial linear portion of the curve. In this way, it was found that mercury electrodes had a capacity of 6 $\mu F/cm^2$.

b). Oscillographic methods.

The cathode ray tube is of particular value in recording pre-electrolysis phenomena at electrode surfaces, and consequently it has been widely used as indicating device for charging and other methods. Erdey-Gruź and Kromrey (27) made use of a mechanical oscillograph. Barclay and Butler (28), employing valve circuitry, obtained oscillograms of freshly formed mercury surfaces in 1 N sulphuric acid. Values of 50 $\mu F/cm^2$. on the anodic branch and of 22 $\mu F/cm^2$. on the cathodic branch of the curves were observed. A typical oscillogram is shown.

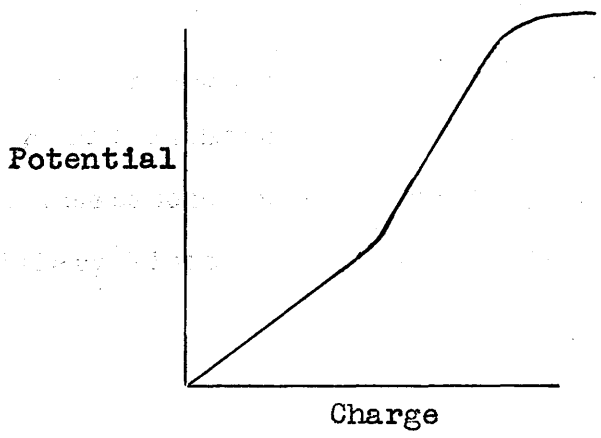

Hickling (29) also has designed electronic circuits to produce cathode ray tube charging curves and to examine anodic phenomena. At a freshly amalgamated copper cathode in 1 N sulphuric acid values of 10 - 11 $\mu F/cm^2$. were found. The same apparatus was used to determine the capacity of nickel in a solution of its own ions. Large values, 430 - 470 $\mu F/cm^2$., were observed for a Ni - 1 N nickel sulphate system.

Loveland and Elving (30) have devised circuitry for the direct cathode ray tube display of differential capacity as a function of potential at a dropping mercury cathode, and have obtained a minimum value of about 16 $\mu F/cm^2$. for mercury in a 0.1 N potassium chloride solution. The above authors have also discussed cathode ray oscillography as applied to polarisable mercury electrodes in general (31).

c). Alternating current methods.

Many authors (32,33) have included the double layer in a wheatstone capacity bridge, and by using a large auxiliary electrode in series with the electrode under examination have measured the effective capacity of the latter. Kruger (34) obtained values of 7 - 10 $\mu F/cm^2$. and Proskurnin and Frumkin (35), 18 - 20 $\mu F/cm^2$. at negatively polarised mercury. Stringent purification of solutions was practised by these workers.

Again, using a mercury electrode, Borrisova and Proskurnin (36) measured capacity by comparing, on a cathode ray tube, the potential developed across the double layer with that across standard condensers when passing a known alternating current.

4) Electrokinetic phenomena.

There is a large group of phenomena which occurs when a liquid is displaced with respect to the surface of a charged solid. Thus, under the influence of an electric field,

a) the movement of charged particles is known as electrophoresis, and

b) the movement of liquid when the charged surface is fixed is referred to as electroendosmosis.

Also, potential differences are set up when

a) a liquid is forced to move relative to a solid thus giving rise to streaming potentials, and
b) charged particles are allowed to move in a liquid under the influence of gravity. This is known as sedimentation potential or Dorn effect.

These effects are important in the study of the double layer, and the first three are useful in the investigation of glass-liquid or quartz-liquid interfaces.

[illegible] using an alternating current bridge method.

The measurement of double layer capacity at a dropping mercury cathode using an alternating current bridge method.

Experimental.

Description of apparatus and method used in determining double layer capacities.

From the previous section it is evident that considerable disagreement among capacity values measured at a mercury surface exists. In 1935 Proskurnin and Frumkin (35) demonstrated that traces of surface active impurities had considerable effect upon experimental values, and it was therefore clear that stringent purification was necessary. Nevertheless, even when strict precautions were taken, discrepancies still persisted. For the determination of double layer capacities therefore, it was decided to adopt a method similar to that introduced by Grahame (37). Two essential features of the method are:

a) capacity is measured by its inclusion in an A.C. bridge, and b) the electrode under examination is a dropping mercury cathode in a solution of some indifferent electrolyte. Considering further these two features -

a) provided adequate precautions of design and construction are taken, an A.C. bridge affords the most accurate method of determining the value of an unknown electrical component.

b) It has already been mentioned that mercury is particularly suitable for double layer study. Some of the

reasons for this are: (i) it is a liquid and therefore free from mechanical strains; its surface is also readily renewed: (ii) its interfacial tension is easily measured: and (iii) it has low chemical activity and a high hydrogen overvoltage. Capacities may therefore be measured at potentials where, in the absence of this overvoltage, the evolution of hydrogen would make it impossible for reliable readings to be taken. The particular advantage in making use of a dropping mercury cathode lies in the fact that the mercury surface is continually being renewed and therefore the difficulties experienced by other workers in obtaining and maintaining a clean surface are largely removed. Any disadvantages are concerned with the rather more elaborate electrical arrangements necessary to detect bridge balance on an expanding surface.

Circuitry description.

The electrical behaviour of the double layer may be represented by a capacitance in series with a resistor. Consequently, capacity measurements were made using a series resistor-capacity Wheatstone bridge, and Fig.1 illustrates the essentials of the circuitry. The oscillator, a mains operated Hartley type, could give eight spot frequencies between 500 and 5000 cycles per second. It was placed about 12 feet from the bridge and coupled by means of a Sullivan balanced and screened transformer

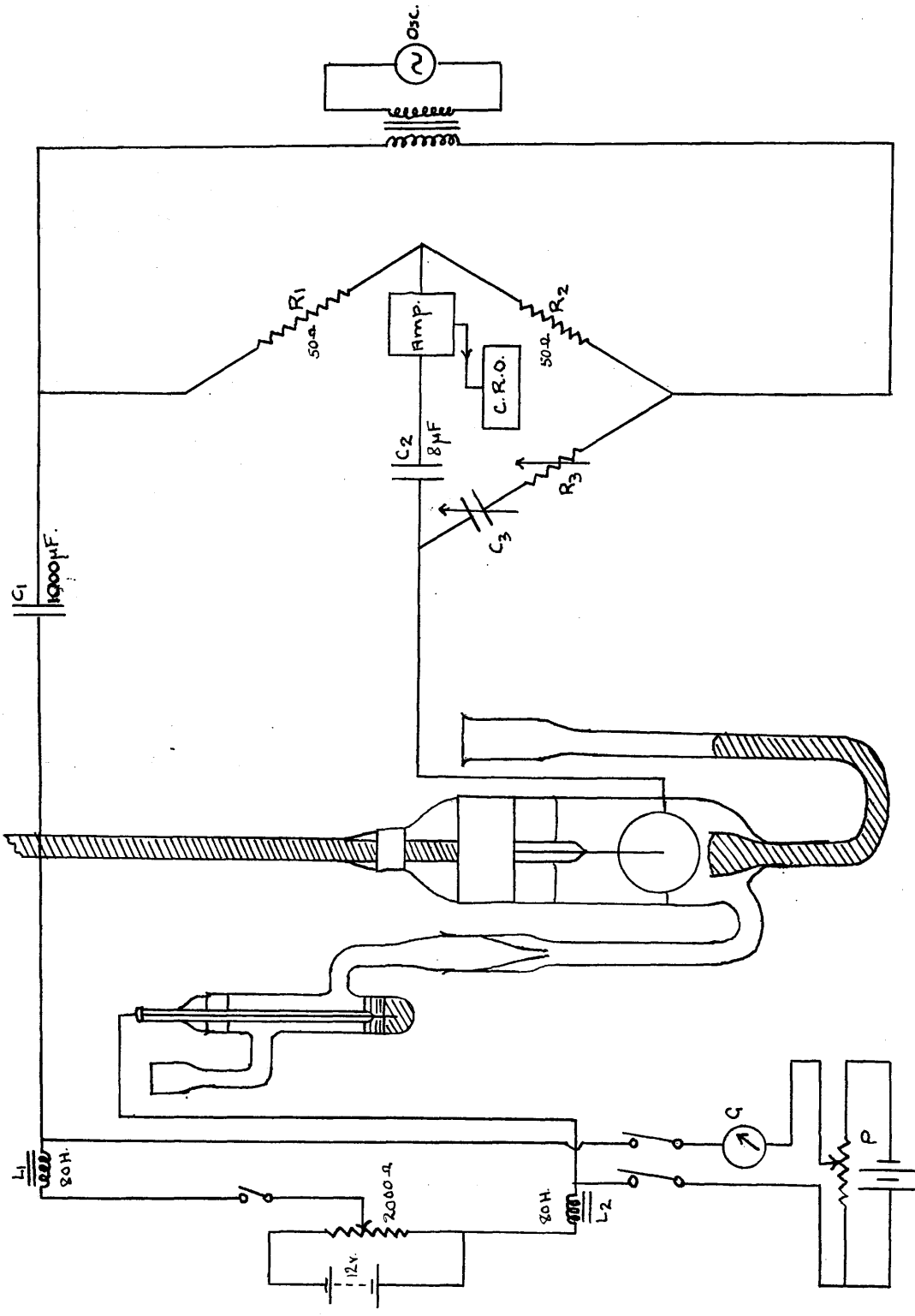
Osc.
R1
50Ω
Amp.
C.R.O.
R2
50Ω
C2
8μF
R3
C3
C1
1000μF.
L1
20H.
2000Ω
12V.
20H.
L2
G
P

Fig 1

which screened the bridge from the source of alternating potential. Grahame (37) has shown that with suitable cell design the results obtained were independent of frequency between 240 and 5000 c.p.s. The frequency used in this work was almost invariably 2000 c.p.s. The amplitude of the alternating potential impressed upon the cell was kept as small as possible consistent with the accurate balancing of the bridge, and was certainly less than 15 m.v. (37). In general, in the measurement of differential capacity, it is desirable to keep the input at a minimum, although where capacity is substantially independent of the applied static potential, this is of less importance. With the exception of the lead between choke L_1 and the mercury cathode, all wiring was screened and grounded. The bridge itself was earthed using a conventional Wagner earth arrangement not shown in the diagram. R_3 was a Sullivan non reactive resistance box reading from 0.1 to 11,111 ohms. The ratio arms R_1 and R_2 consisted of a 100 ohm Sullivan non reactive slide resistance, the total resistance being divided into 10^5 parts by means of two concentric dials. It was customary to set this resistor to give 50 ohms in each arm. Values of about 1000 ohms were also tried but no difference in the measured capacities was observed. C_3 consisted of

two blocks of Muirhead Universal Decade Capacitance Units connected in parallel. These read from 0 to 1 μF in steps of 0.1 and from 0 to 0.1 in steps of 0.01 μFs, their tolerance being ±2%. For third place readings, a Sullivan decade stable mica condenser reading from 0 to 0.01 μFs in steps of 0.001, was also connected.

The static polarisation potential for the mercury cathode was supplied from a variable 2000 ohm resistor connected across a 12 volt bank of lead acid accumulators. Accurate adjustment of potential was made by switching in the potentiometer P and balancing on galvanometer G. The former was a standard type Tinsley potentiometer and the latter a scale and lamp Pye instrument with a maximum sensitivity of 43.5 m.m. per μA. The galvanometer, when switched in, could also be used to record the direct current flowing between cathode and reference electrode during the life of a mercury droplet. The current, of course, increased during the expansion of the surface but maximum flow was of the order of 1 - 2 μA. Any sudden increase in this value was indicative of the deposition of an ionic species which may have been added to the solution on purpose, or of the evolution of hydrogen associated with solvent decomposition. L_1 and L_2 were large inductances (about 80 Henries) which served to isolate A.C. from the

potentiometer system. Condensers C_1 and C_2 prevented direct current from flowing through the bridge, in particular through R_1 and the amplifier. Since C_1 was effectively in series with the cell, its value was large (about 1000 μF). At first it was used alone, but it was found to have a small leakage current which interfered with bridge balancing, and so C_2 was introduced. Its value was much smaller ($\sim$8 μF) since it was contained within the bridge. The bridge output was fed via a two stage, high gain, mains operated amplifier to a Cossor Double Beam Oscilloscope which was used as a balancing device. Its exact function will be described later. The bridge accuracy was checked by measuring the capacity of standard condensers of high quality, both alone and in series with standard resistors. Connection was made at the point where the cell was later inserted.

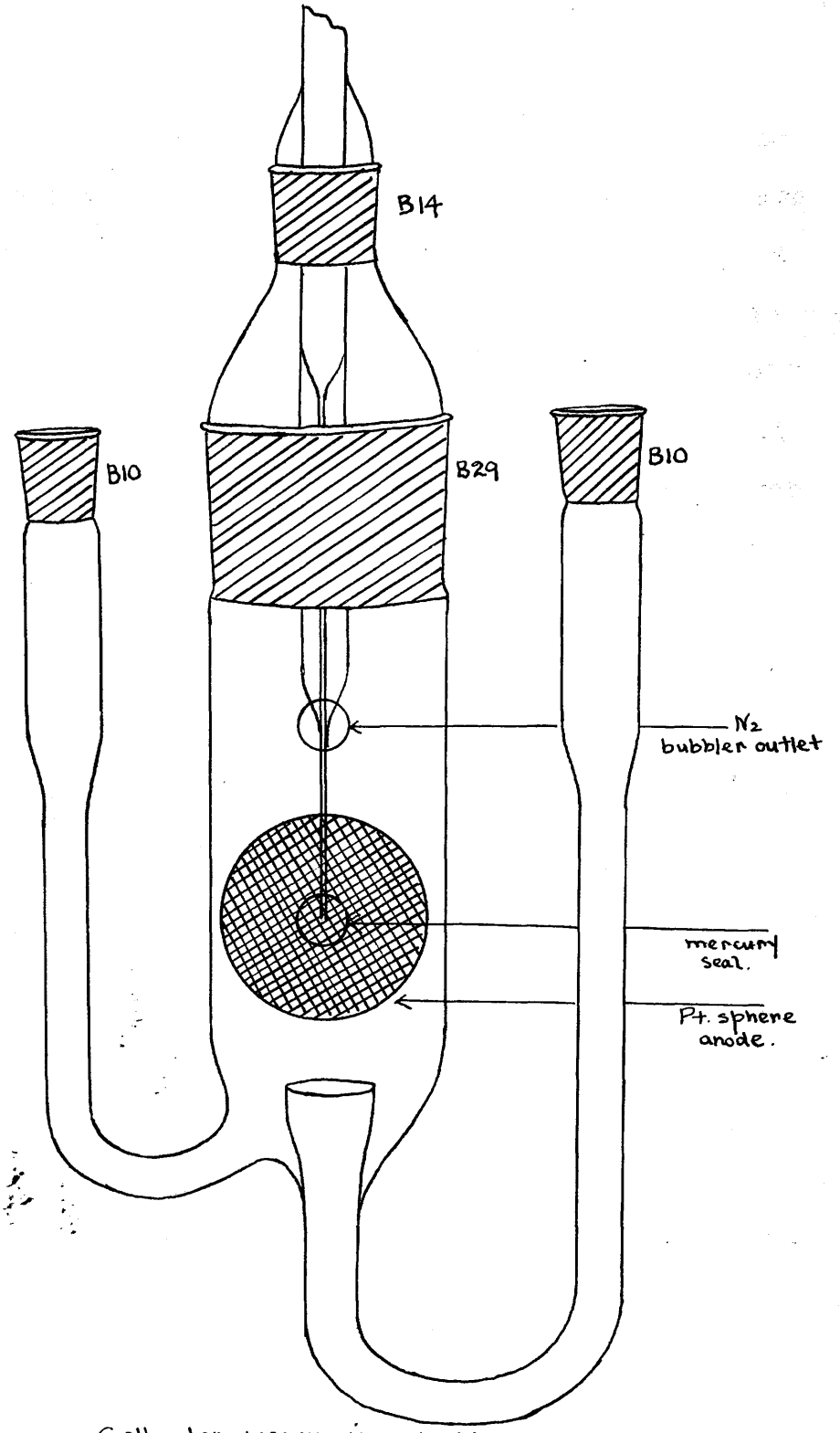

Cell for measuring double layer capacities at a dropping mercury cathode.

Description of the cell.

The cell, which was made entirely of Pyrex glass, had a capacity of about 40 ml. The anode was a sphere of platinum gauze about 2.5 cms. in diameter, attached to the walls of the cell by two pieces of thicker platinum wire, and making electrical contact with the exterior by a mercury seal. The sphere was constructed by sewing with thicker platinum wire two circular pieces of gauze around a beeswax sphere of the correct dimensions, and thereafter dissolving the wax in benzene. Two holes in the sphere 180° apart allowed for the insertion of a fine tipped capillary at the top and for the escape of mercury at the bottom end of the cell. The mercury fell into a cup attached to a curved limb terminating in a B 10 Quickfit socket. In certain cases, a mercury pool in the cup was used as a reference electrode, in which case the solution was dearated by bubbling nitrogen through the solution via the other limb. Alternatively, this limb, which also terminated in a B 10 socket, could be used for the insertion of a calomel electrode, and nitrogen introduced through the central inlet. The nitrogen escaped via a conventional bubbler, the position of which is shown in the diagram. Fine tipped capillaries, e.g., external diameter 0.32 m.m., internal diameter 0.08 m.m., were

drawn from semicapillary tubing joined to normal Pyrex tubing which in turn was sealed into a B 14 cone. A B 29 - B 14 conversion completed the connected to the top of the cell, and the mercury head was attached to the capillary via a short length of polythene tubing. This facilitated the insertion and withdrawal of capillaries, a number of which could, if necessary, be successively drawn from a single length of semi capillary tubing. The tip of the capillary at which the mercury droplet formed was necessarily within the sphere, but it was not imperative that it be central as its exact position was not critical. To avoid any contamination, flexible connection to the mercury reservoir was made by a length of polythene tubing (38). This was also used in the nitrogen input line.

Temperature Control.

The cell was supported in a large glass beaker and partially immersed in water, the temperature of which was kept uniform by an electrically driven paddle system, and maintained at 25 $\pm$0.1^{o}C. by means of a toluene-mercury spiral regulator operating a 60 watt lamp through a Sunvic relay.

The electrical behaviour of the dropping mercury cathode, and the systems devised to detect bridge balance.

It is evident from the circuit diagram that the

small alternating potential from the oscillator is applied between the dropping mercury cathode and the platinum sphere anode. Since the surface area of the latter is large compared with the former, the capacity measured is effectively that of the mercury droplet. The mean cathodic potential with respect to a reference electrode is determined by the setting of potentiometer P, and hence it is clear that the apparatus measures differential capacity as a function of potential. It has already been mentioned that the electrical behaviour of the double layer may be represented by a series capacity resistance network. For an expanding mercury surface, these will be continually changing in such a way that, during the life of a drop, the capacity changes from a minimum to a maximum, and the resistance from a maximum to a minimum. The actual limits will depend upon the drop characteristics and upon the nature of the electrolyte, but provided C_3 and R_3 are suitably set, then at one and only one instant during the life of a drop will the bridge be balanced. When this occurs, C_3 = the double layer capacity at that instant, and R_3 = the series resistance provided by the solution. In practice, the mercury head on the capillary was adjusted to give a drop time of about 6 seconds, and the bridge balanced between 3 and 4 seconds after drop birth. This was done by setting R_3 at a fixed value, and

adjusting C_3 until balance was effected. If the interval between drop birth and balance did not lie between 3 and 4 seconds, R_3 and C_3 were suitably readjusted. Large values of R_3 necessitated a small setting of C_3 and a short time interval, and vice versa.

Indication of bridge balance.

Since the bridge is balanced for an instant only, between 3 and 4 seconds after drop birth, it is necessary that the indicating device show a sharp audible or visual maximum or minimum at that instant. Earphones were first tried and gave a characteristic null point on each side of which was a 2000 cycle note of diminishing and then increasing amplitude. This null point was, however, too insensitive to condenser setting to afford accurate capacity measurements. Two successful systems were evolved:

1) The first made use of a modification of a Hickling thyratron potentiometer circuit (39) designed to measure the amplitude of a transient. The diagram indicates the essentials of the circuit. Value V1 is a thyratron, the grid of which is sufficiently negative with respect to the cathode to prevent the thyratron from striking. Condenser C_1 is thus fully charged to 30 volts, and remains thus

until the grid of V1 is made sufficiently positive to allow the latter to conduct. C_1 is rapidly discharged through V_1, which then destrikes when the H.T. is sufficiently low. C_1 charges relatively slowly through R_1 until V_1 strikes once more. This repetitive cycle causes a series of characteristic sounds on the earphones. It is thus possible to adjust potentiometer P to a value such that the earphones are silent and only the maximum extreme of a positive transient causes the system to go into conduction. By reversing the bias on V_1, a momentary silence may be made to characterise the extreme of a negative input.

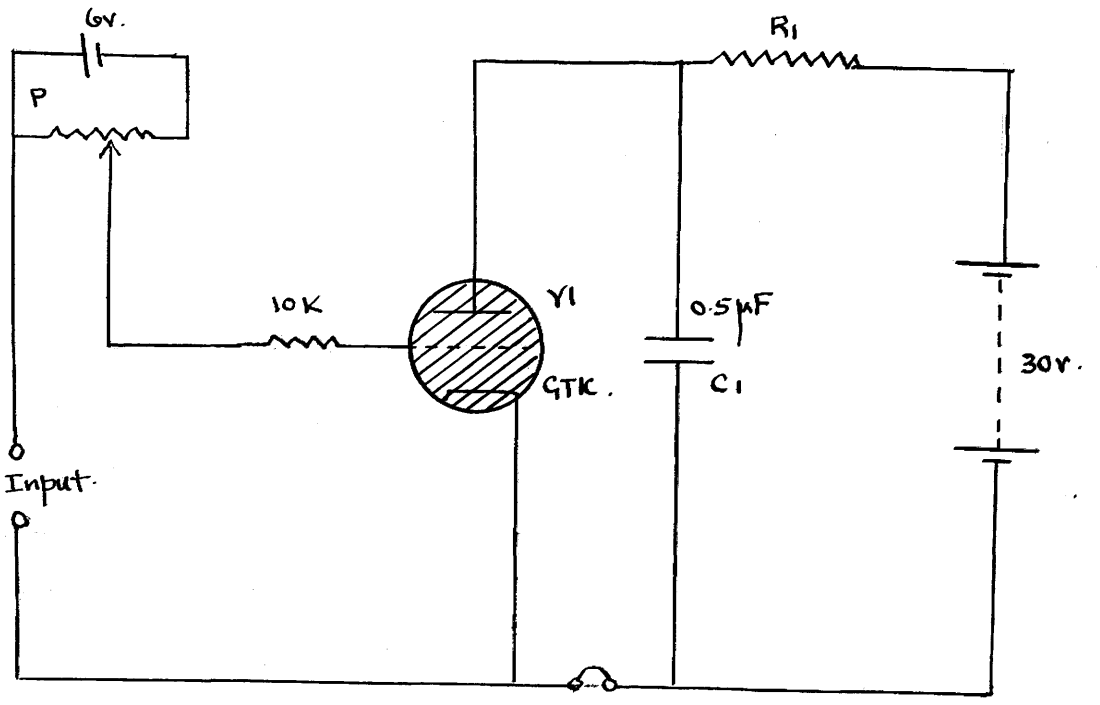

Since the output from the bridge was a minimum on balance, the latter system was first adopted. However, an oscilloscopic investigation of a detected output from the bridge amplifier revealed a sharp maximum of 50 cycle hum at the instant of balance. This was used as a positive transient, and proved to be more satisfactory than the undetected minimum. Adjustment of P could be made so that a single click on the earphones was indicative of balance, whilst silence indicated any out of balance setting. The method was probably sensitive to two places in the third place condenser at the most responsive part of the capacity-potential curve.

2). The second method, which was the one normally employed, made use of a Cossor double beam oscilloscope. The system was evolved as follows. The bridge amplifier output was fed to the A_1 terminal of the oscilloscope and the presentation observed on a free running time base. Being unlocked, however, this was unsatisfactory and so the voltage pulse associated with the fall of a drop was used to trigger the time base, thus giving a locked presentation. The effect was that of a 2000 cycle sine wave decreasing in amplitude until at the moment of balance it appeared to turn inside out. This again, however, was too insensitive to capacity setting and consequently

unsatisfactory. The final technique utilised the detected output already mentioned. This was fed to the A1 terminal of the oscilloscope, but the internal time base was switched off. The resulting presentation was that of a vertical line receiving a large instantaneous deflection when a mercury drop fell, and thereafter, having returned to its original position on the face of the C.R.T., expanding to a sharp maximum at the moment of balance for the next drop. The other oscilloscope beam, now evident as a spot on the tube, was used as a strobing device. Balance was effected by setting R_3 as previously explained, adjusting the larger standard condensers until an approximate maximum was observed, and thereafter obtaining two readings on the third place condenser, one on either side of the correct value such that the maximum excursions of the line were the same distances below the spot. The correct condenser setting thus brought the tip of the line on to the spot, whilst one place on either side caused the line maxima to be a similar distance below the spot. Accurate observations were made by means of a horizontal graticule, and an incorrect setting was characterised by asymmetric differences. In aqueous systems, this method was sensitive to less than one place on the third place condenser.

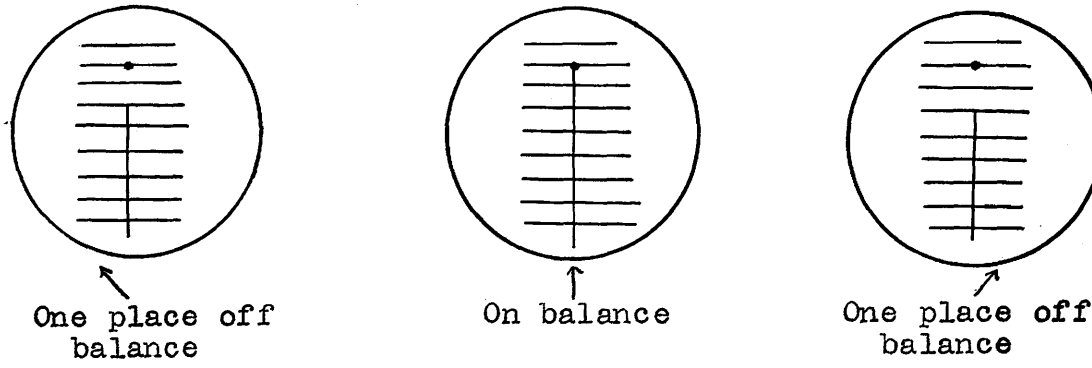

With the bridge balanced, the value of standard condenser hence gave the capacity of the double layer at a mercury droplet at a given time after drop birth. To evaluate capacity per unit area it was therefore necessary to know the surface area of the droplet at that instant. Hence, two additional factors were required:

a) the exact time interval between drop birth and balance, and

b) the mass rate of the dropping mercury electrode.

These are related thus

$$A = Km^{2/3}t^{2/3}$$

Where A = droplet area in square cms.,

$K = (4\pi)^{\frac{1}{3}}\left(\frac{3}{d}\right)^{\frac{2}{3}}$, d being the density of mercury,

m = mercury mass rate in mgm. per second, and

t = birth-balance time in seconds.

Hence, capacity per unit area is given by

$$c = \frac{\bar{c}}{Km^{2/3}t^{2/3}}$$

where $\bar{c}$ is the capacitor reading. The time interval was measured by a $1/100^{th}$ second manual stop watch with successive readings reproducible to within five one hundreths of a second. The fact that in the above expression time occurs to the power two-thirds reduces any error due to mistiming. Mercury mass rates were determined by using a special cell, the anode of which was a mercury pool shorted externally to the dropping mercury cathode. The mercury head, measured by a cathetometer, was maintained throughout at the same height as that employed in the capacity readings. The mercury droplets fell through the given solution into a central cup which, by means of a stopcock, could be emptied at any instant into a suitable receiver. Mercury was usually collected at about 3 minute intervals, washed with acetone, dried, and weighed. The rate of flow was of the order of 1 m.gm./sec.

General run procedure.

To set up the apparatus for the purpose of making capacity measurements, the cell was first clamped on the bench. The fine tipped capillary was then inserted so that its tip was within the platinum sphere anode. The cell was clamped in the thermostat, the mercury head connected to the capillary, and the level raised sufficiently to cause the mercury to drop. This ensured that the

capillary was in operation before the solution was introduced into the cell, thus avoiding wetting of the inside of the capillary and possible erratic dropping behaviour. The solution was then introduced via the appropriate side arm, the reference electrode inserted, and the cell sealed by a bubbler. Tank nitrogen was bubbled through the solution for about 15 minutes to remove oxygen. The mercury head was then adjusted so that the drop time was about 6 seconds, and the exact head measured by a cathetometer. When the cell had been given sufficient time to come to temperature, the appropriate static potential was applied between reference electrode and cathode, and thereafter the bridge was balanced as described. In aqueous systems, the potential range covered with respect to the 0.1 N calomel electrode was from 0 to -1.8 volts. In general, the balancing system was at its most sensitive on the cathodic branch of the curve, i.e., negative with respect to the E.Cap.Max., and least sensitive on the anodic limb where the capacity values were, as a rule, of a much higher order. R_3 was adjusted from time to time to keep the balance point approximately 3.5 seconds after drop birth. In some cases, however, where drop time decreased with decrease in potential, it was necessary to balance after a shorter interval. Little difference in

capacity values measured at the same potential but at different balance times was ever observed. This may be expected, since the mercury drops are spherical, at least until the last half second before falling (37,40). Since, for a given capillary and constant mercury head, $c = \bar{c} / K m^{2/3} t^{2/3}$ capacity reading should be directly proportional to $t^{2/3}$ The accompanying graph indicates this relationship. The data are for 0.1 N potassium chloride solution at E = -1.2 volt with respect to a 0.1 N calomel electrode.

Mercury purification.

After use, mercury was washed with water, filtered by piercing a small hole in normal filter paper and washed with acetone. It was sprayed down a two foot column of 10% nitric acid, and then allowed to stand under concentrated sulphuric acid for 24 hours. After being washed with water and acetone, it was thoroughly dried and finally twice distilled under vacuum.

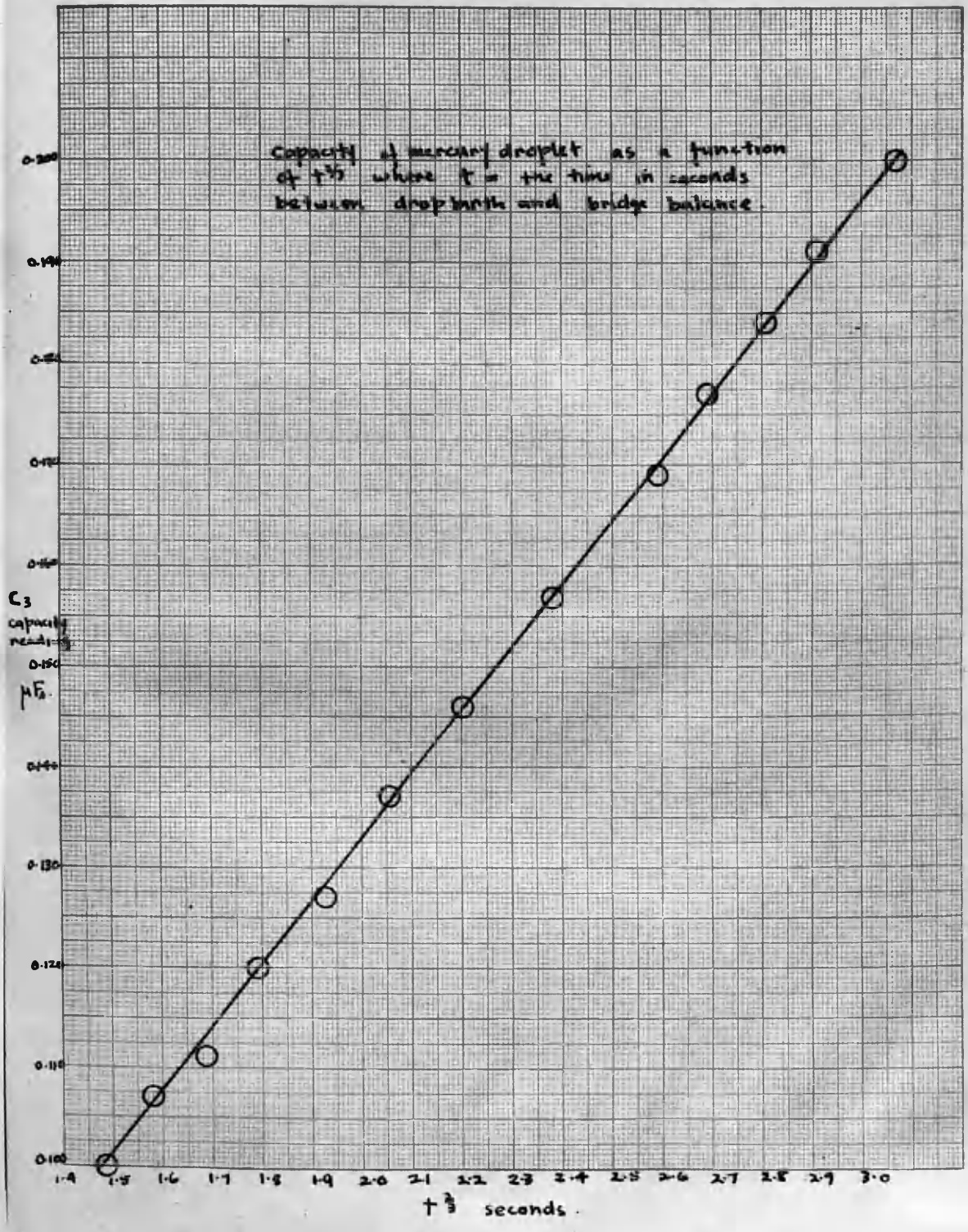
Capacity of mercury droplet as a function of $t^{\frac{2}{3}}$ where t = the time in seconds between drop birth and bridge balance.
C_3 capacity read in μF_0.
0.200
0.190
0.180
0.170
0.160
0.150
0.140
0.130
0.120
0.110
0.100
1.4 1.5 1.6 1.7 1.8 1.9 2.0 2.1 2.2 2.3 2.4 2.5 2.6 2.7 2.8 2.9 3.0
$t^{\frac{2}{3}}$ seconds.

Results and Discussion.

The effects of addition reagents on double layer capacity.

The effects of traces of non-electrolytes on the properties of polarographic waves have been widely studied, but less data are available on their effects on the capacity of the electrical double layer. Gouy (41), in his extensive electrocapillarity work, showed that the curve was flattened, or the E.Cap.Max. shifted on adding slightly soluble organic substances to the solution. Direct capacity observations were made by Proskurnin and Frumkin (35), who demonstrated the effect on capacity of picein and octyl alcohol at a mercury electrode in a solution of sodium sulphate. Abrupt increases in capacity were evident at potentials where the alcohol was adsorbed and desorbed and a lowering of capacity was shown between these potentials. Grahame (37) has studied capacity, resistance, and frequency effects at a mercury electrode in various solutions saturated with octyl alcohol and in sodium sulphate solution with n-heptyl alcohol present, whilst Loveland and Elving (30), also using a dropping mercury electrode, have made an oscillographic investigation of adsorption-desorption and other phenomena in the presence of n-amyl, n-hexyl, n-heptyl, and n-octyl alcohols. Gorodetskaya and collaborators (42,43) have also studied the effects of surface films and have found

a progressive decrease in capacity with increasing chain length in an alcohol series. Doss and Kalyanasundram (44) have recently observed capacity lowering at a mercury cathode on the addition of a number of organic reagents such as toluene, amyl alcohol, and xylene.

The present work, which is semi quantitative in nature, has investigated the effects on differential capacity of the following reagents: i) gelatin, ii) eosin, iii) methyl red, and iv) pyridine. The supporting electrolyte in all cases was N/10 potassium chloride using an N/10 calomel or mercury pool as a reference electrode. Pseudo capacity effects with thallium, cadmium, and lead have also been obtained, and the behaviour of these ions in the presence of gelatin, eosin, and methyl red examined.

The reference electrode.

Comparison of results observed in the presence of methyl red using a) an N/10 calomel electrode and b) a mercury pool revealed no deviations attributable to the replacement of the former by the latter. Also, the potential difference between a mercury pool and an N/10 calomel electrode in the same cell and in the presence of any of the addition reagents was found to be zero. Consequently, for convenience, a mercury pool was frequently used as reference electrode.

Purification of materials.

Conductivity water was used throughout. Analar potassium chloride was twice recrystallised from conductivity water and made up as required. The gelatin was a B.D.H. sample, while eosin and methyl red were prepared by normal organic methods. Ultra pure German pyridine was used after redistillation. Cadmium chloride, lead and thallium nitrates were analar samples.

0.1 N potassium chloride alone.

The capacity-potential curve for 0.1 N potassium chloride is shown in Graph 1 with the associated data in Table 1. The results are in substantial agreement with those of Grahame (37), a minimum capacity of 16.7 $\mu F/cm^2$. corresponding to his value of 16.1 $\mu F/cm^2$. The significance of the shape of this curve has already been discussed by Grahame (8), but it may be pointed out that it is characteristic of capacity-potential curves obtained in general, both in aqueous and in non aqueous systems. The large values of capacity obtained on the anodic branch of the curve are due to specific adsorption of the chloride ions which are held with increasing strength as the potential becomes more positive. The gentle rise in capacity on the cathodic limb may be attributed to increasing coulombic distortion of the cations, whilst the

relatively flat portion of the curve, in the absence of specific adsorption, is characteristic of the solvent. The "hump" on the anodic branch has not yet been satisfactorily explained.

The effects of gelatin addition.

Graph 1 also shows the effect on capacity of 0.25% gelatin. In common with other surface active materials, it lowers the capacity, the value of which on the flat portion of the curve is about 10-11 $\mu F/cm^2$. Gelatin is perhaps exceptional in that it lowers the capacity evenly over almost the entire potential range without there being any evidence of adsorption or desorption at specific potentials.

It was also thought to be of interest to determine how capacity varies with gelatin concentration at a fixed potential. The only similar data in the literature are those of Butler (28), who obtained an oscillogram of t-amyl alcohol in hydrochloric acid at a static mercury surface. The isotherm curve shown in Graph 2 was obtained by adding 0.5% gelatin - N/10 potassium chloride solution to the cell solution at the potential of the E.Cap.Max., i.e., -0.559 volt with respect to the N/10 calomel electrode. Additions were made by means of a weight burette, and nitrogen bubbled through the cell each time to ensure thorough mixing. Since the weight of N/10

potassium chloride solution in the cell was known, the percentage gelatin present was readily calculated. It is evident that small traces of gelatin cause an immediate lowering of the capacity, and that this lowering is an almost linear function of gelatin concentration until the value of the latter is about 0.03%. Thereafter, further additions have no effect on the capacity, which remains substantially constant at a value of about 12.5 $\mu F/cm^2$. Since the capacity-potential curve in Graph 1 was obtained with 0.25% gelatin, the results must show the maximum effect on capacity of this addition reagent. These effects are undoubtedly due to the adsorption on the mercury surface of a thin film of gelatin which interferes with the normal ionic adsorptive processes and spacing of the double layer, thus causing a lowering of capacity. The isotherm curve is indicative of progressive adsorption and of the fact that minimum capacity is associated with a specific maximum gelatin surface concentration.

Weisner (45), who has investigated the effect of eosin on polarographic reduction processes, found that small quantities of the dyestuff caused a reduction in diffusion current. He obtained a curve, the approximate shape of which is shown. The main point of interest is

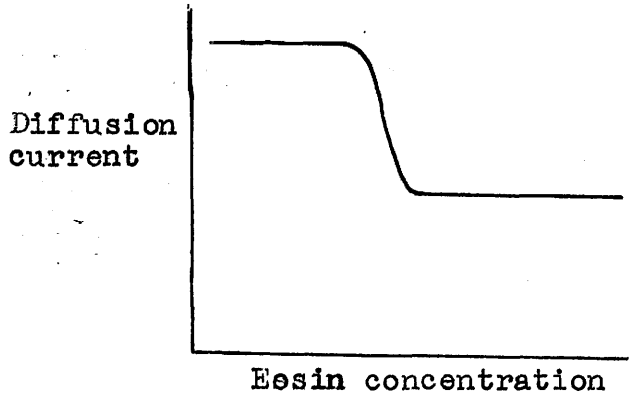

the initial flat portion. This indicates that a critical eosin concentration is necessary before the diffusion current is affected. Wiesner referred to the initial quiescence as "an incubation period", and an investigation of double layer capacity in the presence of gelatin has shown similar effects. This was undertaken in two ways:-

1) Maintaining a constant time interval between drop birth and bridge balance, isotherm curves were drawn at different potentials. The results at the E.Cap.Max. have already shown that at this potential, capacity lowering is immediate. However, Graph 3 indicates that at E = -0.7 volt. and E = -0.9 volt., incubation periods are in evidence and that there is a longer period at the more negative potential. In all these cases the birth-balance time was about 3.5 second. These results show that at potentials more negative than the E.Cap.Max., a critical gelatin concentration is necessary before adsorption takes place. Furthermore, since this concentration is greater, the

more negative the potential, it may be concluded that adsorption is becoming correspondingly weaker.

2) In the second case, the potential was fixed and isotherms obtained for different birth-balance times. Graph 3 also shows the commencement of two isotherms, both at E = -0.9 volt, but at balance times of 5 and 3 seconds respectively. It is clear from the results that the shorter the balance time the longer the incubation period and vice versa. Again, a critical gelatin concentration is necessary before adsorption takes place, and this occurs at a particular instant during the life of a drop. By polarographic techniques, and by the observation of drop times taken as a measure of surface tension, Meites (46) has examined the behaviour of gelatin and methyl red in 0.1 M phosphate and other solutions. He observed that critical concentrations of the reagents were necessary before the polarographic waves or drop times were affected, and attributes these effects to micelle formation. It is, however, difficult to reconcile the capacity results presented here with any gelatin aggregation, since such an occurrence would be independent of potential and of drop characteristics.

Another method of investigation of incubation periods was attempted. It was essentially that of Kay and

Stonehill (47), who made an oscillographic polarographic study of the electro reduction of acridine. During the life of a droplet, as already observed, a small current of the order of 1 - 2 μA flows through the D.C. circuit concerned. This current has the form of a sixth order parabola and may be translated into potential by the inclusion of a series resistor. The potential-time curve may then be observed, after suitable amplification, on a cathode ray tube. Since the drop life is of the order of six seconds, it is necessary to use a D.C. amplifier to avoid waveform differentiation. This scheme was carried out, but although the sudden adsorption of gelatin during the life of a mercury droplet should be accompanied by a sudden decrease in the small direct current flowing, no such discontinuity was observed with the amplification used.

The effects of eosin.

Graph 4 shows the capacity-potential curve for 0.014% eosin. Considerable adsorption is evident on the anodic branch of the curve where the capacity is reduced to about 9 $\mu F/cm^2$. A small desorption hump appears at -1.25 volt, after which the normal cathodic values for N/10 potassium chloride are reverted to. An isotherm curve at the E.Cap.Max. potential is shown in Graph 5.

The results are similar to those obtained with gelatin, but, a) the capacity is lowered to 9.0 $\mu F/cm^2$., whereas with gelatin the value is 12.5 $\mu F/cm^2$, and, b) the minimum capacity is reached at a concentration of slightly less than 0.005%, whereas the corresponding gelatin concentration is 0.25%. With eosin, no capacity incubation period was observed in the potential range over which the dyestuff is adsorbed.

The effects of methyl red.

The capacity-potential curve for 0.005% methyl red appears in Graph 4. Methyl red is reduced cathodically at potentials more negative than -0.3 volt, and consequently the capacity lowering between this potential and about -1.1 volt, at which value the normal potassium chloride figures are reverted to, must be attributed to reduction products.

Effects of pyridine.

Graph 6 reproduces the capacity-potential curve for 1% pyridine. The interesting feature of the curve is the large capacity increase observed at about -1.45 volt. This is undoubtedly due to the break up and desorption of the pyridine film, and is in direct confirmation of the work of Heyrovsky (48) who, from oscillographic observations, predicted an increase in capacity at -1.5 volt with

respect to the normal calomel electrode.

Also shown in the same graph are the desorption peaks for 0.5% and 0.1% pyridine. It is clear that decreasing pyridine concentration is accompanied by
a) a decrease in the adsorption peak amplitude, and
b) a progressive movement of the peak towards a more positive potential.

The last effect is again in agreement with Heyrovsky who regarded V, the desorption potential, as being indicative of the maximum number of adsorbed molecules, and by use of the Langmuir isotherm, predicted values of V for given pyridine concentrations.

Attempted quantitative approach.

It had been hoped to make a quantitative estimation of the surface excess of capillary active material necessary for maximum capacity lowering. From the Gibb's expression $\Gamma_{eosin} = \left(\frac{d\sigma}{d\mu_{eosin}}\right)_{E,KCl}$ where Γ represents the surface excess, σ is the surface tension, and μ the chemical potential, it should be possible to evaluate T by observing the rate of change of surface tension with concentration of reagent, at a fixed potential. This was attempted with both gelatin and eosin, using a Lipmann capillary electrometer with N/10 potassium chloride as supporting electrolyte. The results were

unsatisfactory. Two reasons may be advanced,

a) the surface tension change corresponding to a fairly extensive capacity depression is not large enough for accurate measurement by this method:

b) the surface active material causes severe capillary sticking which reduces to a prohibitive degree the accuracy of the readings.

Capacity effects in the presence of lead, cadmium and thallium ions.

Graphs 7, 8 and 9 show the capacity-potential relations for the solutions a) 0.001 M cadmium chloride - 0.1 N potassium chloride, b) 0.001 M lead nitrate - 0.1 N potassium chloride, and c) 0.001 M thallium nitrate - 0.1 N potassium chloride, respectively. The most noticeable feature of these results is the sudden and extensive capacity rise which in each case takes place at a specific potential characteristic of the cation concerned. This abnormal behaviour is referred to as "pseudo capacity", and occurs at the polarographic half wave potential of the ionic species responsible for the effect. The small alternating potential, superimposed upon the critical static potential, is responsible at the mercury surface for the successive deposition and solution of the cation. This gives rise to a relatively large out of phase alternating

current which produces a sudden increase in observed capacity. The magnitude of the capacity is frequency dependent, the lower the frequency the greater being the effect and vice versa. The frequency here employed was 2000 cycles per second. The half wave potentials of cadmium, lead and thallium lie within the range 0 to -1.8 volt with respect to the N/10 calomel electrode, whereas potassium, the cation of the supporting electrolyte, does not deposit until more extreme polarisation is applied. The technique of studying electrode kinetics by applying a small alternating voltage to an electrode at which an electrochemical reaction is in equilibrium has been employed by a number of workers including Randles (49), Ershler (50), and Breyer and Gutmann (51). As used here, the pseudo capacity effect may be translated in two ways:-

a) as a fairly sensitive indication of the presence of small concentrations of ions, and

b) as a criterion of thermodynamic reversibility.

It was therefore possible to investigate the effect of adsorbed films on the reversible reduction of cations.

The effects of gelatin.

From the potassium chloride - gelatin isotherm shown in Graph 2, it is evident that a minimum value of about 0.03% gelatin produces a maximum lowering of capacity.

Graphs 7, 8 and 9 also show the effect of this gelatin concentration on the pseudo capacity maxima of cadmium, lead and thallium. It is apparent that the ions are affected in the order given, the reversible deposition of cadmium being completely inhibited, that of lead being only partially affected and that of thallium being influenced scarcely at all. Further gelatin additions made little difference to these maxima. In an oscillographic investigation of the effect of adsorbed films on the reversible cathodic reduction of an ion, Heyrovsky (52) concludes that thallium is reversible under all circumstances. This is in keeping with what is presented here. It is suggested that the reduction of a divalent ion is much more likely to be affected by the adsorbed film than that of a monovalent ion. The effect is explained by supposing that the divalent cation acquires only one electron on first touching the electrode, and that the second electron is acquired as a result of a dismutation process thus:-

$$2Cd^{+} \rightleftharpoons Cd + Cd^{++}$$

It is this latter reaction that is hindered by the adsorbed film. Although the presence of gelatin adequately suppressed the cadmium maximum, that of lead was only partially affected. Nevertheless, the peak value of about 154 $\mu F/cm^2$. is approximately two and a half times

that observed with gelatin added.

Since the cadmium maximum was most readily suppressed, it was decided to investigate how the peak capacity varied with gelatin concentration. Graph 10 indicates that the reversible reduction of the ion is not immediately inhibited, but that a critical concentration of gelatin is necessary before suppression commences. The corresponding behaviour of the pseudo capacity as a function of potential at varying gelatin concentrations is illustrated by the family of curves in Graph 11. The "hump" narrows and diminishes in amplitude until about 0.0122% gelatin, after which the peak steadily collapses until it disappears almost completely. These results are in general agreement with those of Randles (49), who concludes, from cathode ray polarographic studies, that gelatin markedly decreases the discharge rate for zinc and cadmium.

The effects of eosin and methyl red.

No observable effect on the pseudo capacity maxima of any of the ions already investigated was obtained on the addition of these reagents.

Table 1.

Capacity data for N/10 potassium chloride.

Potential in volts. -ve V N/10 calomel	Condenser reading in μF (C_3)	Balance time in secs. t.	Solution resistance in ohms (R_3)	Capacity in $\mu F/cm^2$.
-0.10	0.680	3.85	295	69.9
0.15	0.500	3.85	295	51.4
0.20	0.425	3.80	295	44.09
0.25	0.391	3.85	295	40.20
0.30	0.382	3.85	295	39.27
0.35	0.385	3.85	295	39.59
0.40	0.388	3.85	295	39.89
0.45	0.383	3.80	295	39.24
0.50	0.357	3.88	295	36.53
0.55	0.332	4.28	290	31.81
0.60	0.285	4.22	290	27.55
0.65	0.260	4.50	285	24.09
0.70	0.236	4.45	285	22.03
0.75	0.221	4.42	285	20.72
0.80	0.210	4.38	285	19.80
0.85	0.203	4.42	285	19.04
0.90	0.194	4.42	285	18.18
0.95	0.189	4.38	285	17.82
1.00	0.184	4.42	285	17.25
1.05	0.181	4.45	285	16.89
1.10	0.177	4.35	285	16.80
1.15	0.176	4.35	285	16.71
1.20	0.175	4.26	285	16.81
1.25	0.162	3.78	295	16.87
1.30	0.177	4.28	295	16.95
1.35	0.179	4.28	285	17.15
1.40	0.181	4.18	285	17.61
1.45	0.184	4.18	285	17.90
1.50	0.187	4.18	285	18.19
1.55	0.191	4.10	285	18.83
1.60	0.196	4.10	285	19.32
1.65	0.201	4.18	285	19.55
1.70	0.207	4.10	285	20.40
1.75	0.214	4.18	285	20.82
1.80	0.222	4.10	285	21.88

Capillary constant = 3960:

Table 1A

Capacity data for N/10 KCl - 0·25% gelatin

Potential volts - ve	C_3 μFs.	t seconds	Capacity μF/cm^2
0·10	1·42	3·67	72·9
0·15	1·24	3·80	62·2
0·20	1·00	3·96	48·81
0·25	0·764	3·81	38·26
0·30	0·692	4·50	23·24
0·40	0·447	4·10	21·64
0·50	0·316	4·07	15·14
0·60	0·263	4·23	12·28
0·70	0·244	4·37	11·15
0·80	0·238	4·40	10·83
0·90	0·239	4.51	10·69
1·00	0·242	4.63	10·64
1·10	0·243	4·53	10·84
1·20	0·246	4·55	10·94
1·30	0·243	4·22	11·37
1·40	0·248	4·27	11·51
1·50	0·241	3·79	12·11
1·60	0·257	3·71	13·10
1·70	0·270	3·27	14·97
1·80	0·302	3·06	17·66
1·90			

Capillary constant = 8187

Table 2

Gelatin isotherm data for N/10 KCl at E = -0·559 volt vs. N/10 calomel electrode

C_3 μFs.	t seconds	Percentage gelatin	capacity μF/cm^2.
0·548	3·16	0	31·07
0·545	3·35	0·0005	29·73
0·528	3·34	0·0017	28·85
0·498	3·38	0·0033	27·01
0·440	3·88	0·0061	23·41
0·389	3·61	0·0084	20·19
0·344	3·65	0·0115	17·73
0·328	3·97	0·0154	15·98
0·306	4·68	0·0226	13·36
0·278	4·36	0·0750	12·70
0·275	4·35	0·1500	12·60
0·278	4·35	0·2000	12·70

Capillary constant = 8187

TABLE 3

Gelatin incubation period data

A :- at E = -0·7 volt v. N/10 calomel.

B :- at E = -0·9 volt v. N/10 calomel.

Gelatin additions dropwise	A Capacity $\mu F/cm^2$	B Capacity $\mu F/cm^2$
0	22·75	18·50
1	22·00	18·52
2	21·60	18·51
3	21·00	18·50
4	20·70	18·45
5	20·20	18·24
6	19·62	18·00
7	18·27	17·26
8	17·63	16·10
9	16·70	--
10	15·80	--
11	15·15	--
12	14·50	--
13	13·55	--
14	12·65	--

Gelatin additions dropwise	A C_3 $\mu Fs.$	B C_3 μFs
0	400	465
½	405	415
2	404	415
3	397	397
4	398	373
5	376	349
6	352	322
7	326	301

A :- balance time = 3 seconds.

B :- balance time = 5 seconds.

Table 4

Capacity data for 0·014% eosin - N/10 KCl

Potential in volts - ve	C_3 μFs	t seconds	Capacity $\mu F/cm^2$
0·02	0·320	3·90	15·05
0·05	0·250	3·20	13·41
0·10	0·205	3·14	11·40
0·20	0·170	3·08	9.35
0·30	0·163	3·05	9·03
0·40	0·161	3·05	8·92
0·50	0·162	3·05	8·97
0·60	0·168	3·05	9·30
0·70	0·181	3·05	10·02
0·80	0·200	3·05	11·08
0·90	0·229	3·00	12·82
1·00	0·271	3·00	15·18
1·10	0·292	3·15	15·83
1·20	0·410	3·54	20·56
1·30	0.390	3·30	25·50
1·40	0·322	3·35	16·75
1·50	0·332	3·20	17·80
1·60	0·349	3·15	17·67
1·70	0·368	3·15	18·64
1·80	0·367	2·80	21·51
1·23	0·490	3·75	23·65
1·25	0·490	3·70	23·86
1·27	0·470	3·75	22·69

Capillary constant = 8585

Table 4A

Capacity data for 0·005% methyl red - N/10 KCl

Potential in volts - ve	C_3 μFs	t seconds	Capacity μF/cm^2
0·1	0·835	3·20	44·43
0·2	0·660	3·32	34·28
0·3	0·441	3.20	23·46
0·4	0·346	3·30	18·04
0·5	0·380	3·43	19·31
0·6	0·392	3.85	18·44
0·7	0·322	3·60	15·85
0·8	0·267	3·10	14·51
0·9	0·319	3·60	15·70
1·0	0.333	3·35	17·19
1·1	0·351	3·50	17·60
1·2	0·345	3.42	17·56
1·3	0·328	3·18	17·52
1·4	0·327	3·05	17·97
1·5	0·352	3·30	18·36
1·6	0·368	3·35	18·99
1·7	0.389	3·35	20·08
1·8	0·418	3·20	22·24
1·9	0·440	3·00	24·45

Capillary constant = 8653

Table 5

Eosin isotherm data for N/10 KCl

at E = -0·3 volt vs N/10 calomel electrode

C_3 μFs	t seconds	Percentage eosin	Capacity μF/cm^2
0·693	3·23	0	36·94
0·628	3·20	0·00056	33·68
0·548	3·20	0·00119	29·39
0·458	3·20	0·00179	24·56
0·357	3·25	0·00234	18·95
0·281	3·20	0·00289	15·07
0·215	3·25	0·00343	11·41
0·192	3·55	0·00400	9 ·61
0·185	3·60	0·00460	9·18
0·184	3·55	0·00524	9. 21
0·183	3·55	0·00594	9·16
0·185	3·55	0. 00721	9·16
0·183	3·55	0·00936	9·16
0·183	3·55	0·01230	9·16

Capillary constant = 8585

Table 6

Capacity data for 1% pyridine - N/10 KCl

Potential volts - ve	C_3 μFs	t seconds	Capacity $\mu F/cm^2$
0·1	1·48	2·70	88·0
0·2	0·805	2·85	46·51
0.3	0·745	2·90	42·55
0·4	0·625	2·85	36·11
0·5	0·473	3·75	22·76
0·6	0·363	3·94	16·90
0·7	0·302	3·45	15·36
0·8	0·253	3·65	12·40
0·9	0·210	3·80	10·02
1·0	0·167	3·65	8·18
1·1	0·144	3·70	6·99
1·2	0·136	3·85	6·43
1·3	0·140	4·05	6·40
1·4	--	--	Very high
1·5	0·465	2·75	27·51
1·55	0·495	3·88	23·28
1·6	0·474	3·95	22·02
1·7	0·432	3·55	21·56
1·8	0·435	3·22	23·16

Capillary constant = 8611

Table 6A

Capacity data for 0·5% pyridine - N/10 KCl

Potential volts - ve	C_3 μFs	t seconds	Capacity μF/cm^2
1·00	0·102	3·65	10·88
1.10	0·084	3·15	9·88
1·20	0·170	4·05	16·90
1·25	0·250	3·25	29·11
1·275	0·298	3·93	30·23
1·30	0·278	3·68	29·48
1·35	0·255	3·70	26·93
1·40	0·224	3·55	24·31
1·50	0·192	3·48	21·12
1·60	0·182	3·37	20·44
1·70	0·186	3·37	20·88
	0·1% pyridine - N/10 KCl		
0·60	0.220	4·05	21·86
0·80	0·156	3.58	16·84
0·90	0·163	3·58	17·59
1·00	0·216	4·95	18·78
1·05	0·177	3·58	19·10
1·10	0·178	3·58	19·21
1·20	0·175	3·58	18·84
1·30	0·167	3·43	18·51
1·40	0·163	3·34	18·42

Capillary constant = 3960

Table 7

Capacity data for 0·001 M $CdCl_2$ - N/10 KCl

Potential volts. - ve	C_3 μFs	t seconds	Capacity μF/cm^2
0·10	1·010	3·97	50·0
0·20	0·774	3·48	42·0
0·30	0·722	3·49	39·13
0·40	0·731	3·49	39·62
0·50	0·673	3·47	36·60
0·60	0·434	3·62	22·95
0·65	0·620	3·00	37·16
0·675	2·100	3·68	109
0·70	2·220	3·23	126
0·75	0·640	3·53	34·42
0·80	0·380	3·48	20·63
0·90	0·345	3·48	18·73
1·00	0·327	3·46	17·82
1·10	0·317	3·48	17·21
1·20	0·315	3·47	17·10
1·30	0·318	3·47	17·30
1·40	0·325	3·37	18·20

Capillary constant = 8022

Table 7A

Capacity data for 0·001 M $CdCl_2$ - N/10 KCl - 0·03% gelatin

Potential volts. - ve	C_3 μFs	t seconds	Capacity $\mu F/cm^2$
0·10	1·30	2·75	80·0
0·20	0·930	3·45	49·75
0·30	0·660	3·44	35·37
0·40	0·455	3·88	22·51
0·50	0·343	4·14	16·25
0·60	0·295	4·50	13·22
0·65	0·287	4·40	13·06
0·70	0·309	4·46	13·93
0·75	0·229	3·34	12·51
0·80	0·200	2·90	12·02
0·90	0·219	3·34	11·96
1·00	0·238	3·76	12·03
1·10	0·243	3·74	12·32
1·20	0·252	3·68	12·92
1·30	0·257	3·50	13·62
1·40	0·263	3·50	13·94

Capillary constant = 8187

Table 8

Capacity data for 0·001 M $Pb(NO_3)_2$ - N/10 KCl

Potential volts. - ve	Cg μFs	t seconds	Capacity μF/cm²
0·20	0·775	3·42	42·55
0·30	0·730	3·45	39·86
0·25	0·731	3·45	39·91
0·35	0·748	3·50	40·51
0·40	0·771	3·67	40·41
0·45	1·210	4·02	59·6
0·50	3·100	3·98	153
0·55	1·100	4·07	53·8
0·60	0·530	3·40	29·22
0·70	0·488	4·41	22·62
0·80	0·437	4·49	20·02
0·90	0·401	4·42	18·56
1·00	0·363	4·15	17·52
1·10	0·373	4·60	16·81
1·20	0·364	4·51	19·18
1·30	0·367	4·53	19·23
1·40	0·373	4·44	17·21

Capillary constant = 8022

Table 8A

Capacity data for 0·001 M $Pb(NO_3)_2$ + N/10 KCl + 0·03% gelatin

Potential volts. - ve	C_3 μFs	t seconds	Capacity μ/Fcm²
0·10	1·40	3·00	82
0·20	0·94	3·00	55
0·30	0·72	3·70	36·76
0·40	0·50	4·00	24·23
0·50	1·14	3·36	62
0·45	0·54o	3·05	33·36
0·55	0·42o	3·60	21·85
0·60	0·284	3·90	14·00
0·70	0·233	3·50	12·35
0·80	0·224	3·50	11·87
0·90	0·223	3·50	11·82
1·00	0·224	3·50	11·87
1·10	0·229	3·50	12·13
1·20	0·235	3·50	12·45
1·30	0·240	3·50	12·72
1·40	0·248	3·50	13·14
1·50	0·256	3·30	14·11

Capillary constant = 8187

Table 9

Capacity data for 0·001 M $TlNO_3$ - N/10 KCl

Potential volts. - ve	C_3 μFs	t seconds	Capacity μF/cm²
0·10	1·23	3·73	63·8
0·15	0·885	3·46	48·73
0·20	0·850	3·73	44·10
0·25	0·753	3·58	40·11
0·30	0·705	3·30	39·66
0·35	0·754	3·56	40·32
0·40	0·735	3·31	41·25
0·45	0·781	3·33	43·68
0·50	0·955	3·36	53·07
0·55	1·55	3·74	80·2
0·60	1·08	3·50	58·4
0·70	0·429	3·21	24·58
0·80	0·340	3·18	19·59
0·90	0·322	3·20	18·53
1·00	0·305	3·14	17·73
1·10	0·297	3·21	17·01
1·20	0·291	3·20	16·74

Capillary constant = 8022

Table 9A

Capacity data for 0·001 M $Tl(NO_3)$ - N/10 KCl - 0·03% gelatin

Potential volts. - ve	C_3 μFs	t seconds	Capacity μF/cm²
0·10	1·40	2·70	88·2
0·20	0·880	3·37	47·81
0·30	0·630	4·55	33·07
0·40	0·468	4·08	22·38
0·50	0·720	4·28	33·36
0·45	0·443	3·85	22·02
0·55	1·60	4·32	73·7
0·60	0·750	4·60	33·12
0·70	0·257	3·87	12·73
0·80	0·228	3·75	11·54
0·90	0·225	3·75	11·39
1·10	0·228	3·80	11·69
1·20	0·239	3·75	12·10
1·30	0·246	3·65	12·68
1·40	0·255	3·65	13·14

Capillary constant = 8187

Table 10

Capacity data for gelatin concentration isotherm at the cadmium pseudo capacity maximum i.e. - 0·7 volt vs. mercury pool in 0·001 M $CdCl_2$ - N/10 KCl

Percentage gelatin	Capacity $\mu F/cm^2$
0	122
0·0043	122
0·0065	122
0·0070	122
0·0077	122
0·0085	122
0·0093	122
0·0101	122
0·0110	61·5
0·0117	39.2
0·0135	36·3
0·0146	25·2
0·0180	21·4

Table 11

Capacity data at potentials around -0·7 volt for varying gelatin concentration in 0·001 $CdCl_2$ - N/10 KCl solution

Percentage gelatin	Potential volts. -ve	Capacity $\mu F/cm^2$
0	0·60	27·75
	0·65	43·01
	0·70	123
	0·75	26·72
	0·80	20·53
0·011	0·60	15·51
	0·65	23·48
	0·70	61·1
	0·75	22·22
	0·80	20·05
0·012	0·60	12·53
	0·65	16·61
	0·70	44·11
	0·75	20·04
	0·80	15·00
0·0122	0·65	13·61
	0·70	35·90
	0·75	18·00
0·0147	0·7	21·25
0·0180	0·7	21·32
0·0210	0·7	17·54
0·0240	0·7	15·73

Graph 1

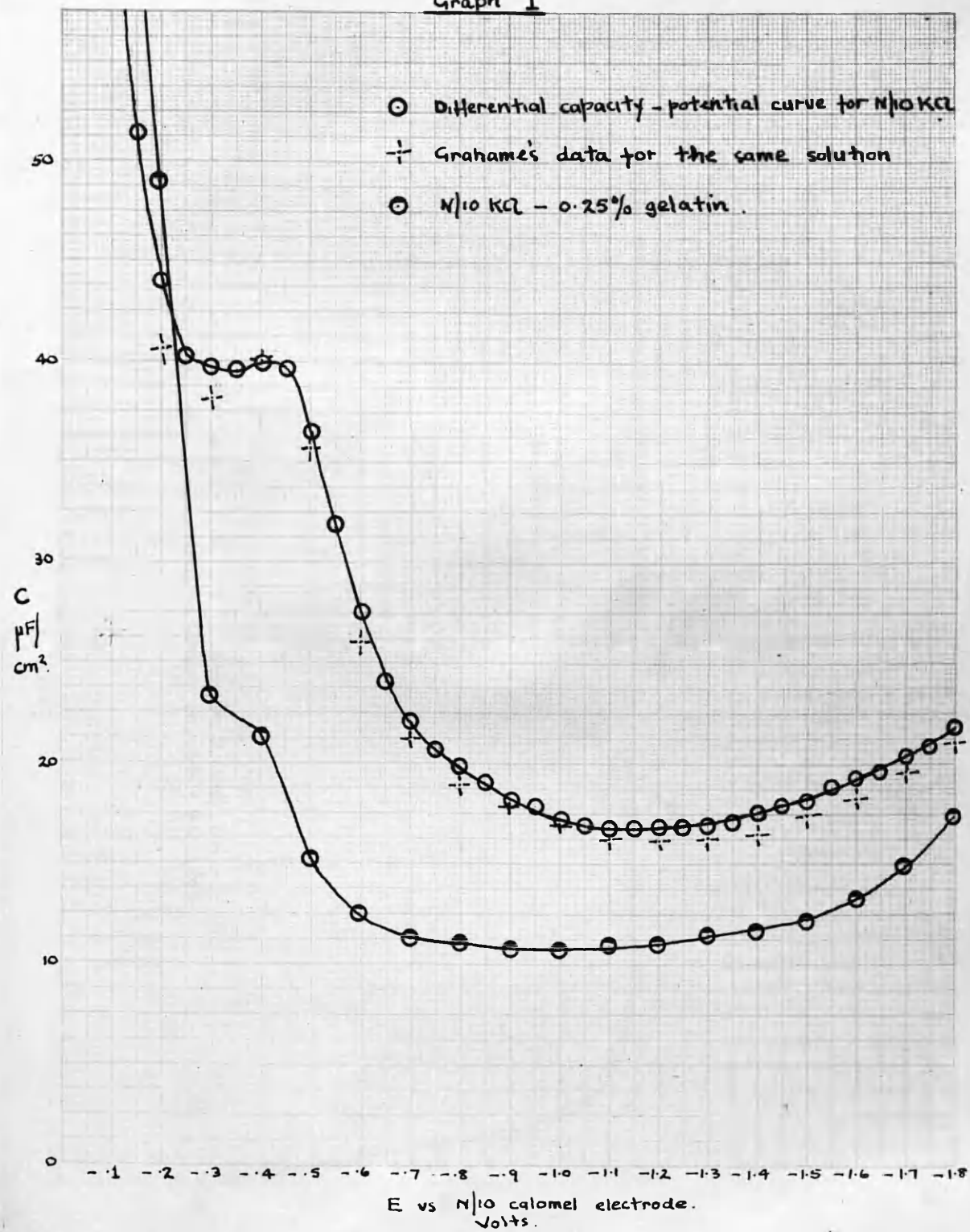
⊙ Differential capacity - potential curve for N/10 KCl
⊹ Grahame's data for the same solution
⊙ N/10 KCl – 0·25% gelatin.
C
μF/cm².
50
40
30
20
10
0
-·1 -·2 -·3 -·4 -·5 -·6 -·7 -·8 -·9 -1·0 -1·1 -1·2 -1·3 -1·4 -1·5 -1·6 -1·7 -1·8
E vs N/10 calomel electrode.
Volts.

Graph 2

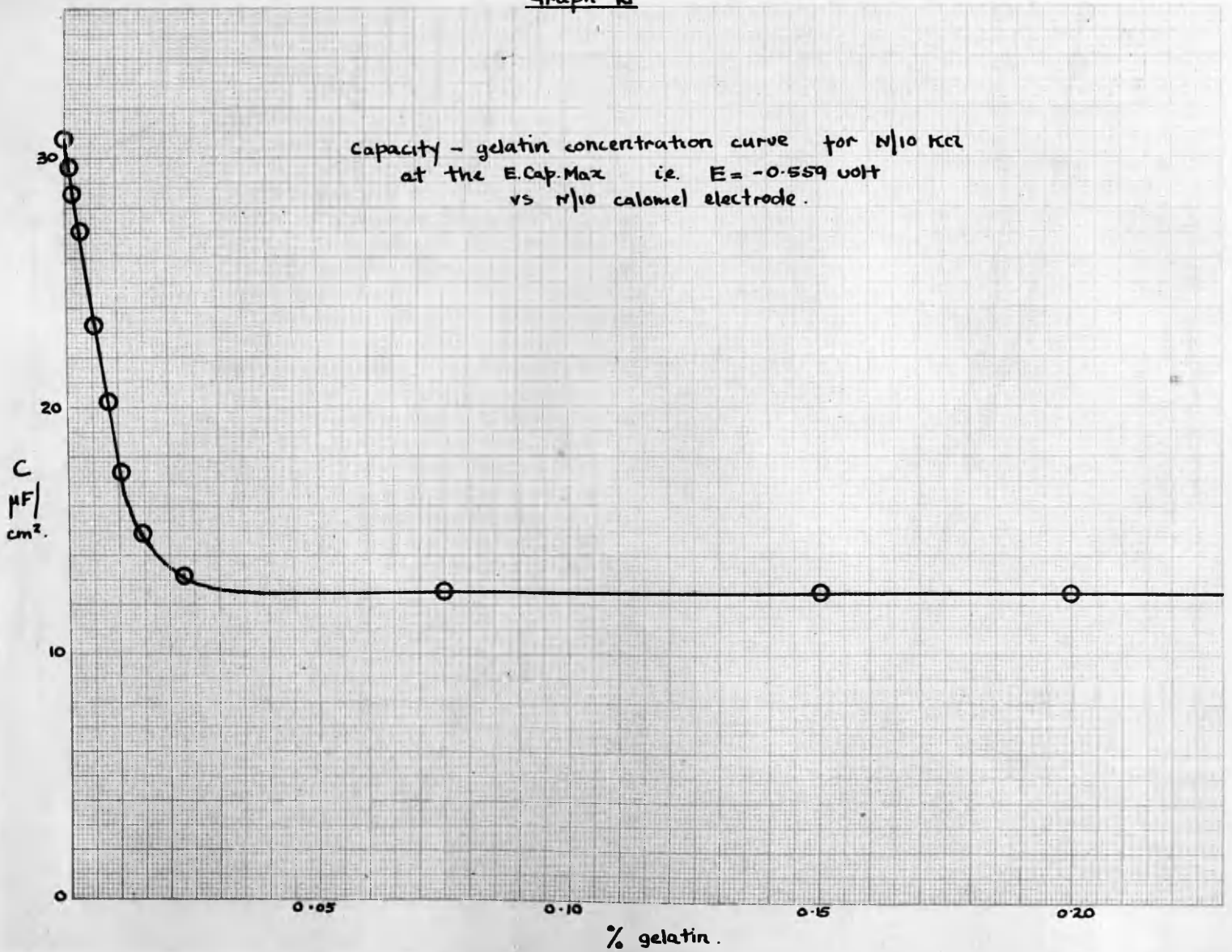
Capacity - gelatin concentration curve for N/10 KCl
at the E.Cap.Max i.e. E = -0.559 volt
vs N/10 calomel electrode.
30
20
10
0
C
μF/
cm².
0·05
0·10
0·15
0·20
% gelatin.

Graph 3

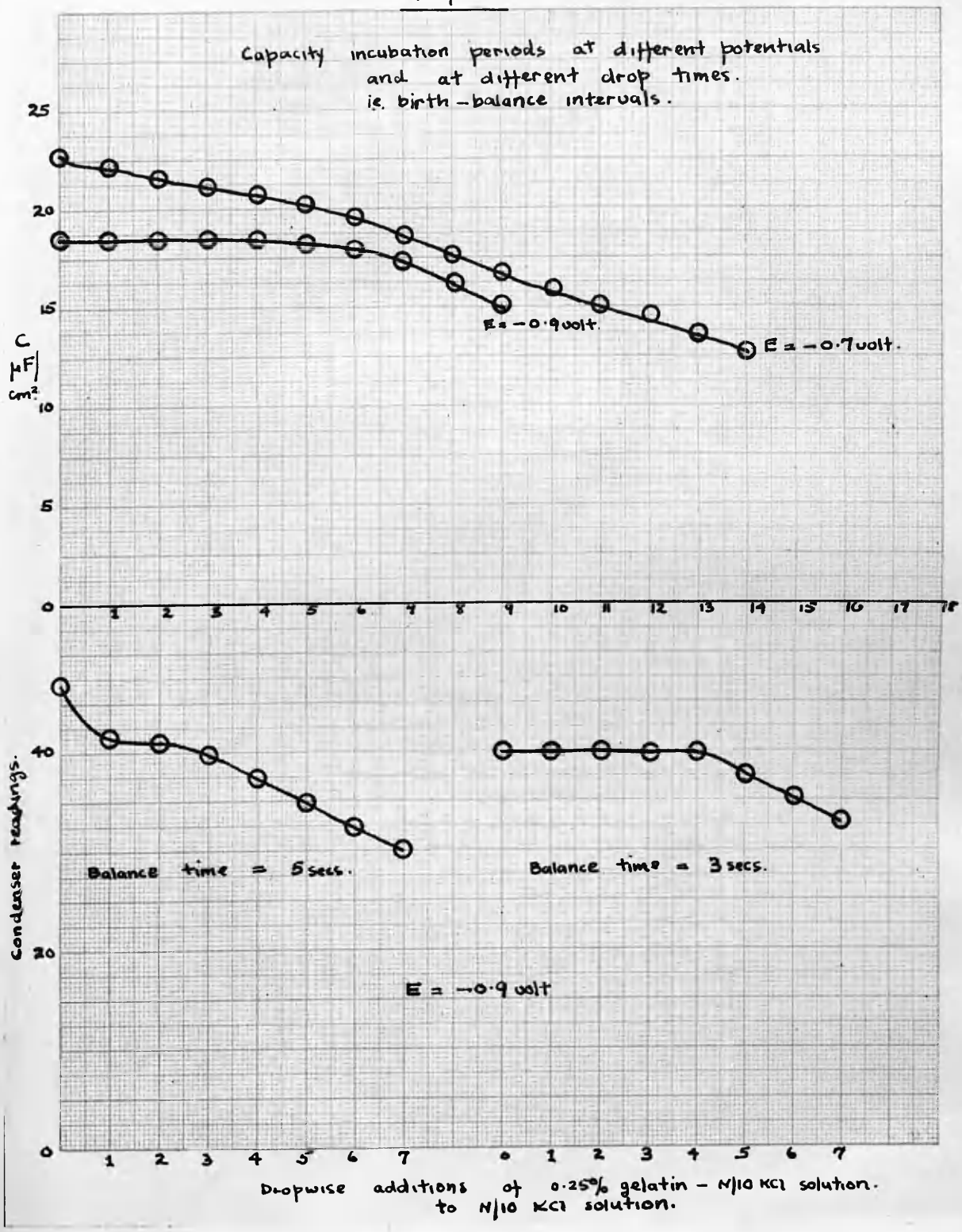
Capacity incubation periods at different potentials and at different drop times.
ie. birth – balance intervals.
C μF/cm²
E = −0·9 volt.
E = −0·7 volt.
Condenser readings.
Balance time = 5 secs.
Balance time = 3 secs.
E = −0·9 volt
Dropwise additions of 0·25% gelatin – N/10 KCl solution to N/10 KCl solution.

Graph 4

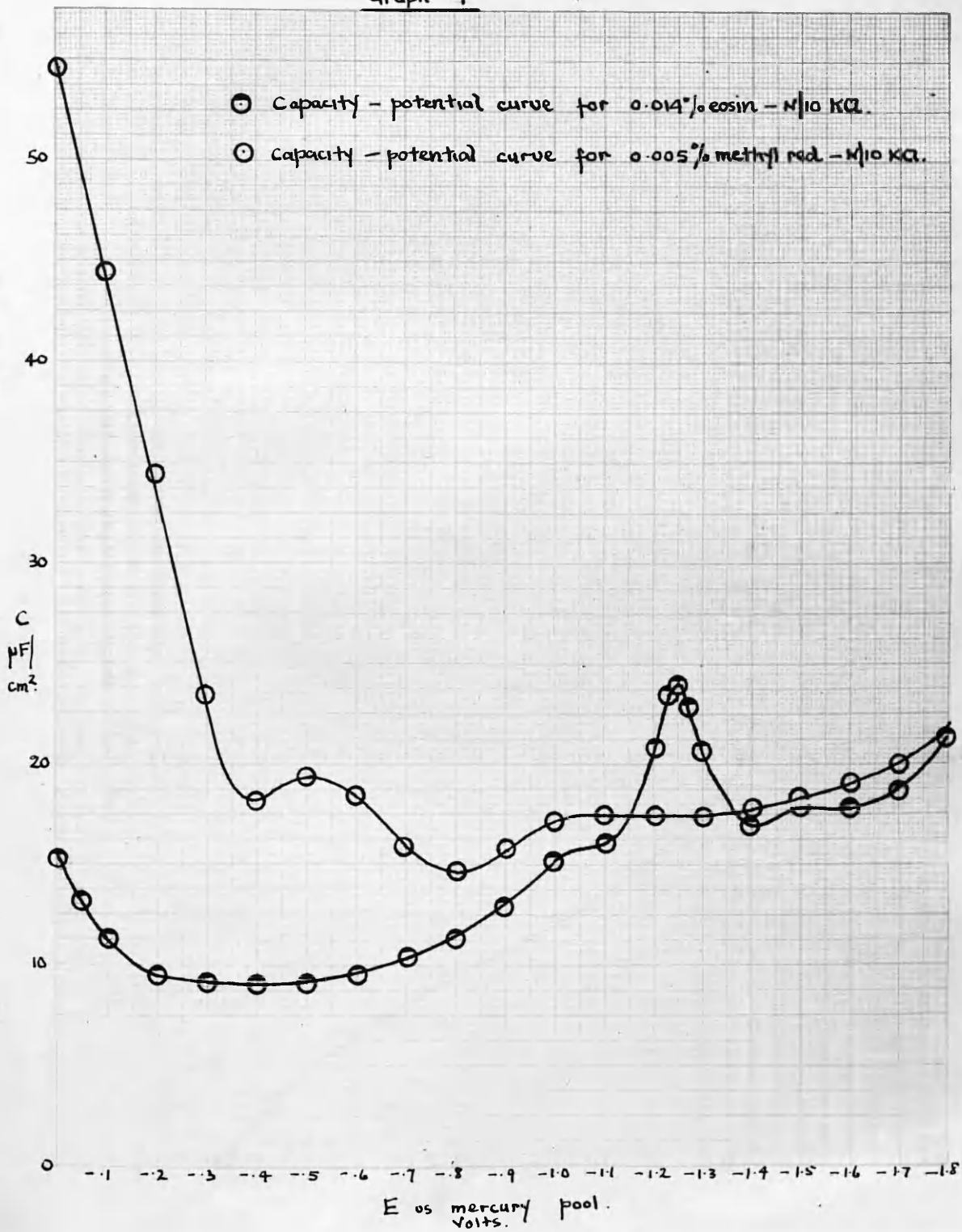
Capacity – potential curve for 0·014% eosin – N/10 KCl.
Capacity – potential curve for 0·005% methyl red – N/10 KCl.
C μF/cm²
50
40
30
20
10
0
-·1 -·2 -·3 -·4 -·5 -·6 -·7 -·8 -·9 -1·0 -1·1 -1·2 -1·3 -1·4 -1·5 -1·6 -1·7 -1·8
E vs mercury pool. Volts.

Graph 5

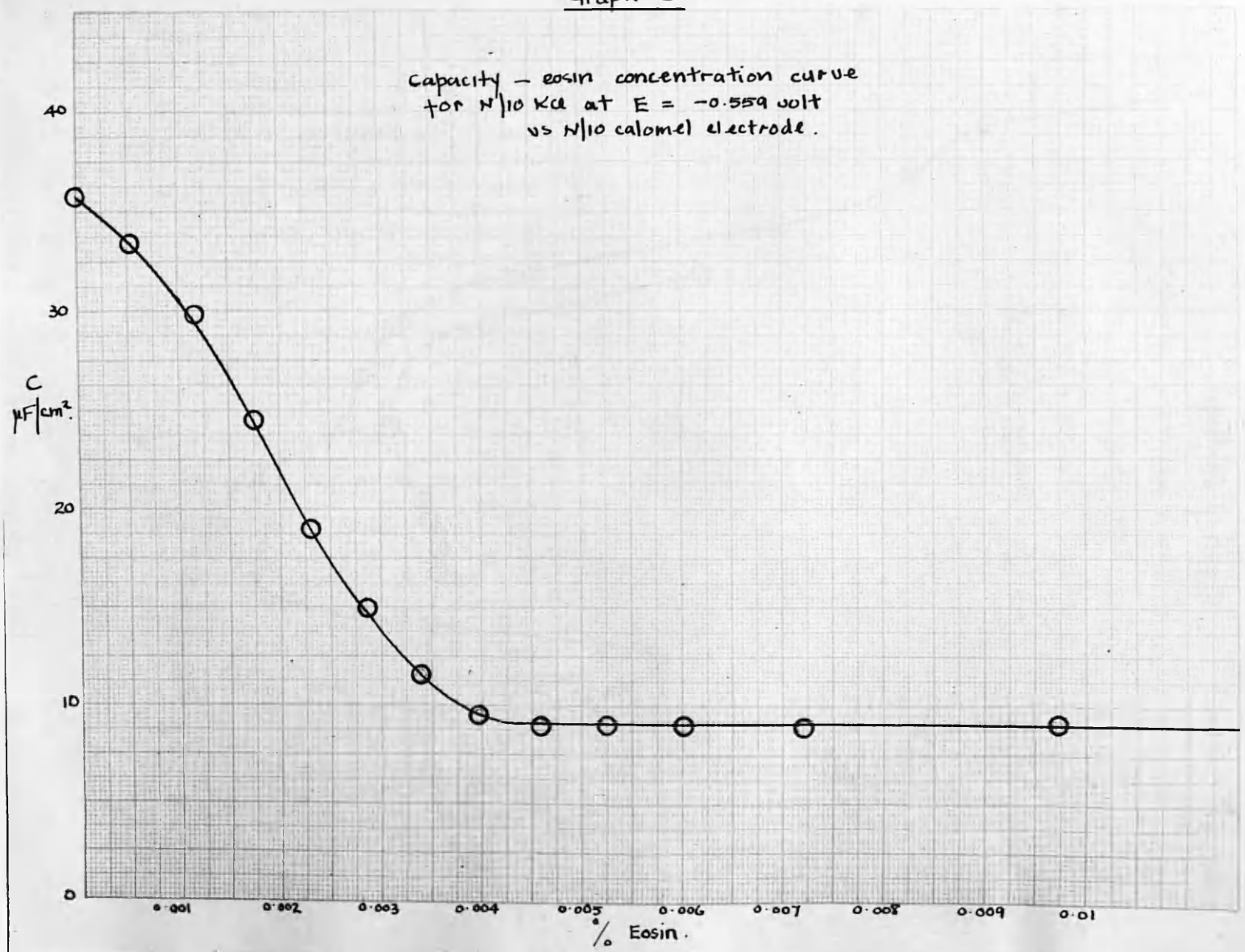
Capacity – eosin concentration curve
for N/10 KCl at E = −0.559 volt
vs N/10 calomel electrode.
C
μF/cm².
40
30
20
10
0
0·001
0·002
0·003
0·004
0·005
0·006
0·007
0·008
0·009
0·01
% Eosin.

Graph 6

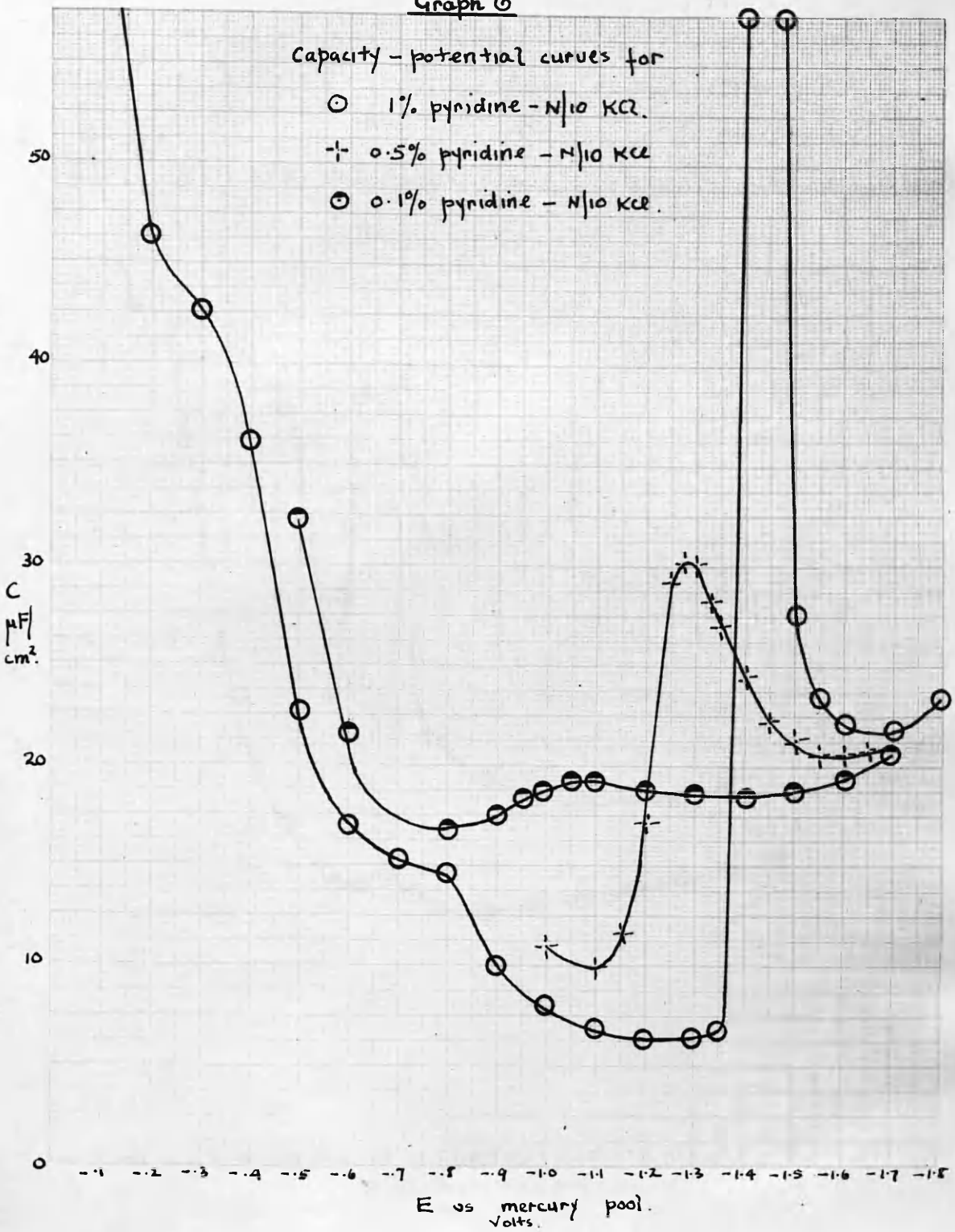
Capacity – potential curves for
⊙ 1% pyridine – N/10 KCl.
-|- 0.5% pyridine – N/10 KCl
⊙ 0.1% pyridine – N/10 KCl.
50
40
30
20
10
0
C
μF/
cm².
-·1 -·2 -·3 -·4 -·5 -·6 -·7 -·8 -·9 -1·0 -1·1 -1·2 -1·3 -1·4 -1·5 -1·6 -1·7 -1·8
E vs mercury pool.
Volts.

Graph 7

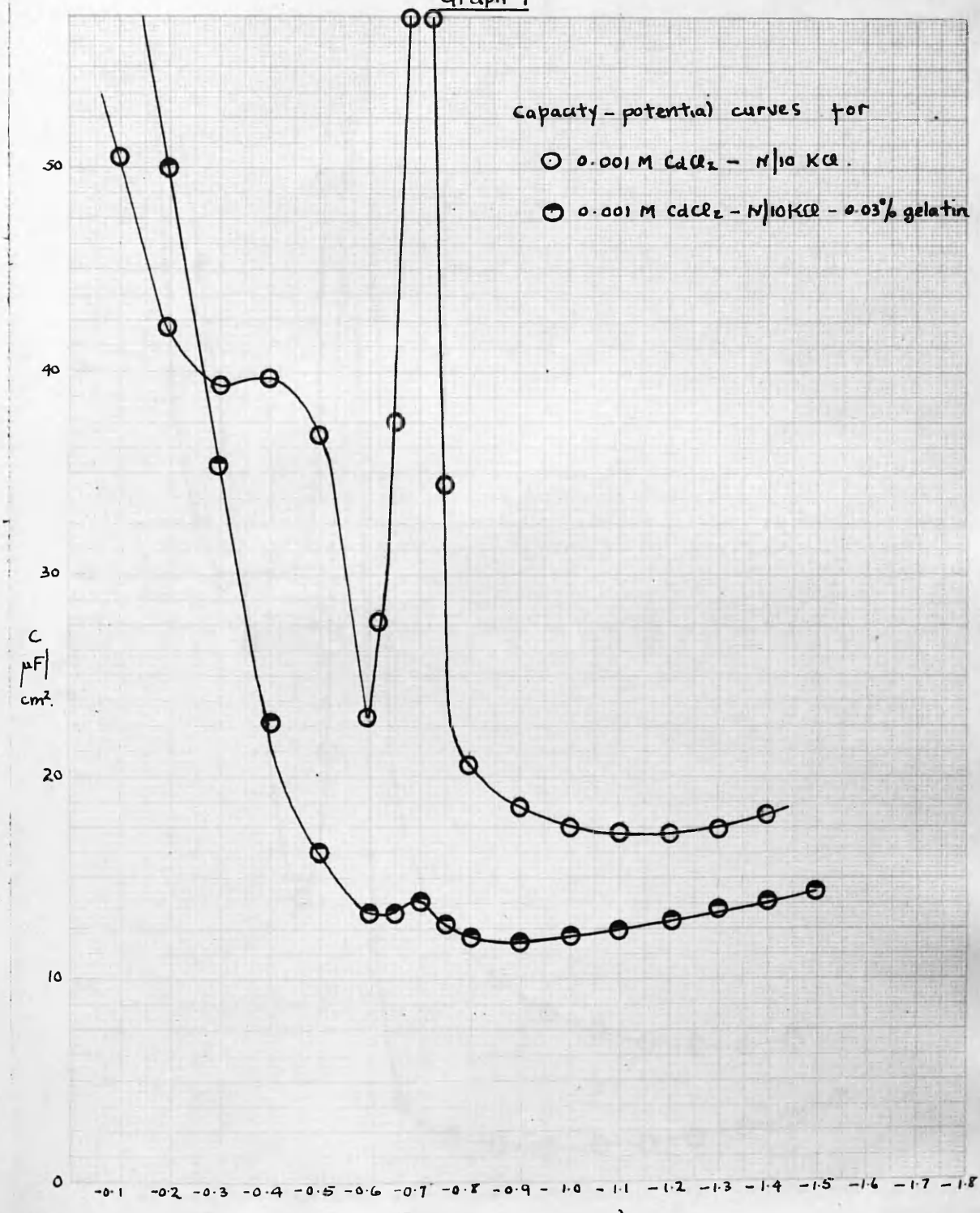
Capacity - potential curves for
⊙ 0.001 M $CdCl_2$ - N/10 KCl.
⊙ 0.001 M $CdCl_2$ - N/10 KCl - 0.03% gelatin
50
40
30
20
10
0
C μF/cm².
-0·1 -0·2 -0·3 -0·4 -0·5 -0·6 -0·7 -0·8 -0·9 -1·0 -1·1 -1·2 -1·3 -1·4 -1·5 -1·6 -1·7 -1·8
E vs. mercury pool.
Volts.

Graph 8

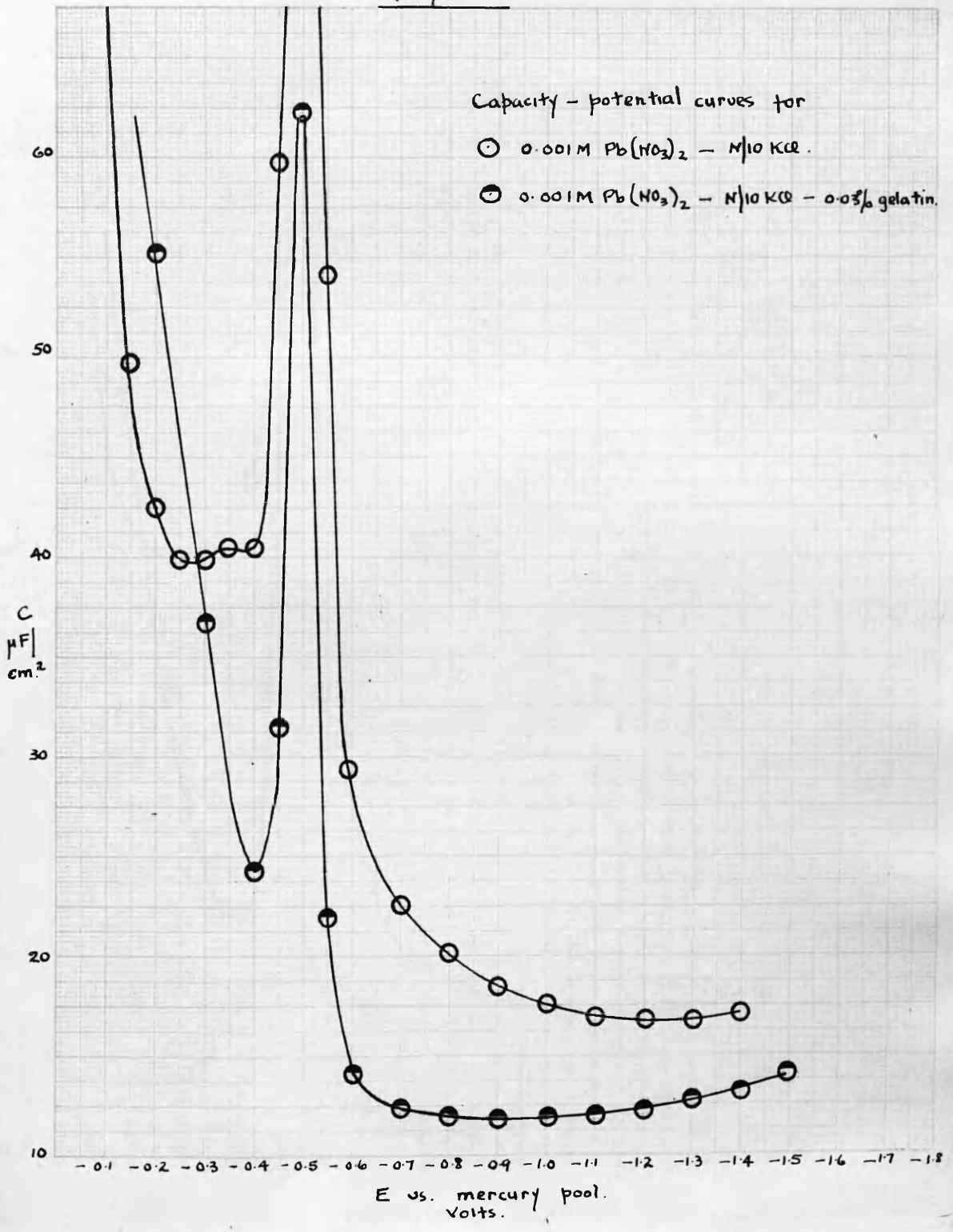
Capacity - potential curves for
0·001 M Pb(NO3)2 — N/10 KCl.
0·001 M Pb(NO3)2 — N/10 KCl — 0·03% gelatin.
60
50
40
30
20
10
C
μF/cm.²
-0·1 -0·2 -0·3 -0·4 -0·5 -0·6 -0·7 -0·8 -0·9 -1·0 -1·1 -1·2 -1·3 -1·4 -1·5 -1·6 -1·7 -1·8
E vs. mercury pool.
Volts.

Graph 9

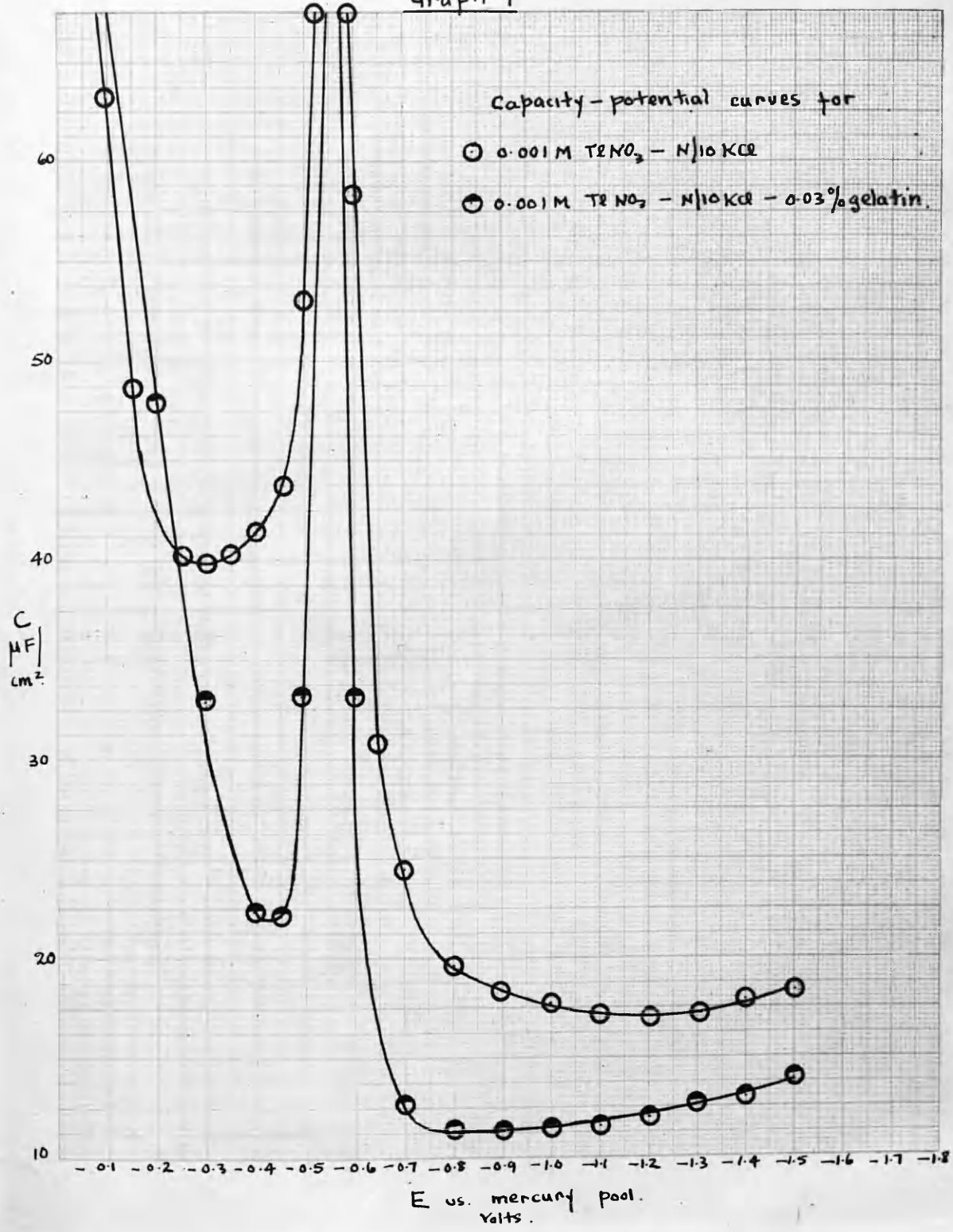
Capacity - potential curves for
⊙ 0·001 M $TlNO_3$ - N/10 KCl
◓ 0·001 M $TlNO_3$ - N/10 KCl - 0·03% gelatin.
60
50
40
30
20
10
C
μF/cm²
- 0·1 - 0·2 - 0·3 - 0·4 - 0·5 - 0·6 - 0·7 - 0·8 - 0·9 - 1·0 - 1·1 - 1·2 - 1·3 - 1·4 - 1·5 - 1·6 - 1·7 - 1·8
E us. mercury pool.
Volts.

Graph 10

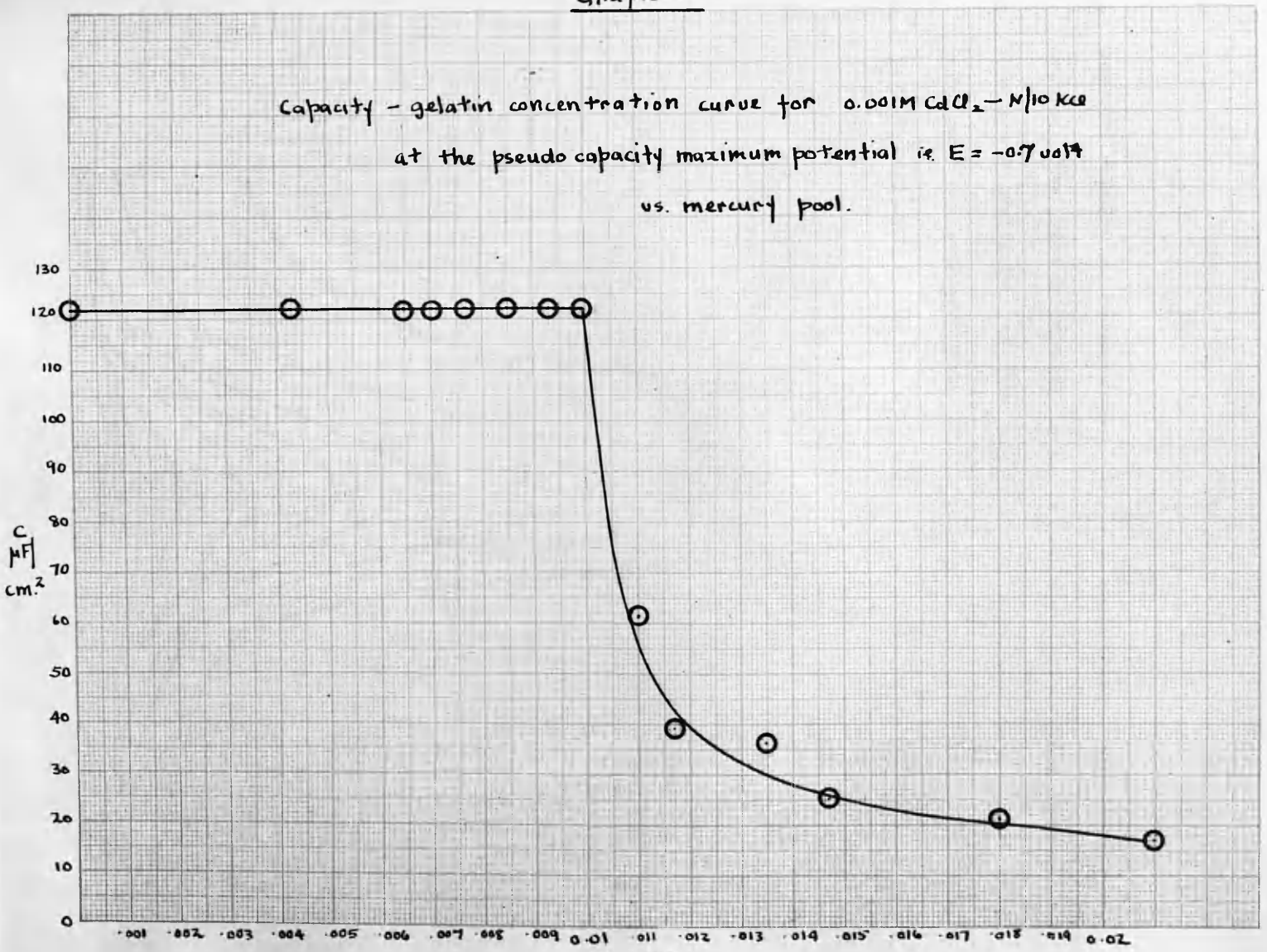
Capacity - gelatin concentration curve for 0.001M $CdCl_2$ — N/10 KCl
at the pseudo capacity maximum potential ie. E = -0.7 volts
vs. mercury pool.
C μF/cm.²
130
120
110
100
90
80
70
60
50
40
30
20
10
0
.001 .002 .003 .004 .005 .006 .007 .008 .009 0.01 .011 .012 .013 .014 .015 .016 .017 .018 .019 0.02
% gelatin

Graph 11

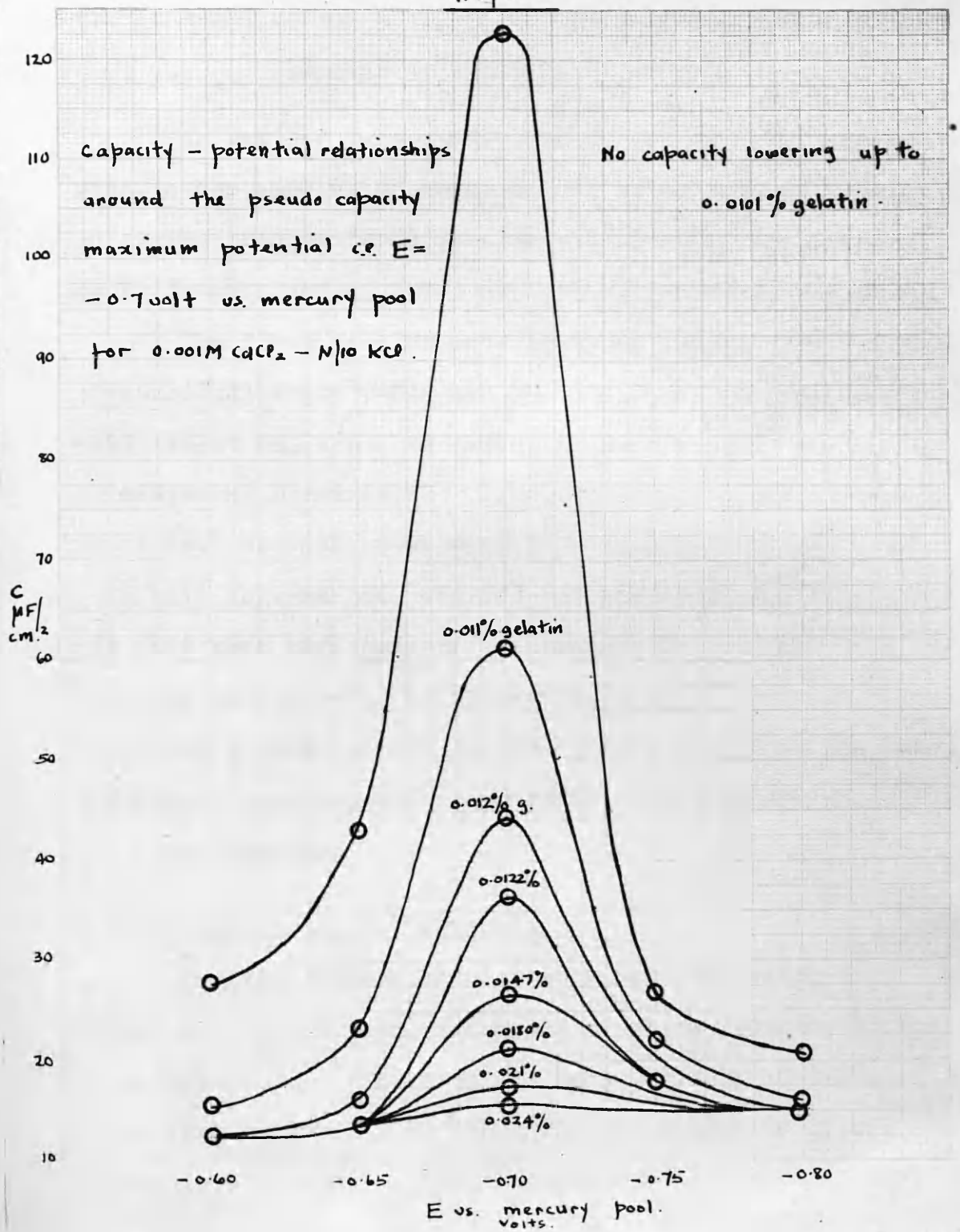
Capacity – potential relationships around the pseudo capacity maximum potential ie. E= −0·7 volt vs. mercury pool for 0·001M CdCl₂ – N/10 KCl.
No capacity lowering up to 0·0101% gelatin.
C μF/cm.²
120
110
100
90
80
70
60
50
40
30
20
10
0·011% gelatin
0·012% g.
0·0122%
0·0147%
0·0180%
0·021%
0·024%
−0·60
−0·65
−0·70
−0·75
−0·80
E vs. mercury pool. volts.

Double layer capacity and electrocapillarity measurements in some non aqueous solvents.

As yet, no systematic data on double layer capacities in non aqueous solvents appear to be available, and so it was thought to be of interest to carry out measurements in such media. The work is presented in two parts.

The first part makes a study of capacity and related electrocapillarity phenomena in a) concentrated sulphuric acid (about 98% w/w), b) anhydrous acetic acid, and c) anhydrous formic acid. Dielectric constant measurements have recently been made in sulphuric acid (53), and both this solvent (54, 55, 56) and anhydrous acetic acid (57, 58) have been used in polarographic studies. Capacity data are therefore of additional interest. The effects of eosin and gelatin on the acetate system have been observed, and pseudo capacity measurements on lead and cadmium salts are also described.

Electrocapillarity measurements.

Surface tension results were obtained using a capillary electrometer, a diagram of which illustrates the essential parts. The cell was made entirely of Pyrex glass with suitable side limbs for the insertion of a reference electrode or the introduction of a mercury pool

anode. Capillaries, drawn in the manner already described, were slightly tapering and had an internal diameter of about 0.06 mm. Cleaning of capillaries was effected by hot chromate solution or by a brief treatment with 50% hydrofluoric acid as recommended by Grahame (59). The mercury head was connected by a short length of polythene tubing to a B 14 quickfit cone which accommodated the capillary and fitted the top of the cell. All flexible connections in the apparatus were made by polythene tubing. A travelling microscope was used to view the capillary which was illuminated by a 24 volt D.C. lamp, the light from which was focussed on the capillary tip by a suitable lens. The direction of incidence of the beam was at right angles to that of capillary observation, and by suitable manipulation of the lamp the mercury thread could be made to appear as a fine line of silver with a sharp point clearly defined against a dark background. When readings were taken, the mercury point was brought to the capillary tip by altering the head of mercury. The latter was controllable by a reservoir clamped to a rack and pinion stand, while oscillation of the mercury in the capillary could be effected by blowing gently through a calcium chloride drying tube connected by a quickfit cone and socket to the open end of the manometer. This facilitated the taking of readings

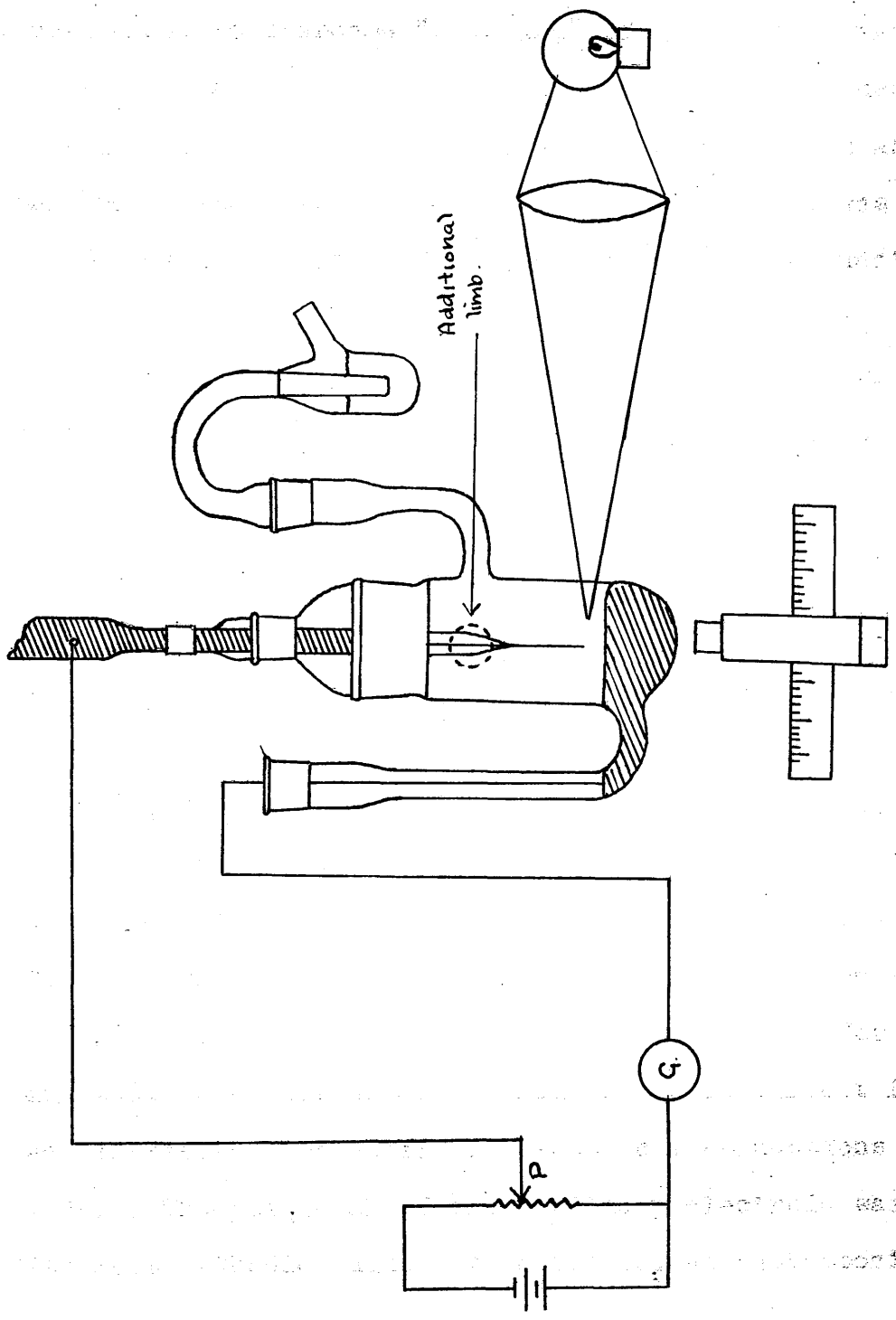

Capillary Electrometer.

and helped to overcome "sticking" of the mercury meniscus (60). A cathetometer, reading to 0.05 mm., was used to measure the mercury head, the height of which was about 40 cms. The potential of the mercury meniscus was adjusted using a student Pye potentiometer in conjunction with a galvanometer of the type already described. The series connection of the latter with the two electrodes was permissible since any current flow was of the order of 1 - 2 μA. The entire apparatus was set up in a room where the temperature was maintained thermostatically at 25±1°C.

General run procedure.

The apparatus was set up as shown, and the mercury head adjusted to about 50 cms. so that mercury was freely expelled from the capillary. A cathetometer reading corresponding to the capillary tip was taken. Solution was then introduced to the cell and the capillary sharply focussed on the microscope with the tip aligned on the cross wire. Tank nitrogen was bubbled through for 10 minutes, to effect deaeration and to reduce current flow, and thereafter the necessary electrical connections were made. The potential of the capillary electrode was set at its most cathodic value within the solvent decomposition range, and the mercury head adjusted to bring the tip of

the mercury thread to the microscope cross wire. A cathetometer reading on the mercury head was then taken. Between readings, the potential was switched to the maximum cathodic setting, thus causing the mercury to flow from the capillary tip which was hence cleared of any adsorbed species liable to cause sticking. The anodic branch of the curve was particularly susceptible to this fault, and in general, sluggish capillary behaviour was more common in non aqueous solutions than in their aqueous counterparts. However, the adoption of the above techniques enabled satisfactory reproducibility to be obtained. When the run had been completed, the solution was sucked from the cell, which was then thoroughly washed before N/10 potassium chloride solution was introduced in situ. The capillary was calibrated by assuming the interfacial tension at the E.C.ap.Max. of N/10 potassium chloride at 25°C to be 426.7 dynes per cm. (61).

Capacity measurements.

The technique was almost exactly similar to that described for aqueous media. However, since accurate capacity values for N/10 potassium chloride were known both from Grahame's data and from those reported here, it was not necessary to determine the mercury mass rate in every

case. At the end of a run, a B 10 quickfit adaptor enabled the experimental solution to be sucked from the cell, which was then thoroughly washed with conductivity water. N/10 potassium chloride solution was finally introduced, and readings taken at selected potentials where the capacity values were most accurately known. The capillary constant was then evaluated. However, mass rates were directly determined for acetic and sulphuric acids, and for a given capillary, little difference from aqueous solutions was observed. In general, capacity readings were somewhat less sensitive than in aqueous systems, but they were again most reproducible on cathodic polarisation. At least two capacity runs were made on each solution and typical results are recorded in the graphs and tables. A mercury pool was used as reference electrode.

Purification of materials.

The sulphuric acid was analar of strength about 98% (w/w), while the 100% sample was prepared by the method of Brand (62). Analar acetic acid was purified and dried as described by Orton and Bradfield (63), who distilled the acid from chromic oxide. A calculated quantity of acetic anhydride was added to accommodate the water produced by the oxidation of impurities by the chromic oxide. From

the melting point of the purified sample (16.50°C) less than 0.05% water was present. Analar formic acid, strength 98 - 100%, was repeatedly distilled from phosphorous pentoxide under reduced pressure until the feeezing point temperature was 8.40°C. Ammonium acetate was purified by recrystallising an analar sample from glacial acetic acid and drying in vacuo over potassium hydroxide. Analar ammonium formate was recrystallised from ethanol, while sodium acetate was recrystallised from conductivity water and dehydrated at 150°C for one week (64). Lead and cadmium acetates were analar samples dehydrated at 110°C for a week (65).

Sulphuric Acid.

The self ionisation of this acid is so extensive that no supporting electrolyte is required. Measurements in this solvent, however, are somewhat restricted by its low decomposition potential, which, for 98.65% acid, is about -0.7 to -0.8 volt. The potential becomes more negative for weaker acids (-0.8 to -0.9 volt for 86.8% H_2SO_4), while for concentrations above 99%, the potential falls off sharply and above about 100% mercury is attacked at room temperature.

Differential capacity as a function of potential for acid of strength about 98% (w/w) is shown in Graph 12.

The associated table records the results. These were reproducible to 0.3 $\mu F/cm^2$. except on extreme anodic polarisation where there was lower sensitivity. Reproducibility here was about 0.5 $\mu F/cm^2$. Although restricted in range, the curve is essentially similar to those obtained in aqueous solutions. At potentials approaching zero, a sharp capacity rise to values greater than 45 $\mu F/cm^2$. was observed, while on more negative polarisation, capacities progressively decreased, until at -0.6 volt a value of about 17 - 18 $\mu F/cm^2$. was obtained. The effect of the addition of small quantities of water was investigated. Although the solvent resistance was markedly lowered by a small increase in water concentration, double layer capacity values were not affected by such an increase. Graph 13 illustrates the electrocapillarity curve, the average of four runs. The curve appears to be normal except that solvent decomposition occurs before the E.Cap.Max. is reached. Graphical differentiation of this curve at intervals of 0.05 volt, giving surface charge density as a function of potential is shown in Graph 14. Although some scatter is evident, an average slope gives a capacity of 18.4 $\mu F/cm^2$., which is in reasonable agreement with the minimum value of about 18 $\mu F/cm^2$. obtained by direct measurement. The relation between surface charge density and potential may be more accurately determined by graphical

integration of the capacity data. The constant of integration is, however, fixed by taking the surface charge density value corresponding to a given potential from the electrocapillary differentiation. Graph 14 also illustrates the result of such an integration at intervals of 0.025 volt taking q = 19.7 μ couls./cm^2. at E = -0.25 volt. A comparison between the two sets of data is thus afforded.

Although the decomposition potential was only about -0.2 volt, a few capacity measurements on 100.29% sulphuric acid were made. These are shown on Graph 12, and although showing the same trends as the more aqueous acid, are nevertheless somewhat higher within the narrow potential range concerned.

Employing the method of Ilkovic (25), Vlcek (55) obtained a value for 92% sulphuric acid of 52.5 μF/cm^2., which is 25% greater than the value determined by Ilkovic for aqueous solutions. On the cathodic limb, the result reported by this method for N/10 potassium chloride solution was 22.6 μF/cm^2. Although,in the results presented here, comparison with aqueous solutions is somewhat difficult because of the aqueous "hump", it is nevertheless clear that at corresponding potentials the sulphuric acid values are lower than their aqueous equivalents. At -0.6 volt the capacity ratio is 1.5/1. Vlcek makes a

comparison of capacity values on the basis of dielectric constant variation. The recently measured value of 110 for anhydrous sulphuric acid would indicate that the value for 98% sulphuric should be not far removed from this and should not be as low as 80, that of pure water. On this basis, acid capacities ought to be higher than those observed in aqueous solution. However, the nature and concentration of the anion exert a profound influence on capacity values and therefore the anodic limb of the curve is perhaps the least suitable for comparison.

Anhydrous acetic acid.

Since the decomposition potential of acetic acid does not occur before -1.8 volt, it was possible to evaluate capacities over the potential range encountered in aqueous measurements. In the first case, ammonium acetate was used as supporting electrolyte, and Graph 15 shows the capacity-potential curve for the system acetic acid - 1 molal ammonium acetate. The resemblance to a typical aqueous curve is evident. The steep anodic rise in capacity due to specific adsorption is followed by a region of minimum capacity and thereafter by the customary cathodic increase due to coulombic distortion of cations. It is perhaps noteworthy that the region of minimum capacitance

at -0.75 volt follows closely on the E.Cap.Max. at -0.65 volt. The minimum value obtained was about 7 $\mu F/cm^2$., which is less than half a typical aqueous capacity. This may in part be attributed to the low dielectric constant of acetic acid, i.e., 6.13, compared with that of water which is about 80. No anodic "hump" in this or in any other non aqueous solvent was observed.

The acetate electro capillarity curve, the average of eight runs, is illustrated in Graph 16. In the case of the acids, reproducibility was not as good as that obtained in later work on alcohols and pyridine. However, since the method of measuring capacities is capable of considerable accuracy, a reliable outline of the electrocapillarity curve was obtained by a double integration of the capacity data. For its absolute determination, a) the E.Cap.Max. and b) a surface tension value at this potential were selected from experimental values. Taking $q = 0$ and $= 393.0$ dynes/cm. at -0.65 volt, a double graphical integration was effected at intervals of 0.025 volt, and the results are shown also on Graph 16. Reasonable agreement between the experimental and calculated values is shown. Bachman and Astle (66) have stated that the electro capillarity curve of ammonium acetate in anhydrous acetic acid differs markedly from the same curve in water

in that two maxima instead of one are present. Such a case, if authenticated, would be of considerable interest to double layer theory, since it implies that the surface charge density on the mercury is zero at two potentials. The data presented here, determined by two techniques, show no such anomalies. Craxford (67) has observed that the drop weight method - that used by Bachman and Astle - involves special difficulties, and that failure to recognise these has, in the past, led to the production of fictitious maxima (68). Surface charge density as a function of potential, derived from a single integration of the capacity data, is shown in Graph 17, while Graph 18 illustrates the results of graphical differentiation of both limbs of the electrocapillarity curve at intervals of 0.05 volt. Average slopes gave values of 9.3 $\mu F/cm^2$. on the cathodic, and 35 $\mu F/cm^2$. on the anodic branches of the curve.

Capacity and electrocapillarity data for the system acetic acid - 0.8 molal sodium acetate are illustrated in Graphs 15 and 16 respectively. This concentration of sodium acetate represents the maximum solubility of the salt in acetic acid. However, since capacity is largely independent of concentration over such a limited range, comparison may be made with the 1 molal

ammonium acetate curve. The general characteristics of the two curves are the same, with each showing a minimum capacity of 6.8 $\mu F/cm^2$. at almost the same potential, i.e., -0.75 volt. Although the effect of cation variation for a given anion on double layer capacity in a non aqueous solvent has been more fully investigated later, nevertheless a comparison of the cathodic values for the two acetate systems reveals that, for a given potential, the ammonium capacity is higher than that of the sodium. In aqueous solutions, these ions show a capacity difference in the same order but of a smaller magnitude than that in evidence here. The acetate capacities were reproducible to about 0.2 $\mu F/cm^2$. at the most sensitive part, i.e., on the cathodic branch of the curve. The effect of the addition of small quantities of water to the acetate systems was also examined. Again, although the solution resistance was considerably reduced, no significant capacity change was observed.

Pseudo capacity effects shown by cadmium and lead acetates are illustrated in Graph 19. As in aqueous solutions, thermodynamic reversibility is in evidence, but for the same ionic concentration, i.e., 0.001 M, the maximum capacity for cadmium is less than one quarter while that for lead is about one fifth the value in aqueous

solution. The half wave potentials corresponding to these peak capacities are also of course different from their aqueous equivalents.

	$E_{1/2}$ v. S.C.E. volts.	Pseudo Capacity Max. v mercury pool. volts
Cd	1NKCl -0.642	1M $NH_4\bar{A}c$ -0.825
Pb	1N KCl -0.435	1M $NH_4\bar{A}c$ -0.570

The effects of 0.05% gelatin and of 0.014% eosin on acetate capacities are indicated in Graph 20. Although the eosin concentration was the same as that used in aqueous solution, the corresponding gelatin concentration, i.e., 0.25%, caused erratic capillary behaviour. The actual concentration used was only one fifth of this value: nevertheless an overall flattening and depression of the capacity values was obtained. This behaviour is analogous to that observed in aqueous media, and again indicates adsorption over a wide potential range. Eosin also shows similar effects to those found in water. Capacity depression is confined largely to the anodic branch of the curve, and in both solvents the value is reduced to about 9 $\mu F/cm^2$. The small desorption peak is again in evidence, but in acetic acid it occurs at -0.8 volt

compared with -1.25 volt in water.

Anhydrous formic acid.

The decomposition potential for pure formic acid is about -1.3 volt, and capacity measurements therefore were made within the potential range 0 to -1.3 volt. The supporting electrolyte was ammonium formate and Graph 21 shows the capacity-potential curve for a 1 molal solution of this salt. The general shape of the curve is somewhat different from that previously encountered in that there is an approximate symmetry between the anodic and cathodic branches. A minimum value of about 11 $\mu F/cm^2$. was observed at approximately -0.9 volt, and thereafter the cathodic values rose steeply to 17 $\mu F/cm^2$. at -1.3 volt. On the basis of dielectric constant variation, 6.3 for acetic acid and 57 for formic acid, the higher values in the latter medium are to be expected. For 1 molal formate, the solution resistance was relatively low (3,500 Ω for acetate and 100 Ω for formate), and it was found that, for a given setting of R_3, the bridge balanced over a fairly wide range of C_3 settings. For each setting of C_3 however, birth-balance time altered accordingly, and recorded capacities for a given potential were substantially constant. This is illustrated in Table 21. In order to revert to the usual system of balance and to observe

capacity behaviour with varying concentration of supporting electrolyte, capacities were measured using 0.1 molal formate as supporting electrolyte. The results are recorded on Graph 21 also. The bridge behaviour was now normal. The values of capacity were substantially lower than those observed with the higher formate concentration, the minimum being about 9.5 $\mu F/cm^2$. at -0.95 volt. This is in keeping with aqueous behaviour, where a decrease in the supporting electrolyte concentration is also associated with capacity diminution. Graph 17 gives surface charge density as a function of potential for the 0.1 molal formate system - the result of a single graphical integration of capacity data at 0.025 volt intervals taking $q = 0$ at -0.75 volt. Graph 22 compares the experimental with the calculated electrocapillarity curve obtained by further integration taking $\sigma = 401.01$ dynes/cm. at -0.75 volt. The result of graphical differentiation of the cathodic limb of the electrocapillarity curve at intervals of 0.05 volt giving an average capacity of 10.9 $\mu F/cm^2$. is shown in Graph 18. As in previous systems, small traces of water had no effect upon capacity measurements. Reproducibility for formic acid was about 0.1 $\mu F/cm^2$. except on extremes of anodic or cathodic polarisation. The values here reported are considerably lower than those found by

Bowden and Grew (69) who give 67 $\mu F/cm^2$. as the capacity for pure formic acid.

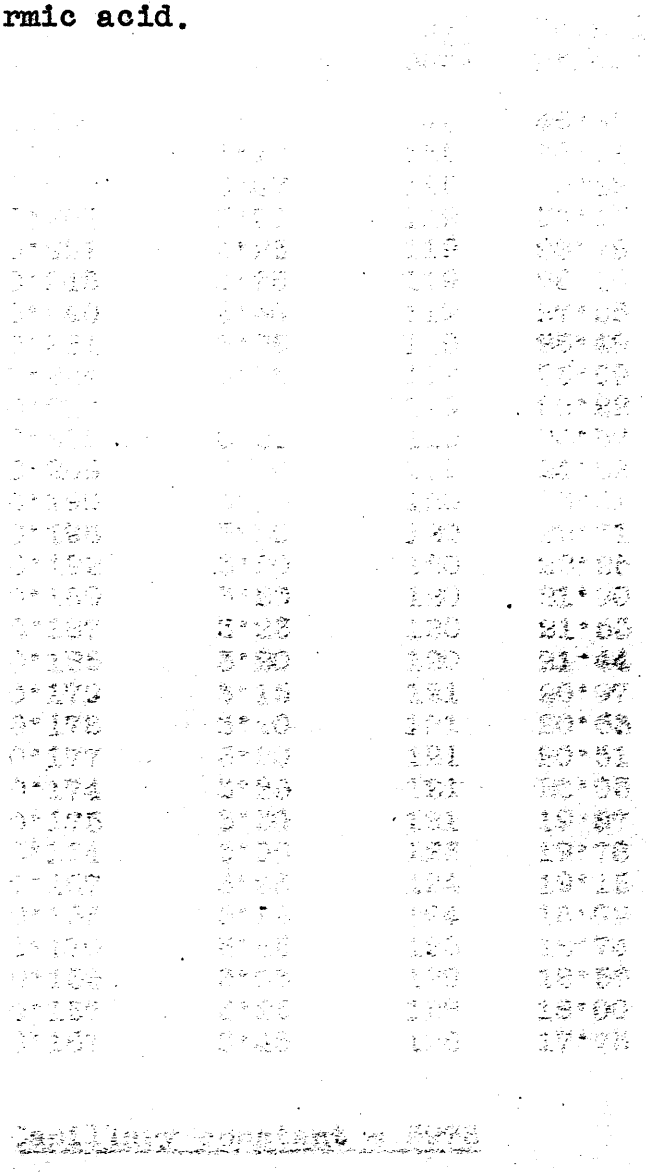

Table 12

Capacity data for 98% (W/W) sulphuric acid mercury pool reference electrode

Potential volts. -ve	C_3 μFs.	t seconds	R_3 ohms.	Capacity $\mu F/cm^2$
0·02	0·400	3·20	145	46·35
0·04	0·310	3·10	135	36·71
0·06	0·260	2·87	125	32·42
0·08	0·262	3·25	119	30·04
0·10	0·251	3·25	119	28·78
0·12	0·245	3·25	119	28·10
0·14	0·240	3·30	119	27·25
0·16	0·231	3·25	119	26·49
0·18	0·224	3·25	119	25·69
0·20	0·213	3·10	119	25·22
0·22	0·212	3·20	119	24·57
0·24	0·209	3·20	119	24·22
0·26	0·199	3·15	120	23·31
0·28	0·196	3·20	120	22·71
0·30	0·192	3·20	120	22·25
0·32	0·189	3·20	120	21·90
0·34	0·187	3·23	120	21·53
0·36	0·185	3·20	120	21·44
0·38	0·179	3·15	121	20·97
0·40	0·178	3·20	121	20·63
0·42	0·177	3·20	121	20·51
0·44	0·174	3·23	121	20·03
0·46	0·175	3·30	121	19·87
0·48	0·164	3·08	123	19·78
0·50	0·167	3·25	124	19·15
0·52	0·165	3·25	124	18·92
0·54	0·170	3·45	128	18·74
0·56	0·155	3·05	128	18·56
0·58	0·157	3·25	128	18·00
0·60	0·161	3·45	128	17·75

Capillary constant = 3973

Table 13

Electrocapillarity data for 98% (w/w) sulphuric acid

mercury pool reference electrode

Potential volts -ve	A dynes/cm.	B dynes/cm.	C dynes/cm.	D dynes/cm.	Average
0	218·9	222·2	223·0	222·6	221·7
0·05	230·2	235·1	233·6	237·8	234·2
0·10	243·0	243·8	251·4	247·3	246·4
0·15	255·9	258·7	262·7	259·8	259·3
0·20	266·4	269·8	273·5	270·1	270·0
0·25	277·6	274·8	282·2	281·0	278·9
0·30	287·6	287·9	292·8	289·8	289·5
0·35	296·2	297·2	301·9	299·2	299·1
0·40	305·2	307·9	311·0	307·9	308·0
0·45	314·2	317·7	315·9	316·4	316·1
0·50	320·4	326·2	324·7	323·8	323·8
0·55	329·2	---	334·8	331·3	331·8

Table 15

Capacity data for A:- 1 molal ammonium acetate - acetic acid

B:- 0·8 molal sodium acetate - acetic acid

Potential volts -ve	Capacity $\mu F/cm^2$ A	Capacity $\mu F/cm^2$ B
0·10	89·7	45·66
0·20	50·5	33·57
0·30	40·23	28·90
0·40	31·81	24·92
0·50	22·22	18·14
0·60	11·83	10·76
0·70	7·19	7·21
0·725	7·01	6·91
0·750	6·84	6·81
0·775	6·84	6·81
0·80	7·21	6·81
0·85	7·37	7·11
0·90	7·75	7·41
1·00	8·45	7·70
1·10	9·15	8·00
1·20	9·95	8·20
1·30	10·83	8·21
1·40	11·99	8·40
1·50	13·25	8·69
1·60	15·00	9·28
1·70	18·07	10·46
1·80	24·89	12·04
1·05	8·80	7·90
1·15	9·59	8·10
1·25	10·30	8·11
1·35	11·27	8·30
1·45	12·62	8·50
1·55	14·05	8·89
1·65	16·08	9·67
1·75	21·15	11·25

TABLE 16

Electrocapillarity data for 1 molal ammonium acetate and 0·8 molal sodium acetate - acetic acid. Mercury pool electrode.

A and B :- typical runs for the ammonium acetate system.
C :- average of eight runs for above.
D :- results of graphical integration of capacity data.
E :- results for the sodium acetate system.

Potential volts -ve	A Dynes/cm	B Dynes/cm	C Dynes/cm	D Dynes/cm	E Dynes/cm
0	341·1	--	353·0	--	--
0·05	352·2	--	356·4	--	--
0·10	362·4	360·9	364·0	--	350·4
0·15	367·5	366·0	369·1	--	357·1
0·20	374·2	370·2	373·9	372·9	361·0
0·25	375·7	372·3	376·8	378·3	364·5
0·30	379·6	380·8	382·2	382·7	369·6
0·35	383·9	385·3	385·7	386·1	375·3
0·40	386·7	388·3	388·3	388·7	379·4
0·45	392·1	389·3	390·7	390·5	383·0
0·50	392·7	391·4	391·5	391·7	385·9
0·55	392.9	392·8	392·1	392·5	387·5
0·60	394·7	393·5	393·3	392·9	388·4
0·65	394·9	393·9	393·5	393·0	388·7
0·70	394·4	393·7	393·0	392·1	389·3
0·75	395·5	392·9	393·1	392·6	388·9
0·80	394.1	394·0	393·1	392·2	388·7
0·85	393·3	392·1	391·5	391·5	388·1
0·90	393·9	391·4	391·2	390·7	387·1
0·95	392·5	391·3	390·2	389·7	386·0
1·00	391·7	389·9	388·5	388·5	384·6
1·05	390·7	387·5	386·8	387·1	383·2
1·10	388·2	384·8	384·4	385·4	381·3
1·15	387·3	383·9	383·4	383·6	389·5
1·20	385.0	380·8	380·7	381·4	387·2
1·25	381·2	378·2	377·7	379·0	384·9
1·30	380·0	375·8	375·4	376·4	382·5
1·35	376·4	372·1	371·8	373·5	369·7
1·40	374·2	368·5	368·8	370·3	366·5
1·45	369·5	364·9	364·5	366·8	363·4
1·50	365·9	358·7	359·7	362·9	359·7

TABLE 17

Surface charge density data obtained from integration of capacity values for

A :- 1 molal ammonium acetate - acetic acid.

B :- 0.1 molal ammonium formate - formic acid.

Potential -ve volts	A Surface charge density μ couls./cm^2.	B Surface charge density μ couls./cm^2.
0.10	-	+10.91
0.15	-	9.63
0.20	+12.20	8.44
0.25	9.84	7.34
0.30	7.78	6.32
0.35	5.98	5.38
0.40	4.42	4.52
0.45	3.09	3.72
0.50	2.01	3.00
0.55	1.13	2.31
0.60	0.49	1.68
0.65	0	1.08
0.70	- 0.39	0.53
0.75	0.74	0
0.80	1.08	- 0.50
0.85	1.44	1.00
0.90	1.82	1.46
0.95	2.22	1.94
1.00	2.64	2.41
1.05	3.08	2.90
1.10	3.54	3.41
1.15	4.01	3.96
1.20	4.52	4.53
1.25	5.03	5.16
1.30	5.57	5.40
1.35	6.14	-
1.40	6.73	-
1.45	7.35	-
1.50	8.01	-
1.55	8.71	-
1.60	9.46	-
1.65	10.28	-
1.70	11.17	-
1.75	12.18	-
1.80	13.35	-

TABLE 21

Capacity data for A :- 1 molal ammonium formate - formic acid

B :- 0·1 molal ammonium formate - formic acid

mercury pool reference electrode.

Potential volts -ve	A C_3 μFs	t seconds	Capacity μF/cm²	B Potential volts -ve	Capacity μF/cm²
0·10	0·280	2·65	32·33	0·100	29·83
	0·320	3·15	32·92	0·125	26·64
	0·350	3·75	32·08	0·150	25·86
0·20	0·220	2·60	25·72	0·175	24·69
	0·250	3·20	25·45	0·200	23·70
	0·280	3·78	25·53	0·225	22·74
0·30	0·200	3·00	21·26	0·250	21·66
	0·180	2·57	21·21	0·275	21·05
	0·220	3·45	21·30	0·300	19·95
0·40	0·150	2·40	18·50	0·325	18·90
	0·180	3·25	18·13	0·350	18·03
	0·200	3,68	18·56	0·375	17·48
0·50	0·170	3·68	15·78	0·400	16·72
	0·140	2·65	16·16	0·425	15·93
	0·150	3·00	15·94	0·450	15·39
0·60	0·150	3·45	14·52	0·475	14·81
	0·130	3·00	13·82	0·500	14·32
	0·170	4·30	14·21	0·525	13·71
0·70	0·130	3·43	12·63	0·550	13·19
	0·100	2·20	13·07	0·600	12·32
	0·150	4·10	12·94	0·625	11·84
0·80	0·100	2·50	12·00	0·650	11·55
	0·110	2·95	11·83	0·675	11·28
	0·130	3,70	12·02	0·700	10·90
0·90	0·110	3·05	11·56	0·725	10·61
	0·140	4·38	11·56	0·750	10·42
	0·100	2·68	11·25	0·775	10·13
1·00	0·100	2·60	11·69	0·800	9·85
	0·130	3·82	11·77	0·825	9·75
	0·110	3·05	11·56	0·850	9·65
1·10	0·100	2·30	12·68	0·875	9·46
	0·140	3·85	12·61	0·900	9·36
	0·120	2·95	12·90	0·925	9·27
1·20	0·140	3·10	14·56	0·950	9·27
	0·170	4·15	14·55	0·975	9·35
	0·150	3·55	14·25	1·000	9·34
1·30	0·150	2·70	17·09	1·100	10·46
	0·170	3·20	17·30	1·200	11·61
	0·180	3·60	16·95	1·300	13·53

Capillary constant = 4495

TABLE 22

Electrocapillarity data for 0·1 molal ammonium formate - formic acid.

A :- experimental value.

B :- from integration of capacity data.

Potential volts -ve	A Dynes/cm	B Dynes/cm
0·10	368·4	371·4
0·15	369·6	376·5
0·20	378·8	381·1
0·25	382·6	385·0
0·30	387·2	388·4
0·35	389·8	391·3
0·40	392·3	393·8
0·45	394·9	395·8
0·50	396·6	397·5
0·55	397·9	398·8
0·60	399·4	399·8
0·65	400·3	400·5
0·70	400·9	400·9
0·75	401·0	401·0
0·80	400·9	400·9
0·85	400·6	400·5
0·90	399·9	399·9
0·95	399·4	399·1
1·00	397·9	397·9
1·05	396·4	396·7
1·10	394·7	395·1
1·15	392·8	393·3
1·20	390·6	391·2
1·25	387·9	388·8
1·30	385·0	--
1·35	381·4	--

Graph 12

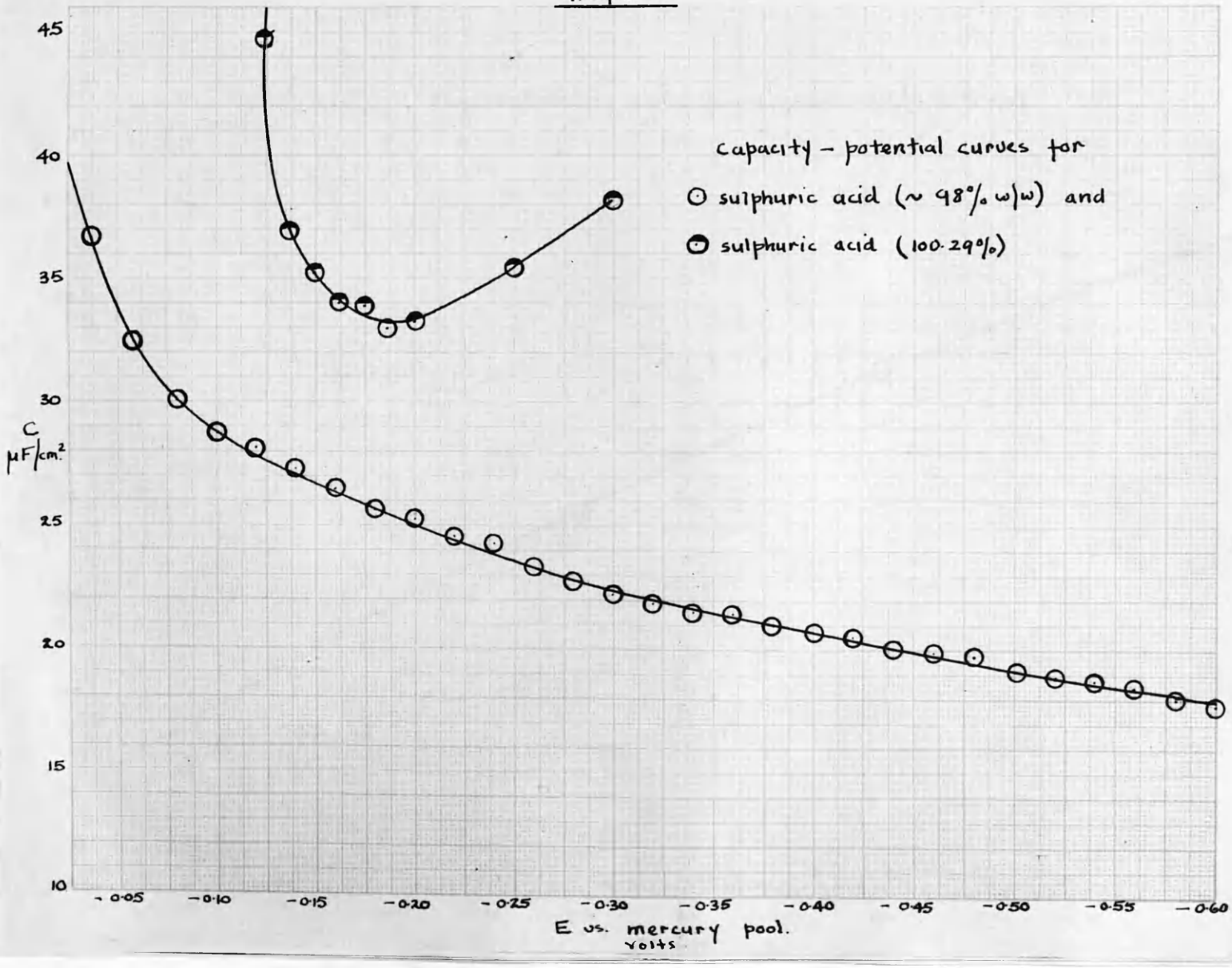
capacity – potential curves for
sulphuric acid (~ 98% w/w) and
sulphuric acid (100.29%)
C
μF/cm²
45
40
35
30
25
20
15
10
-0.05
-0.10
-0.15
-0.20
-0.25
-0.30
-0.35
-0.40
-0.45
-0.50
-0.55
-0.60
E vs. mercury pool.
volts

Graph 13

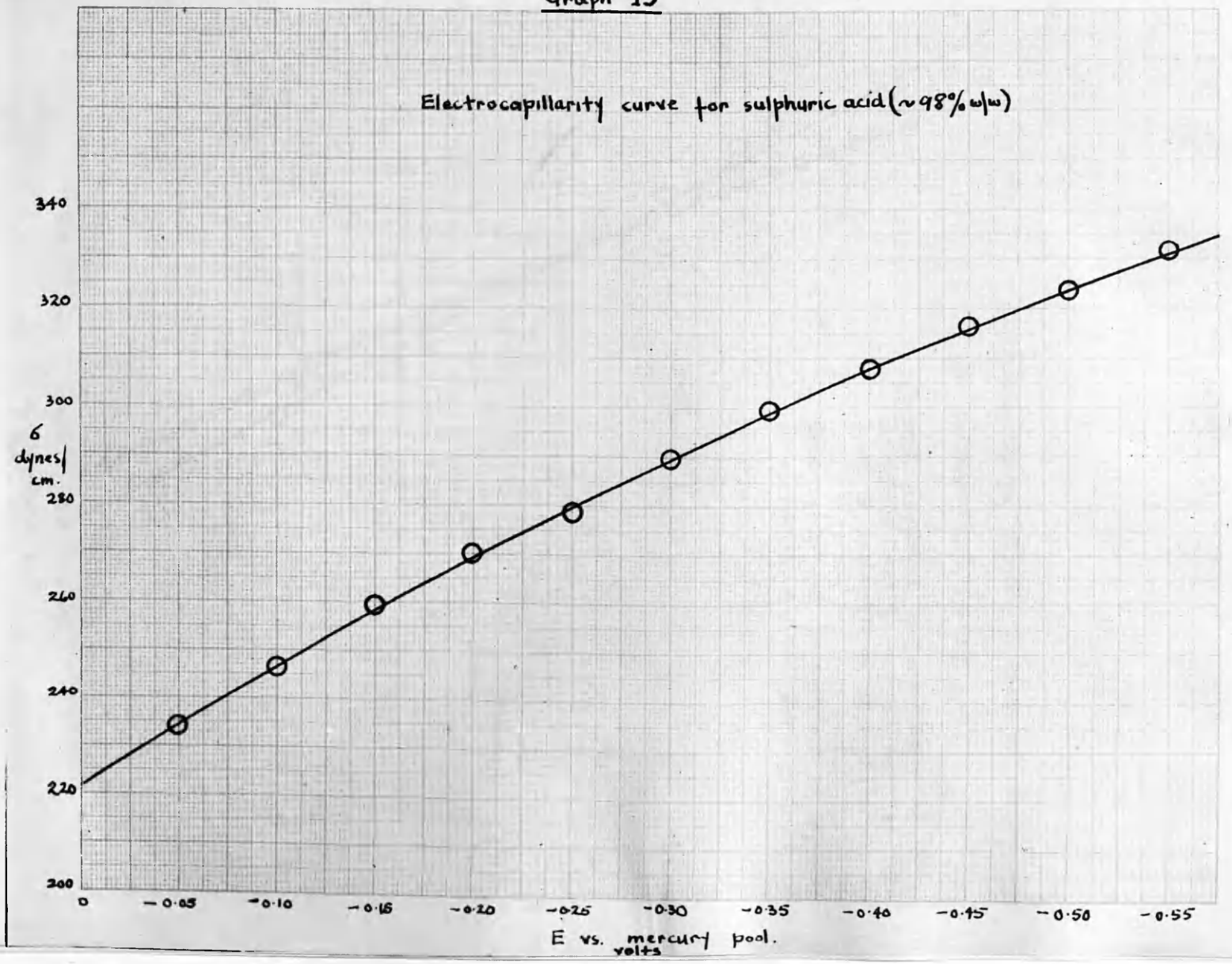
Electrocapillarity curve for sulphuric acid (~98% w/w)
340
320
300
280
260
240
220
200
γ dynes/cm.
0
−0·05
−0·10
−0·15
−0·20
−0·25
−0·30
−0·35
−0·40
−0·45
−0·50
−0·55
E vs. mercury pool. volts

Graph 14

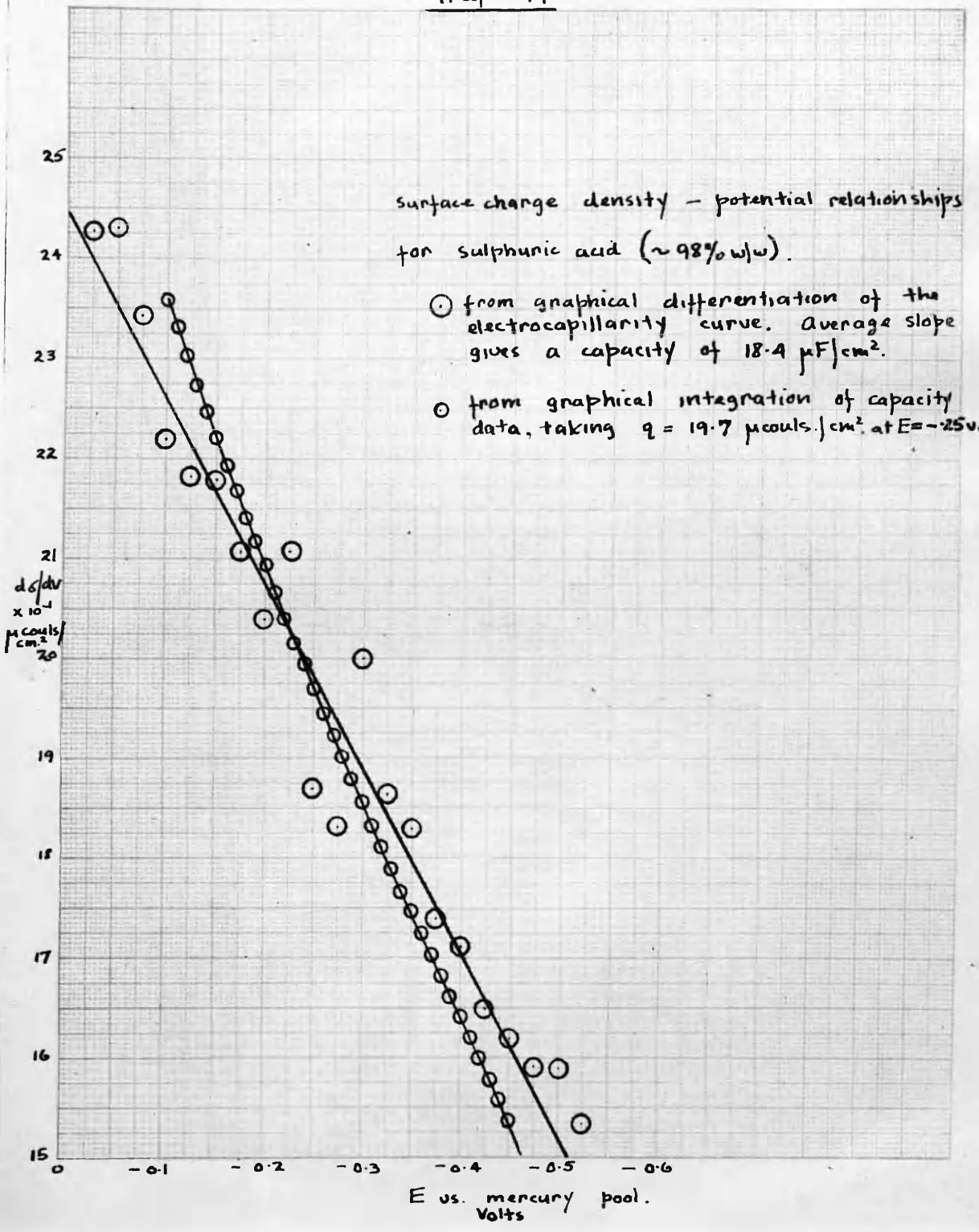

Surface charge density – potential relationships for sulphuric acid (~98% w/w).

⊙ from graphical differentiation of the electrocapillarity curve. Average slope gives a capacity of 18·4 μF/cm².

⊙ from graphical integration of capacity data, taking q = 19·7 μcouls./cm². at E = -·25v.

Graph 15

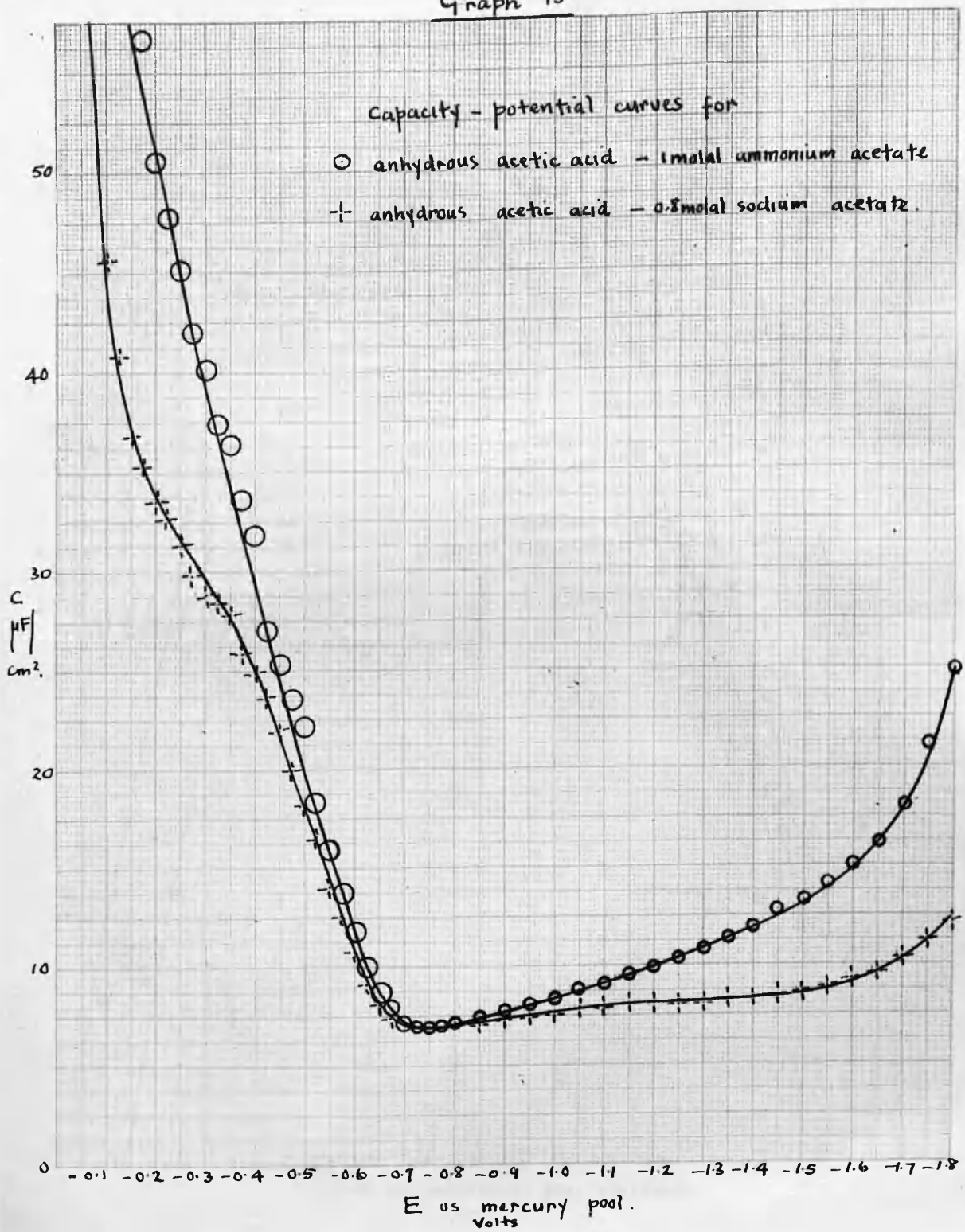
Capacity - potential curves for
○ anhydrous acetic acid – 1molal ammonium acetate
-|- anhydrous acetic acid – 0.8molal sodium acetate.
C μF/cm².
50
40
30
20
10
0
-0·1 -0·2 -0·3 -0·4 -0·5 -0·6 -0·7 -0·8 -0·9 -1·0 -1·1 -1·2 -1·3 -1·4 -1·5 -1·6 -1·7 -1·8
E vs mercury pool.
Volts

Graph 16

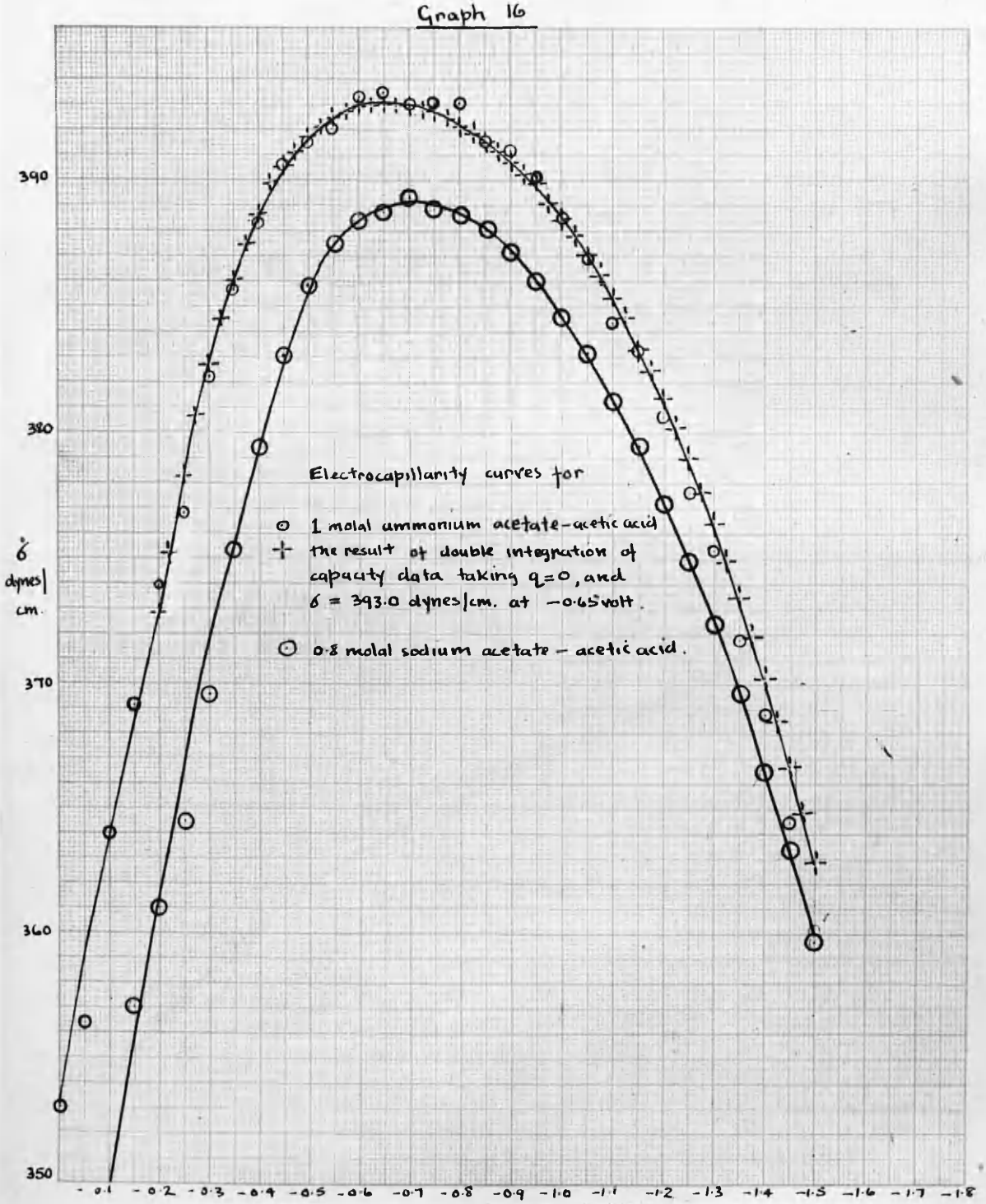
390
380
370
360
350
δ
dynes/
cm.
Electrocapillarity curves for
⊙ 1 molal ammonium acetate-acetic acid
+ the result of double integration of capacity data taking q=0, and δ = 393.0 dynes/cm. at −0.65 volt.
⊙ 0.8 molal sodium acetate – acetic acid.
-0.1 -0.2 -0.3 -0.4 -0.5 -0.6 -0.7 -0.8 -0.9 -1.0 -1.1 -1.2 -1.3 -1.4 -1.5 -1.6 -1.7 -1.8
E vs. mercury pool electrode
Volts.

Graph 17

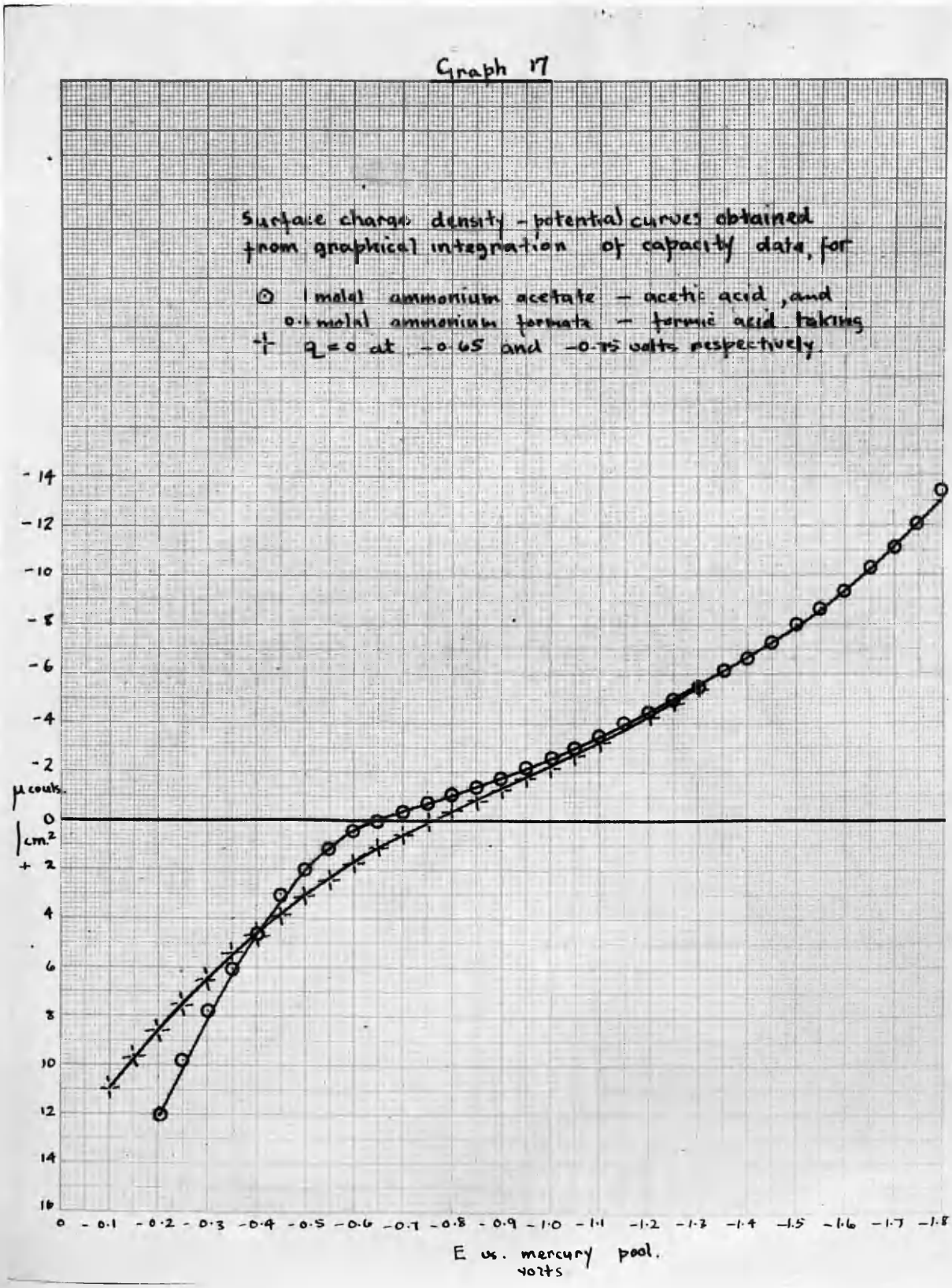
Surface charge density - potential curves obtained from graphical integration of capacity data, for
⊙ 1 molal ammonium acetate – acetic acid, and 0·1 molal ammonium formate – formic acid taking
+ q = 0 at −0·65 and −0·75 volts respectively.
−14
−12
−10
−8
−6
−4
−2
μ coulo.
0
/cm²
+2
4
6
8
10
12
14
16
0 −0·1 −0·2 −0·3 −0·4 −0·5 −0·6 −0·7 −0·8 −0·9 −1·0 −1·1 −1·2 −1·3 −1·4 −1·5 −1·6 −1·7 −1·8
E vs. mercury pool.
volts

Graph 18

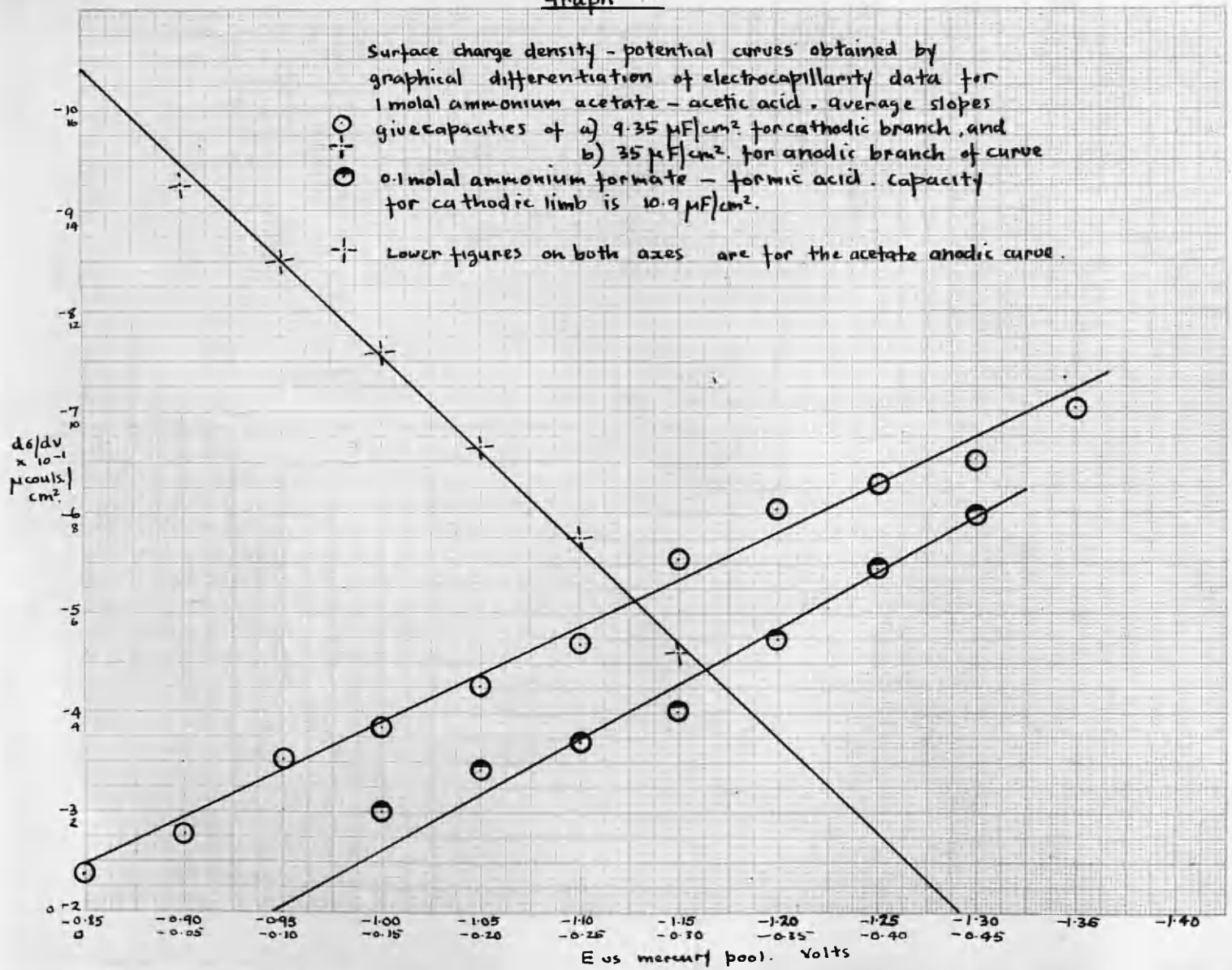
Surface charge density - potential curves obtained by graphical differentiation of electrocapillarity data for 1 molal ammonium acetate – acetic acid. average slopes give capacities of a) 9.35 μF/cm² for cathodic branch, and b) 35 μF/cm². for anodic branch of curve
0.1 molal ammonium formate – formic acid. capacity for cathodic limb is 10.9 μF/cm².
Lower figures on both axes are for the acetate anodic curve.
dσ/dV x 10⁻¹ μcouls./cm²
E vs mercury pool. Volts

Graph 19

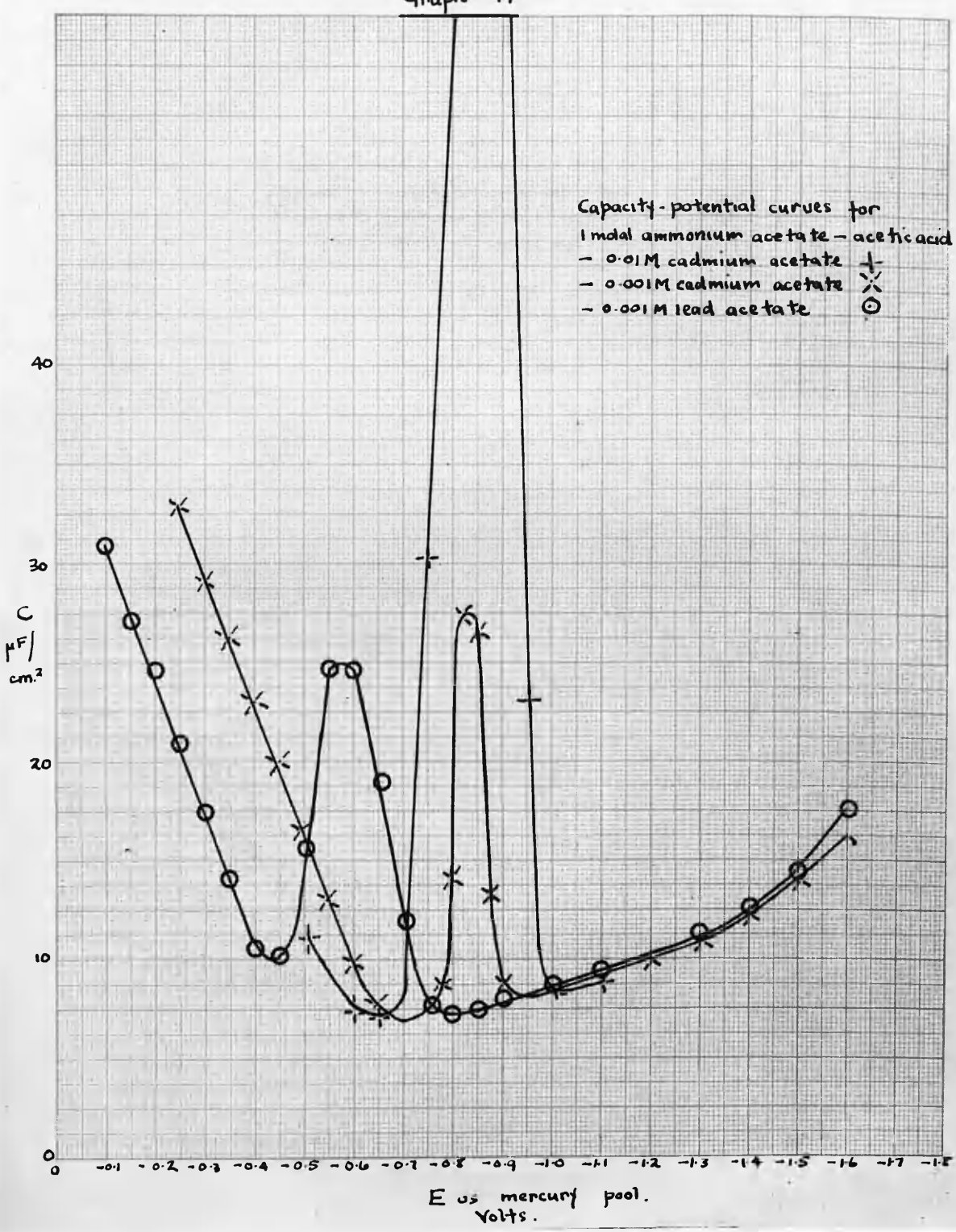
Capacity-potential curves for
1 molal ammonium acetate – acetic acid
– 0·01 M cadmium acetate
– 0·001 M cadmium acetate
– 0·001 M lead acetate
C μF/cm.²
40
30
20
10
0
0 -0·1 -0·2 -0·3 -0·4 -0·5 -0·6 -0·7 -0·8 -0·9 -1·0 -1·1 -1·2 -1·3 -1·4 -1·5 -1·6 -1·7 -1·8
E vs mercury pool.
Volts.

Graph 20

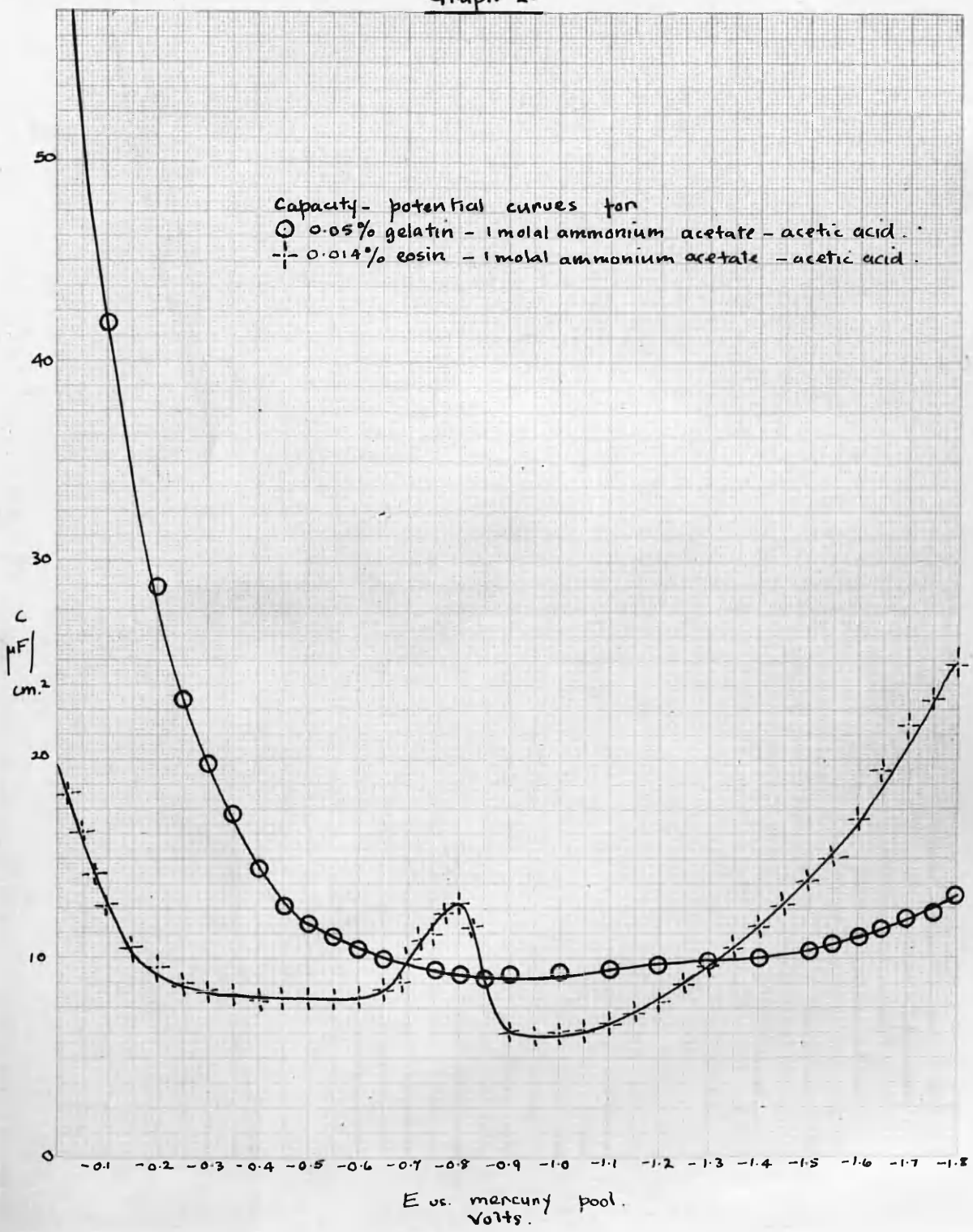
Capacity - potential curves for
⊙ 0.05% gelatin - 1 molal ammonium acetate - acetic acid.
-|- 0.014% eosin - 1 molal ammonium acetate - acetic acid.
C
μF
cm.²
50
40
30
20
10
0
-0.1 -0.2 -0.3 -0.4 -0.5 -0.6 -0.7 -0.8 -0.9 -1.0 -1.1 -1.2 -1.3 -1.4 -1.5 -1.6 -1.7 -1.8
E vs. mercury pool.
Volts.

Graph 21

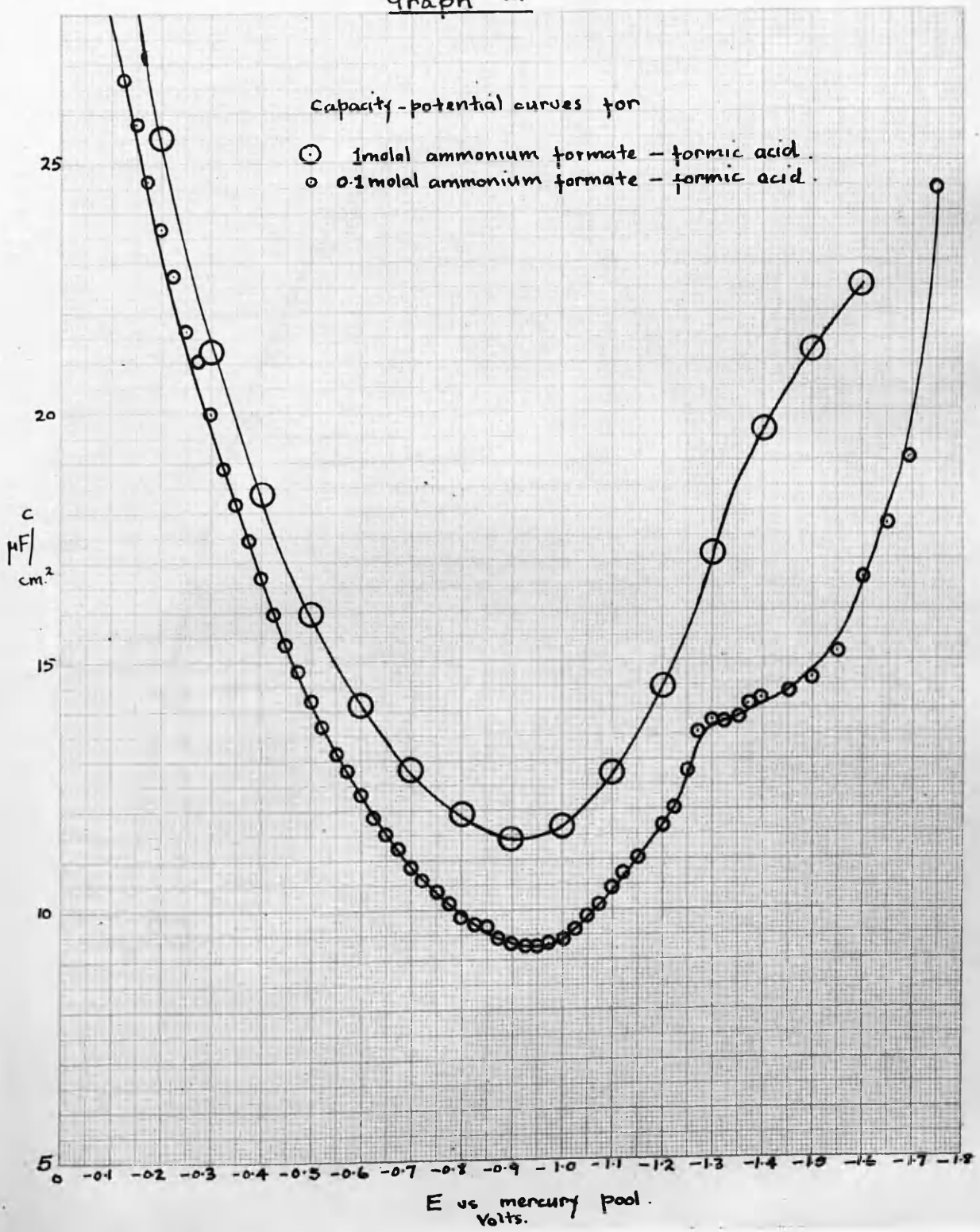
Capacity-potential curves for
1molal ammonium formate – formic acid.
0·1molal ammonium formate – formic acid.
C μF/cm.²
25
20
15
10
5
0 -0·1 -0·2 -0·3 -0·4 -0·5 -0·6 -0·7 -0·8 -0·9 -1·0 -1·1 -1·2 -1·3 -1·4 -1·5 -1·6 -1·7 -1·8
E vs mercury pool. Volts.

Graph 22

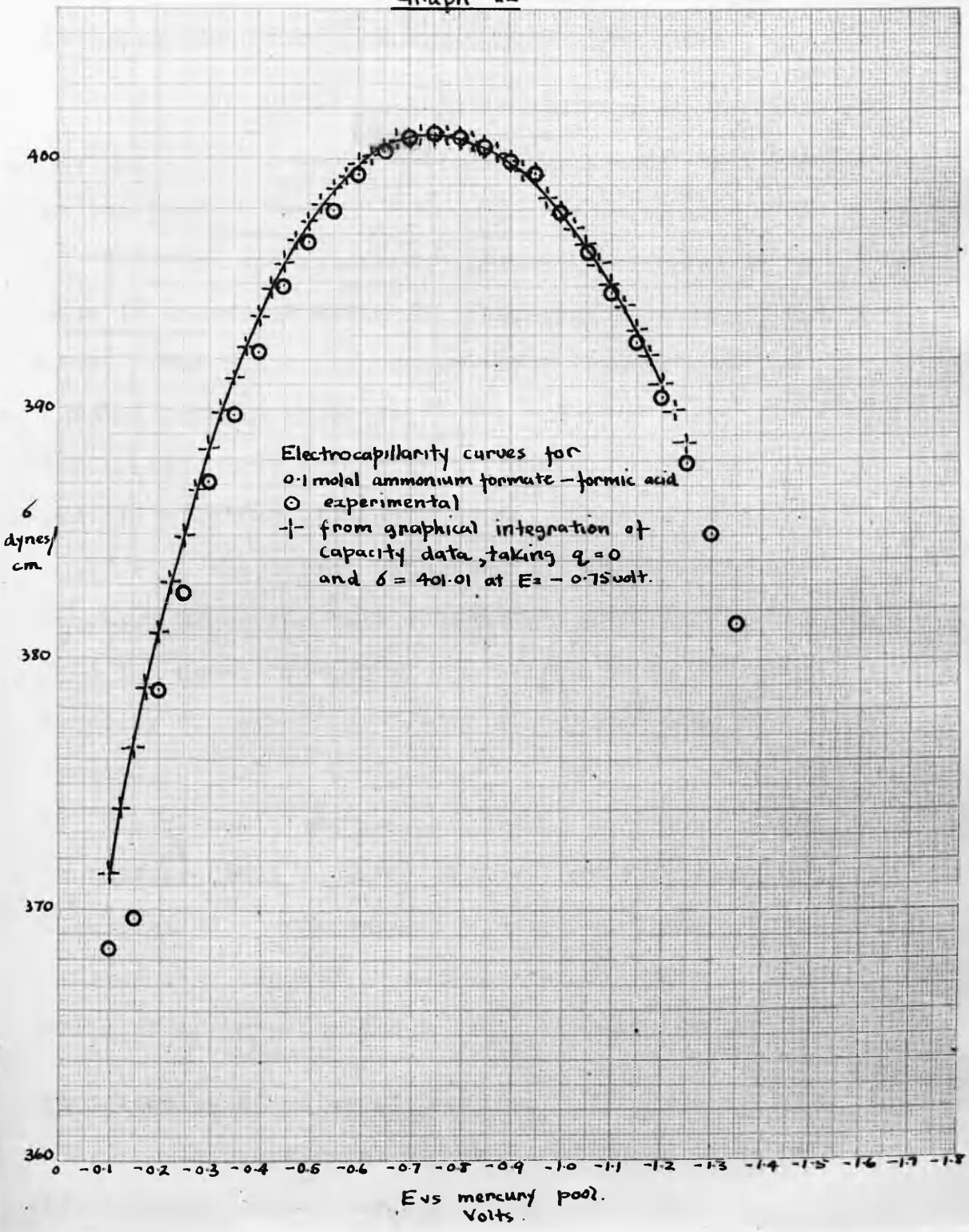
400
390
380
370
360
δ
dynes/
cm
Electrocapillarity curves for
0·1 molal ammonium formate – formic acid
⊙ experimental
-|- from graphical integration of
capacity data, taking q = 0
and δ = 401·01 at E = – 0·75 volt.
0
-0·1
-0·2
-0·3
-0·4
-0·5
-0·6
-0·7
-0·8
-0·9
-1·0
-1·1
-1·2
-1·3
-1·4
-1·5
-1·6
-1·7
-1·8
E vs mercury pool.
Volts.

Further measurements in non aqueous solvents.

The second section of the work on capacity behaviour in non aqueous solvents has itself been undertaken in two parts.

a). Capacity and electrocapillarity measurements have been made in anhydrous methanol, ethanol, n-propanol, and pyridine. The supporting electrolyte was, in all cases, 1 molal lithium chloride. The capacity curves have been integrated, thus affording i) surface charge density data, and ii) electrocapillarity curves, which have been compared with the direct experimental determinations. Further, since the same concentration of supporting electrolyte was used throughout, the effect on double layer capacity of solvent variation has at the same time been studied.

b). The effect of cation variation for a given anion on the differential capacity of the double layer has been investigated. The solvent was methanol and the salts, anhydrous lithium, sodium and potassium iodides. Electrocapillarity data for these salts are also reported.

Purification of materials.

A.R. methanol was refluxed for 6 hours with furfural and 10% sodium hydroxide to remove acetone. It was

then fractionated and subjected to further purification and drying by the method of Lund and Bjerrum (70), i.e., it was refluxed for ½ hour with iodine activated magnesium, distilled off, and finally fractionated from an efficient column. Glass apparatus was used throughout, and adequate precautions, using calcium chloride drying tubes, were taken to exclude moisture during reflux and distillation. The solvent was stored in a Pyrex flask from which moisture was further excluded by fitting an inverted jar to a rubber ring around the flask neck. These precautions and the method of storage applied to all solvents both in this and the previous section.

A.R. ethanol was treated with sodium and refluxed for two hours. It was then distilled, and stored over freshly formed calcium oxide prepared by heating quicklime in a muffle furnace for two to three hours before use. The alcohol was finally redistilled from the quicklime.

Pure commercial n-propanol was treated with activated magnesium, and the same procedure followed as with methanol.

Commercial pyridine, stored over sodium hydroxide pellets, was fractionated and the fraction boiling between 113-117°C collected. The complex $2C_5H_5N.ZnCl_2$ was then precipitated by the addition of zinc chloride solution to

the pyridine (71). This product was twice recrystallised from absolute alcohol and the base finally liberated by the addition of strong caustic soda solution. The pyridine was then dried by refluxing for several hours over caustic soda pellets: it was finally fractionated, the fraction boiling between 115.3° and 115.7°C at 760 mm. being collected. The purified solvent was stored over sodium hydroxide. Hydrated lithium chloride was heated in a platinum crucible to expel moisture. It was recrystallised from dry ethanol, and since there are no hydrates above 98°C, it was desolvated at 200°C and stored in vacuum desiccator. Lithium iodide was prepared by adding pure anhydrous lithium carbonate to freshly distilled A.R. hydriodic acid and evaporating off the excess acid. Sodium iodide loses its water of crystallisation above 65°C. The dehydrated salt was recrystallised from dry ethanol, desolvated at 200°C and kept in a vacuum desiccator. Potassium iodide forms no hydrates. It was recrystallised from aqueous methanol, dried at 200°C and kept in vacuum desiccator. Ammonium iodide was recrystallised from dry ethanol, dried at 200°C and stored in vacuum desiccator. Sodium bromide was recrystallised from conductivity water, dried at 200°C and kept as above.

Preparation of the solution.

The hygroscopic nature of the solvents and of some of the salts, especially lithium chloride, made it necessary to take special precautions to exclude moisture during solution preparation. The salt was quickly weighed into a long necked quickfit flask which was then transferred to an electrically heated asbestos oven. The neck of the flask, which protruded from the top of the oven, was fitted with an adaptor which enabled tank hydrogen to be passed through the flask while the contents were heated to 220°C. The hydrogen was dried by passing it over phosphorous pentoxide, and escaped from the system via a concentrated sulphuric acid bubbler. The heating was continued for about 15 minutes, and after the flask and contents had been allowed to cool, they were reweighed and the correct weight of solvent blown into the flask by a stream of dried air.

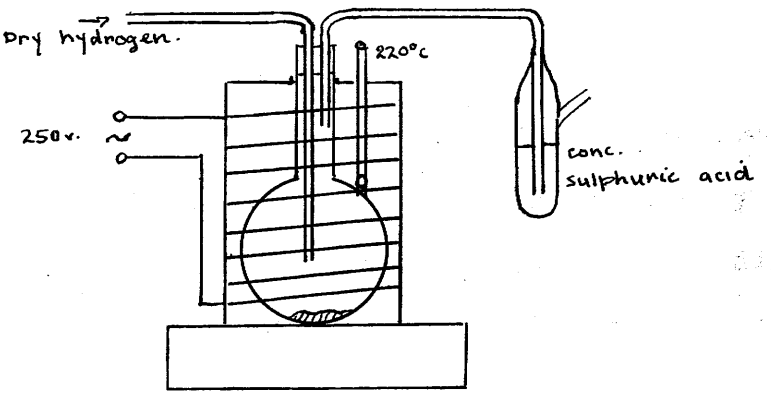

Capacity and electrocapillarity measurements.

The techniques were the same as those previously described and again, at least two runs were made for each set of data. The sensitivity for both types of measurement was somewhat greater than that found with acid solvents. At the most sensitive part of the curve, i.e., around the region of minimum capacitance, reproducibility was between 0.05 and 0.1 $\mu F/cm^2$., while, towards the extreme of anodic polarisation, this was reduced to about 2 $\mu F/cm^2$. Potassium and ammonium iodides however behaved similarly to 1 molal formic acid in that bridge balance was effective over a range of C_3 settings. Consequently sensitivity was somewhat reduced. Electrocapillarity reproducibility was about 0.3 dyne/cm. around the E.Cap.Max., and between 0.5 and 1.0 dyne/cm. toward the extremes of the curve. The iodides, however, were somewhat less satisfactory, there being a greater tendency to induce "sticking" of the mercury meniscus.

The effect of solvent variation.

The choice of lithium chloride as electrolyte was governed largely by the fact that it is adequately soluble in all of the organic solvents mentioned. Thus differential capacity as a function of potential relative to a calomel electrode in the same solution and to a mercury pool in the

case of pyridine is shown in Graph 23 for the systems 1 molal lithium chloride - methanol, ethanol, n-propanol, and pyridine. On the same graph also is the curve for 1 molal lithium chloride in water. The general shape of the curves is similar to that previously encountered with the anhydrous acids. The graphs are drawn on the same scale and so immediate comparison of the relative capacities in the different solvents can be made. The aqueous values are much higher than those of the other four solvents, and with the exception of the cation branch, overlap with ethanol at about -1.05 volt; the values for methanol are next highest. Ethanol and n-propanol capacities are identical within experimental error until about -0.95 volt, when the propanol curve flattens and remains thus until -1.6 volt. The pyridine results are in general of a lower order than those of the other solvents. From the data of Bowden and Grew (69) and of Frumkin (72), it appears that there is no direct relation between capacity and the dielectric constant of the solvent. In the case of Bowden and Grew's results, however, it is difficult to see how any adequate comparison can be made, since the systems chosen for examination contain three different solutes at different concentrations. Grahame has stated (73) that the capacity of the non diffuse part of the double layer, which is the

controlling factor on cathodic polarisation, is strongly influenced by dielectric saturation effects which bear little or no relation to the normal dielectric constant. Nevertheless, from the results presented here, it would appear that, for the series examined, the capacities are in general in the same order as the dielectric constants of the media. The minimum capacities in the solvents, water, methanol, ethanol, n-propanol and pyridine are 16.25, 9.50, 8.00, 8.00 and 5.75 $\mu F/cm^2$. respectively, while the dielectric constants are 78, 31.2, 25.00, 22.2 and 12.00. It was thought that the minimum capacities would be most representative of the solvent, since at this part of the curve anionic specific adsorption is absent and coulombic distortion of cations has not yet commenced. Graph 24, although it does not pass through the origin, indicates that a linear relation exists between minimum differential capacity and the dielectric constant of the medium concerned.

Electrocapillarity curves for the organic solvents are shown in Graph 25, on which the results of double integration of the capacity data are also presented. Agreement between the direct experimental surface tension values and those derived from capacity integration is of the order of 0.5 dyne/cm. or better near the E.Cap.Max. potential and

2 dynes/cm. at the extremes of the curves. As with acetic and formic acids, the E.Cap.Maxima were determined by integrating at small potential intervals around a value selected by inspection of the experimental results until the shape of the resultant curve was as nearly coincident as possible with the experimental curve. In the case of the alcohols, and in particular with pyridine, since the E.Cap.Maxima lay in a region in which there was a rapid change in capacity and hence in surface charge density, a small alteration of the selected potential produced surface tension values considerably at variance with the shape of the experimental curves. As the correct E.Cap.Max. was approached, the symmetry of the calculated surface tensions approached more and more nearly that of the directly determined values. In the case of pyridine, a difference in the selected E.Cap.Max. of 0.0025 volt could be detected. Finally, surface charge densities as a function of potential, the result of a single graphical integration of the capacity data are illustrated in Graph 26.

The effect of cation variation.

Grahame (73,74,75) has made a systematic examination of the effects on double layer capacity in aqueous solution of anion and cation variation. In the latter case, by evaluating the potential of the outer Helmholtz

plane, and knowing the surface charge density and the total potential drop across the interface, he calculated integral capacities for the non diffuse part of the double layer. These calculations were made in the region of cathodic polarisation where anion adsorption was absent, and the results indicated that the nature of the cation is of minor importance. The character of the cation also made little difference to differential capacity, which, according to Grahame, is a sensitive function and tends to magnify any differences that exist. Although no attempt here has been made to evaluate integral capacities, since the effect of salt association on the estimation of the outer Helmholtz plane potential was not known, nevertheless, differential capacities for 1 molal lithium, sodium, potassium and ammonium iodides in methanol have been determined, and the results presented in Graph 27. Although, as mentioned above, in aqueous solution, differential capacity is largely unaffected by the nature of the cation, a definite trend within a series is nevertheless observable. Thus, from Grahame's values (74) for N/10 lithium, sodium, potassium and ammonium chlorides at -1.2^{o} volts relative to an N/10 calomel electrode, the differential capacities are 15.39, 15.73, 16.04 and 16.47 $\mu F/cm^2$. This trend becomes more pronounced on more extreme cathodic polarisation.

With the exception of the ammonium salt at potentials more negative than -0.9 volt with respect to a mercury pool, the same tendency is observable in methanol. Differential capacity is, however, more extensively affected than in aqueous solution by the nature of the cation, e.g., at -1.2 volt with respect to a mercury pool the values for lithium, sodium and potassium are 16.5, 25.0 and 34.7 $\mu F/cm^2$. This order, as in aqueous media, is the opposite to what might be expected, since the small unsolvated lithium ion would supposedly approach the interface more closely than a larger ion. Grahame has concluded that cations are not hydrated in the direction of the interface. If this be true of solvation in the case of methanol, the above results must be attributed to the increasing polarisability of a larger ion, thus bringing the centroid of charge closer to the mercury surface and increasing capacity. Electrocapillarity curves for the iodides in methanol are illustrated in Graph 28. Graph 29 shows differential capacity curves for 1 molal lithium chloride, sodium bromide and sodium iodide in methanol. Although, in the case of the chloride, the cation has changed, anodic capacities increase in the order chloride, bromide and iodide. This again is a similar trend to that observed in aqueous solution (75).

TABLE 23

Capacity data for A :- 1 molal lithium chloride - water

B :- 1 molal lithium chloride - methanol

C :- 1 molal lithium chloride - ethanol

D :- 1 molal lithium chloride - n-propanol

E :- 1 molal lithium chloride - pyridine

Reference electrodes, A - D :- calomel electrode in same solution.
E :- mercury pool.

Potential volts -ve	A Capacity $\mu F/cm^2$	B Capacity $\mu F/cm^2$	C Capacity $\mu F/cm^2$	D Capacity $\mu F/cm^2$	E Capacity $\mu F/cm^2$
0·15	50·6	54·5	49·10	50·5	31·29
0·20	44·46	45·26	39·35	37·70	21·51
0·25	41·10	37·85	30·80	30·52	16·34
0·30	40·95	31·30	23·30	24·20	14·27
0·35	42·62	24·85	17·25	19·00	12·82
0·40	44·34	19·22	13·25	14·25	11·67
0·45	46·12	15·02	10·38	11·35	10·85
0·50	45·52	12·72	9·10	9·50	9·80
0·55	41·07	11·48	8·25	8·42	9·37
0·60	35·63	10·47	8·10	8·12	8·66
0·65	30·55	9·87	8·03	8·02	8·34
0·70	26·39	9·61	8·10	8·12	7·60
0·75	23·36	9·52	8·27	8·27	7·41
0·80	21·11	9·50	8·55	8·65	6·83
0·85	19·44	9·61	8·88	8·90	6·78
0·90	18·12	9·86	9·30	9·27	6·39
0·95	17·61	10·15	9·75	9·70	6·47
1·00	16·91	10·49	10·32	10·10	6·10
1·05	16·50	10·88	10·80	10·35	6·26
1·10	16·43	11·31	11·37	10·70	5·88
1·15	16·33	11·70	11·92	11·00	6·07
1·20	16·36	12·10	12·55	11·20	5·77
1·25	16·43	12·58	13·28	11·40	6·08
1·30	16·64	13·05	13·80	11·42	5·89
1·35	16·72	13·60	14·47	11·42	6·07
1·40	17·16	14·18	15·12	11·46	6·08
1·45	18·14	14·79	15·89	11·35	6·49
1·50	17·82	15·42	16·60	11·34	7·25
1·55	18·13	16·10	17·37	11·34	8·50
1·60	18·92	16·80	18·05	11·45	10·76

TABLE 25

Electrocapillarity data for

A :- 1 molal lithium chloride - methanol.

B :- results of capacity integrations.

C :- 1 molal lithium chloride - ethanol.

D :- results of capacity integrations.

Potential volts -ve	A Dynes/cm	B dynes/cm	C Dynes/cm	D Dynes/cm
0·00	362·7	--	358·0	--
0·025	368·1	--	--	--
0·05	371·9	--	366·2	--
0·075	375·2	--	--	--
0·10	376·7	--	373·9	--
0·15	380·6	380·0	376·7	376·4
0·20	384·0	383·2	379·0	378·7
0·25	385·4	385·3	380·4	380·0
0·30	386·3	386·3	380·9	380·5
0·35	386·7	386·6	381·1	380·4
0·40	385·7	386·4	380·5	379·9
0·45	385·4	385·6	379·7	379·0
0·50	383·5	384·3	378·1	377·9
0·55	382·4	382·8	377·2	376·5
0·60	380·4	381·0	375·1	375·0
0·65	378·8	379·0	373·0	373·3
0·70	376·3	376·7	370·9	371·2
0·75	373·6	374·2	369·1	369·1
0·80	371·4	371·4	366·2	366·7
0·85	367·7	368·3	363·7	364·1
0·90	364·2	365·1	361·2	361·3
0·95	361·1	361·6	358·3	358·3
1·00	357·2	357·8	354·7	355·0
1·05	353·4	353·7	351·3	351·4
1·10	349·2	349·5	347·7	347·6
1·15	344·7	344·9	343·6	343·5
1·20	339·8	340·0	339·0	339·2
1·25	334·8	334·7	333·4	334·5
1·30	329·2	329·2	328·2	329·4
1·35	323·6	323·2	322·7	324·7
1·40	317·6	317·0	316·6	318·1
1·45	310·9	310·5	309·8	312·0
1·50	304·3	303·6	304·0	305·5

TABLE 25A

Electrocapillarity data for

A :- 1 molal lithium chloride - n-propanol.

B :- results of capacity integration.

C :- 1 molal lithium chloride-pyridine.

D :- results of capacity integration.

Potential volts -ve	A Dynes/cm	B Dynes/cm	C Dynes/cm	D Dynes/cm
0·00	358·6	--	357·2	--
0·025	--	--	359·9	--
0·050	368·7	--	361·7	--
0·10	375·7	376·3	362·7	--
0·15	378·7	379·6	361·4	362·1
0·20	381·0	381·6	360·0	360·8
0·25	382·6	382·7	358·5	359·9
0·30	383·9	382·9	356·2	356·7
0·35	383·2	382·7	353·7	354·2
0·40	382·6	382·0	351·1	351·3
0·45	381·3	380·9	347·9	347·9
0·50	379·7	379·5	344·6	344·5
0·55	377·4	377·9	341·0	340·9
0·60	376·4	376·1	337·8	337·0
0·65	374·2	374·1	334·0	332·8
0·70	372·2	371·9	329·5	328·4
0·75	369·9	370·0	324·8	323·8
0·80	366·6	366·9	319·6	319·1
0·85	364·1	364·0	314·8	314·1
0.90	361·3	360·9	309·4	309·0
0·95	357·8	357·7	304·4	303·8
1·00	354·6	354·2	299·2	298·3
1·05	350·4	350·4	293·8	292·7
1·10	346·3	346·4	288·6	287·0
1·15	342·5	342·1	282·5	281·1
1·20	338·2	337·5	277·1	--
1·25	333·4	332·6	270·8	--
1·30	328·1	327·5	265·1	--
1·35	322·6	322·1	--	--
1·40	317·5	316·4	--	--
1·45	--	310·4	--	--
1·50	--	304·1	--	--

TABLE 26

Surface charge densities derived from capacity data for

A :- 1 molal lithium chloride - methanol.

B :- 1 molal lithium chloride - ethanol.

C :- 1 molal lithium chloride - n-propanol.

D :- 1 molal lithium chloride - pyridine.

Potential volts -ve	A μ couls./cm^2	B μ couls./cm^2	C μ couls./cm^2	D μ couls./cm^2
0·15	+ --	+ 5·73	+ 5·19	- 1·89
0·20	5·44	3·51	3·06	3·17
0·25	3·18	1·33	1·36	4·18
0·30	1·26	0·35	0·00	4·84
0·35	- 0·11	- 0·65	- 1·06	5·52
0·40	1·18	1·40	1·88	6·13
0.45	2·06	2·00	2·50	6·69
0·50	2·70	2·50	2·98	7·22
0·55	3·36	2·93	3·41	7·70
0·60	3·87	3·33	3·82	8·15
0·65	4·40	3·73	4·22	8·57
0·70	4·85	4·13	4·62	8·97
0·75	5·36	4·54	5·03	9·35
0·80	5·85	4·96	5·45	9·71
0·85	6·30	5·39	5·89	10·06
0·90	6·77	5·85	6·34	10·40
0·95	7·30	6·32	6·82	10·72
1·00	7·80	6·82	7·30	11·05
1·05	8·38	7·34	7·81	11·36
1·10	8·90	7·89	8·34	11·67
1·15	9·48	8·47	8·89	11·98
1·20	10·05	9·09	9·45	12·28
1·25	10·70	9·73	10·02	12·58
1·30	11·32	10·41	10·59	12·88
1·35	12·00	11·12	11·16	13·19
1·40	12·66	11·86	11·72	13·49
1·45	13·43	12·63	12·29	--
1·50	14·17	13·43	12·86	--
1·55	14·94	14·27	13·43	--
1·60	15·73	15·15	14·00	--

TABLE 27

Capacity data for A :- 1 molal lithium iodide - methanol

B : -1 molal sodium iodide - methanol

C :- 1 molal potassium iodide - methanol

D :- 1 molal ammonium iodide - methanol

mercury pool reference electrode.

Potential volts -ve	A Capacity $\mu F/cm^2$	B Capacity $\mu F/cm^2$	C Capacity $\mu F/cm^2$	D Capacity $\mu F/cm^2$
0·20	74·6	71·2	88·1	86·8
0·25	61·8	57·3	65·5	66·8
0·30	47·67	44·14	48·95	50·3
0·35	35·57	31·54	34·60	35·13
0·40	25·09	23·37	30·24	24·51
0·45	17·45	16·89	17·59	18·09
0·50	13·82	13·11	14·74	14·64
0·55	11·66	11·85	12·76	14·00
0·60	11·09	11·06	12·10	13·17
0·65	11·02	11·19	12·50	14·18
0·70	10·96	11·55	13·12	14·83
0·75	11·33	11·98	15·11	16·50
0·80	11·64	12·44	16·86	18·25
0·85	12·15	13·20	19·13	20·55
0·90	12·68	13·97	21·52	21·95
0·95	13·42	15·17	24·56	23·91
1·00	13·97	16·12	27·20	25·27
1·05	14·58	17·61	29·23	27·51
1·10	15·33	19·32	31·25	30·19
1·15	16·01	22·12	32·88	32·48
1·20	16·58	25·00	34·87	33·67
1·25	17·25	29·07	36·95	--
1·30	17·44	--	41·10	--

TABLE 28

Electrocapillarity data for

A :- 1 molal lithium iodide - methanol.

B :- 1 molal sodium iodide - methanol.

C :- 1 molal potassium iodide - methanol.

D :- 1 molal ammonium iodide - methanol.

mercury pool reference electrode.

Potential volts -ve	A Dynes/cm.	B Dynes/cm.	C Dynes/cm.	D Dynes/cm.
0·00	349·0	345·1	346·3	342·7
0·05	364·5	358·8	328·0	351·4
0·10	372·7	367·6	361·8	358·1
0·15	377·9	373·9	367·4	373·3
0·20	380·4	376·0	369·7	377·6
0·25	381·7	376·9	371·4	379·2
0·30	380·8	376·1	371·4	379·2
0·35	379·4	375·2	366·2	377·8
0·40	376·9	373·7	367·2	375·9
0·45	374·3	370·0	363·5	373·7
0·50	372·5	367·3	361·9	370·4
0·55	369·7	363·1	360·8	367·8
0·60	365·9	360·1	356·6	363·2
0·65	361·9	356·3	351·9	359·0
0·70	358·1	352·6	347·2	354·7
0·75	353·0	347·6	344·0	350·5
0·80	349·3	343·4	339·3	344·6
0·85	344·4	338·3	334·5	339·5
0·90	339·2	332·6	329·5	334·1
0·95	333·8	327·9	323·7	327·0
1·00	327·9	321·9	319·3	320·8
1·05	321·8	315·6	341·3	312·6
1·10	315·4	309·0	305·1	304·3
1·15	308·2	301·8	297·7	295·7
1·20	300·9	294·7	289·2	285·5
1·25	292·8	285·7	280·4	274·8
1·30	--	277·7	--	--
1·35	--	267·3	--	--

Graph 23

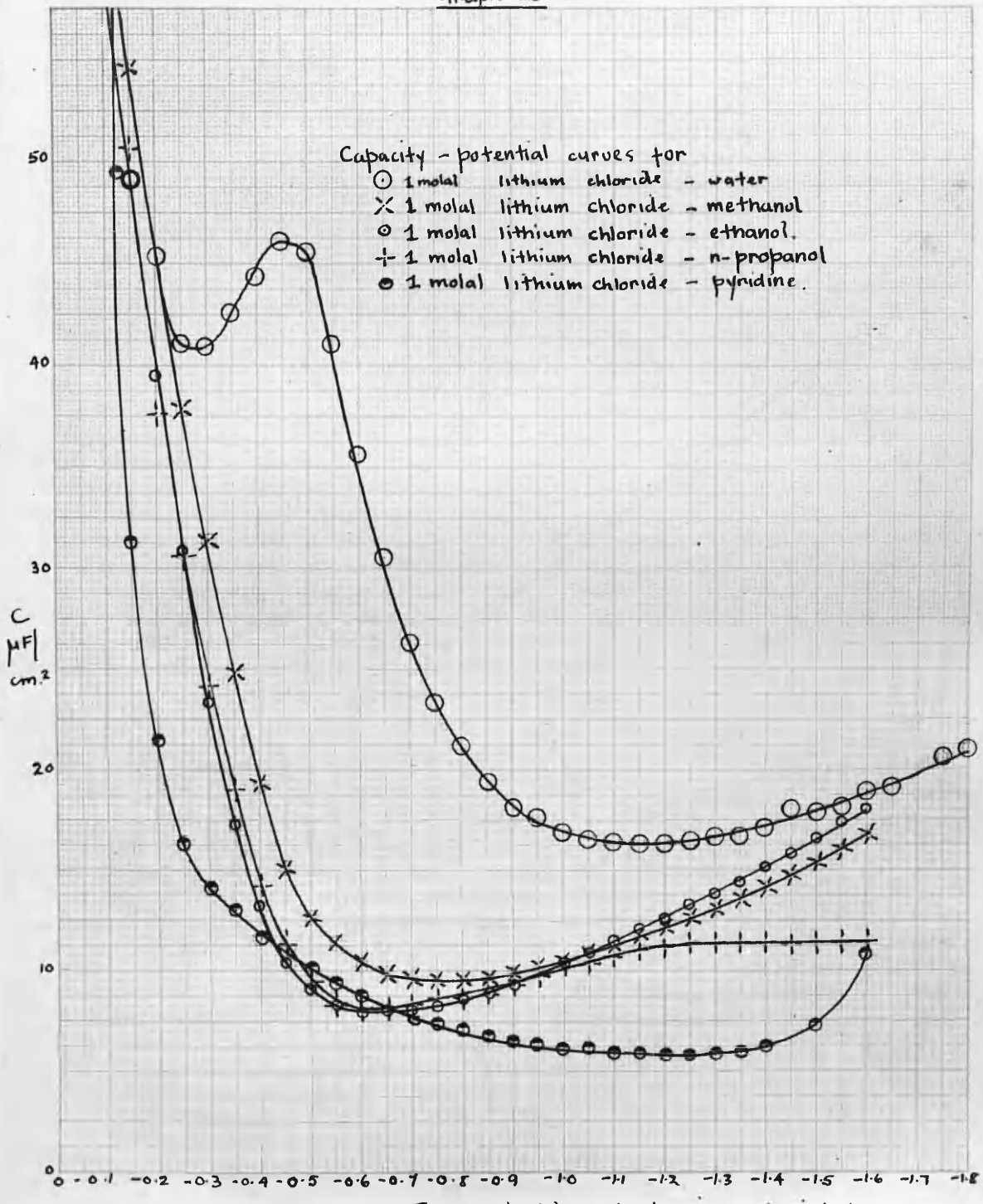

E vs calomel electrode in same solution for water to n-propanol and mercury pool for pyridine.

Graph 24

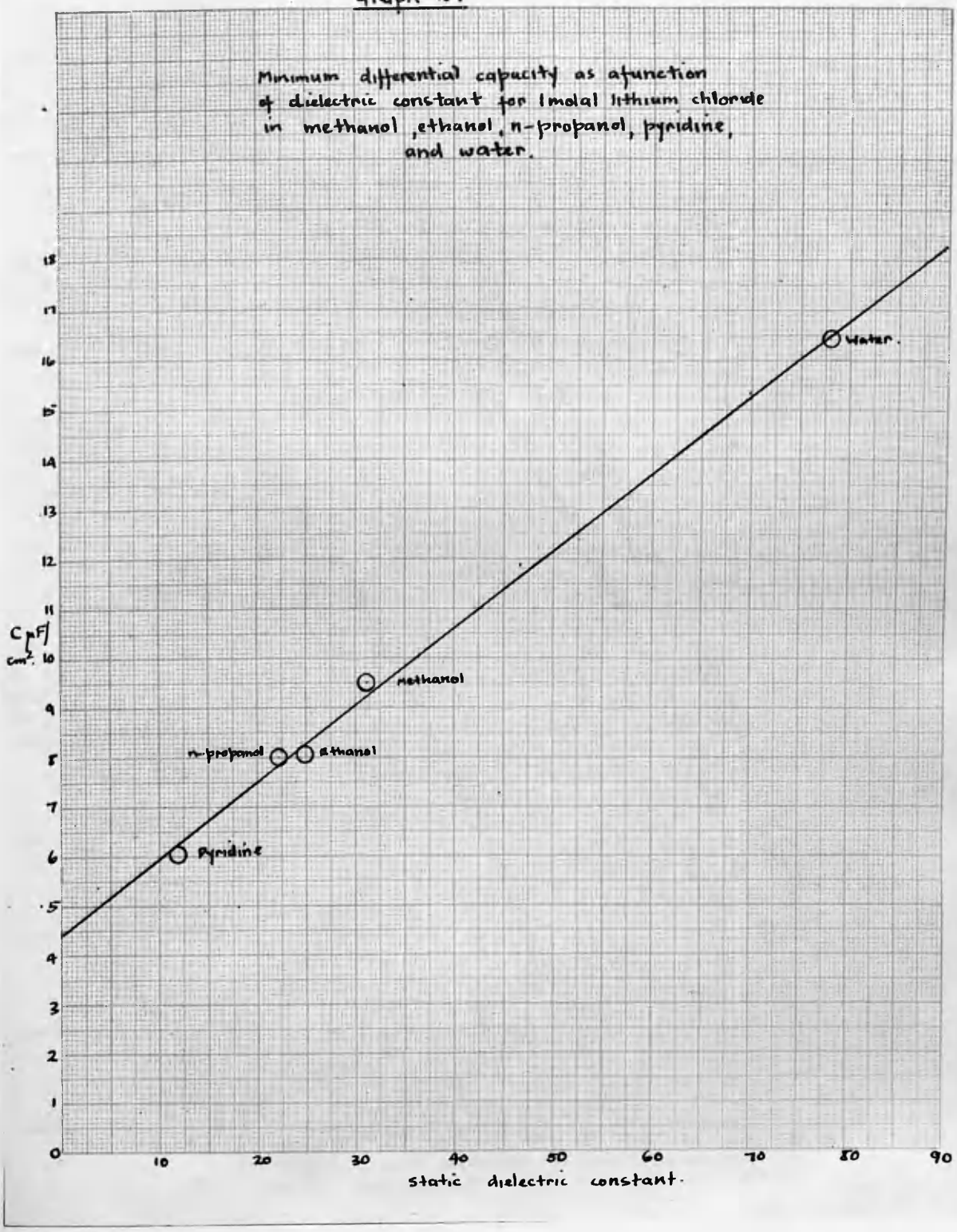
Minimum differential capacity as a function of dielectric constant for 1 molal lithium chloride in methanol, ethanol, n-propanol, pyridine, and water.
C μF/cm²
0
1
2
3
4
5
6
7
8
9
10
11
12
13
14
15
16
17
18
10
20
30
40
50
60
70
80
90
static dielectric constant.
Pyridine
n-propanol
ethanol
methanol
water.

Graph 25

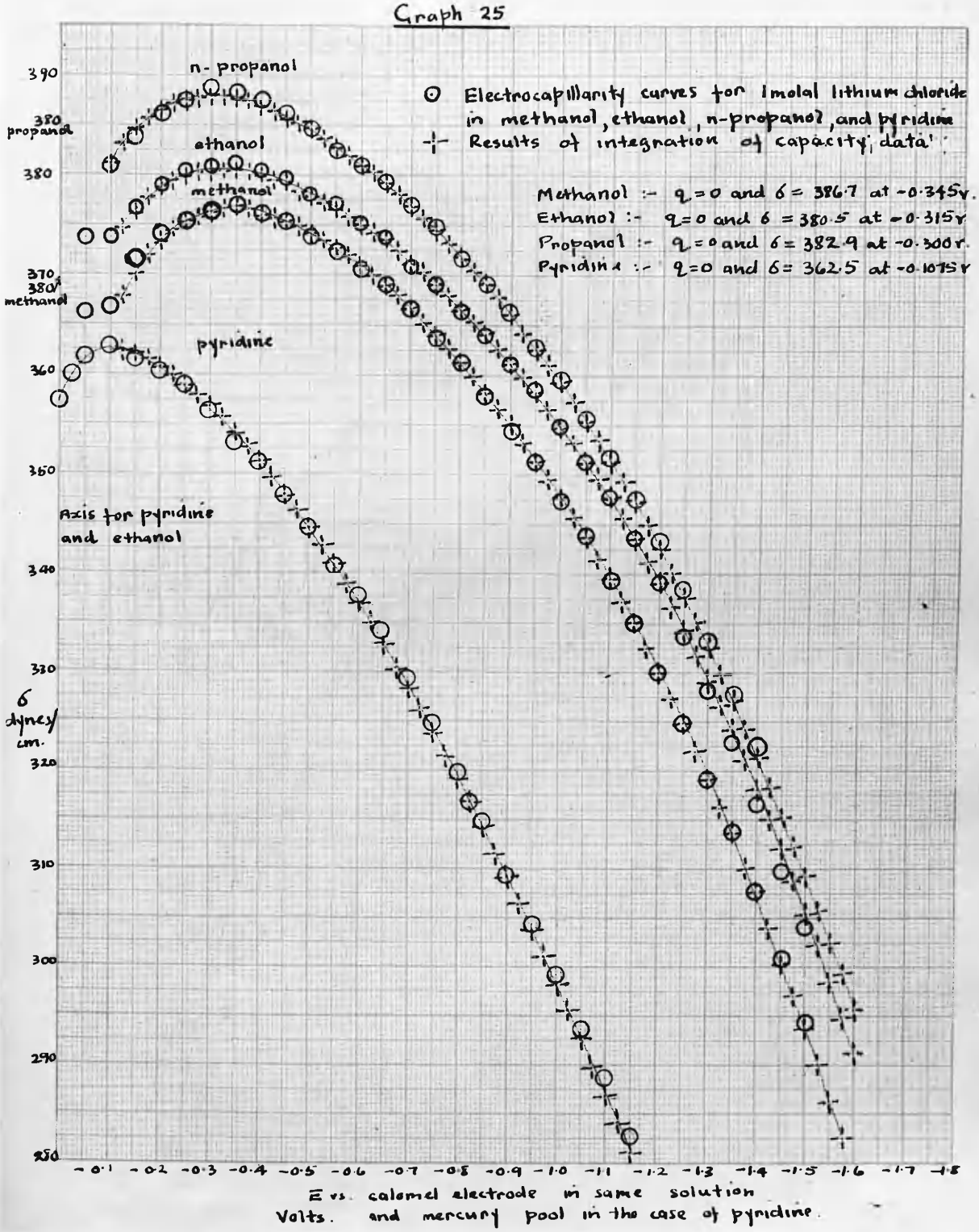
n-propanol
ethanol
methanol
pyridine
propanol
methanol
Axis for pyridine and ethanol
⊙ Electrocapillarity curves for 1 molal lithium chloride in methanol, ethanol, n-propanol, and pyridine
⊣⊢ Results of integration of capacity data.
Methanol :- q=0 and δ = 386.7 at -0.345v.
Ethanol :- q=0 and δ = 380.5 at -0.315v
Propanol :- q=0 and δ = 382.9 at -0.300v.
Pyridine :- q=0 and δ = 362.5 at -0.107v
δ dynes/cm.
390
380
370
360
350
340
330
320
310
300
290
280
-0.1 -0.2 -0.3 -0.4 -0.5 -0.6 -0.7 -0.8 -0.9 -1.0 -1.1 -1.2 -1.3 -1.4 -1.5 -1.6 -1.7 -1.8
E vs. calomel electrode in same solution
Volts. and mercury pool in the case of pyridine.

Graph 26

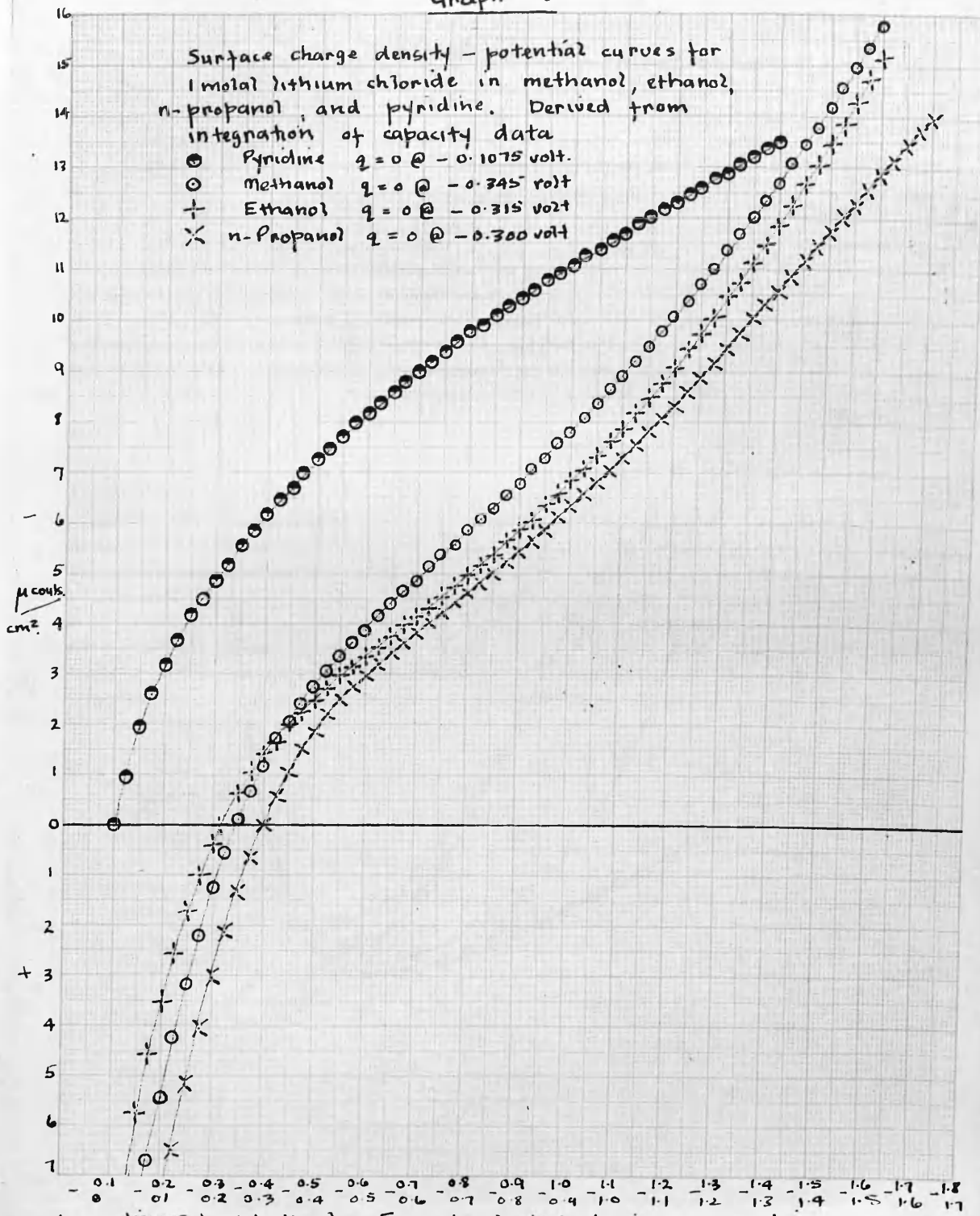
Surface charge density – potential curves for 1 molal lithium chloride in methanol, ethanol, n-propanol, and pyridine. Derived from integration of capacity data
Pyridine q = 0 @ – 0.1075 volt.
Methanol q = 0 @ – 0.345 volt
Ethanol q = 0 @ – 0.315 volt
n-Propanol q = 0 @ – 0.300 volt
μ coulks. / cm²
–
+
16 15 14 13 12 11 10 9 8 7 6 5 4 3 2 1 0 1 2 3 4 5 6 7
– 0.1 0 – 0.2 0.1 – 0.3 0.2 – 0.4 0.3 – 0.5 0.4 – 0.6 0.5 – 0.7 0.6 – 0.8 0.7 – 0.9 0.8 – 1.0 0.9 – 1.1 1.0 – 1.2 1.1 – 1.3 1.2 – 1.4 1.3 – 1.5 1.4 – 1.6 1.5 – 1.7 1.6 – 1.8 1.7
Lower figures for n propanol
E = calomel electrode in same solution and mercury pool for pyridine
Volts.

Graph 27

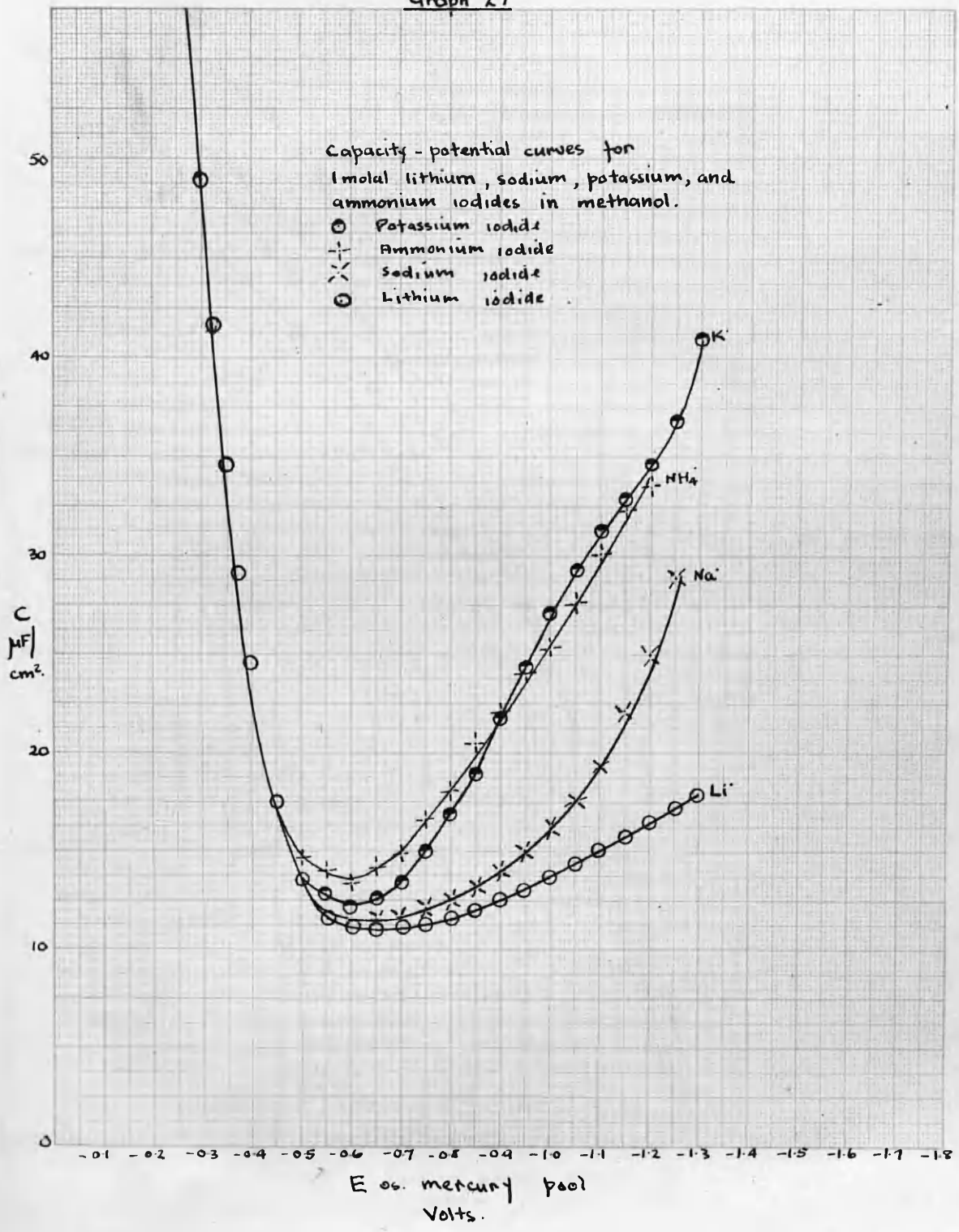
Capacity - potential curves for
1 molal lithium, sodium, potassium, and
ammonium iodides in methanol.
Potassium iodide
Ammonium iodide
Sodium iodide
Lithium iodide
K
NH4
Na
Li
C
μF/
cm².
50
40
30
20
10
0
-01 -02 -03 -04 -05 -06 -07 -08 -09 -10 -11 -12 -13 -14 -15 -16 -17 -18
E vs. mercury pool
Volts.

Graph 28

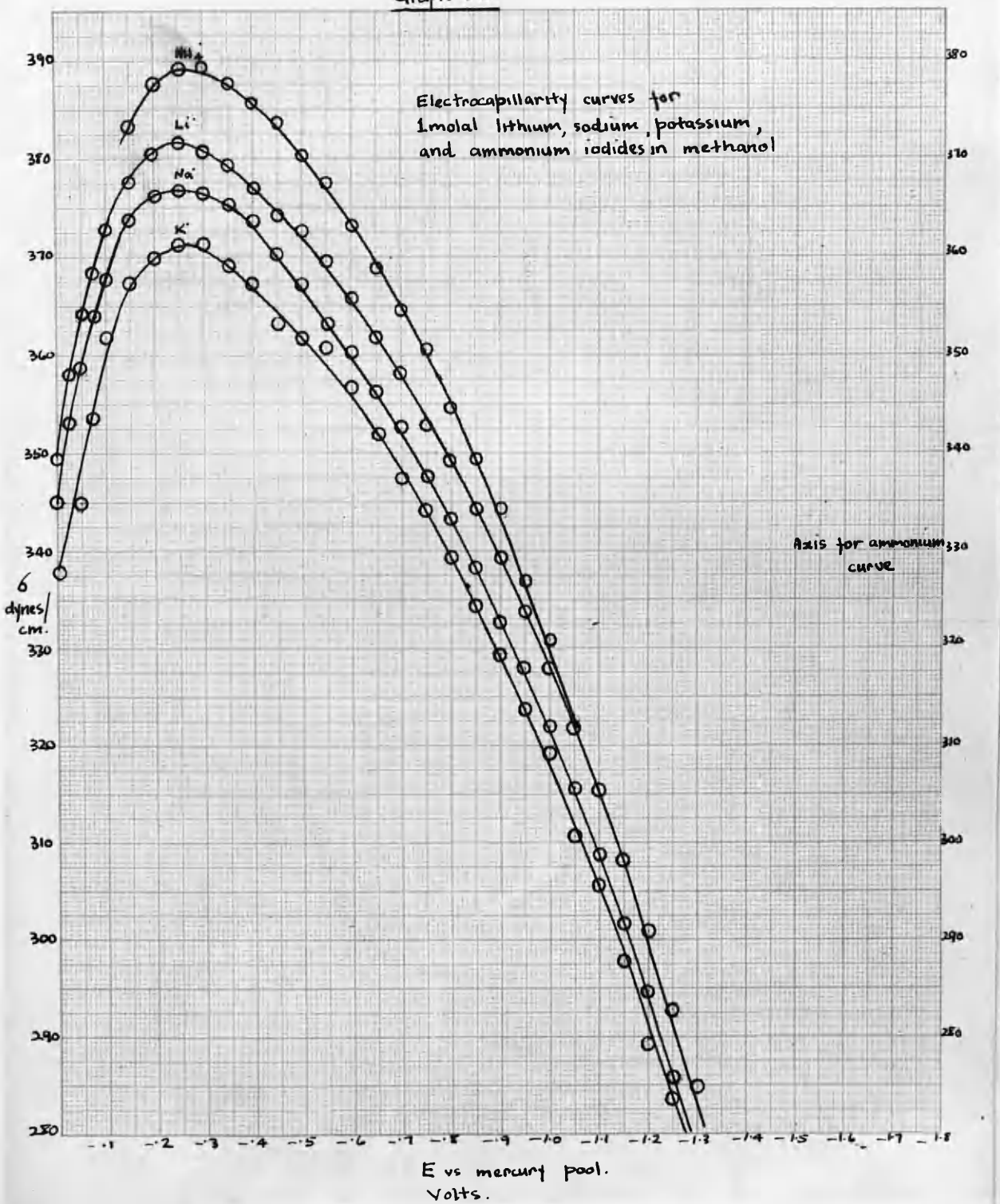
Electrocapillarity curves for
1molal lithium, sodium, potassium,
and ammonium iodides in methanol
NH4
Li
Na
K
Axis for ammonium curve
6 dynes/cm.
E vs mercury pool.
Volts.

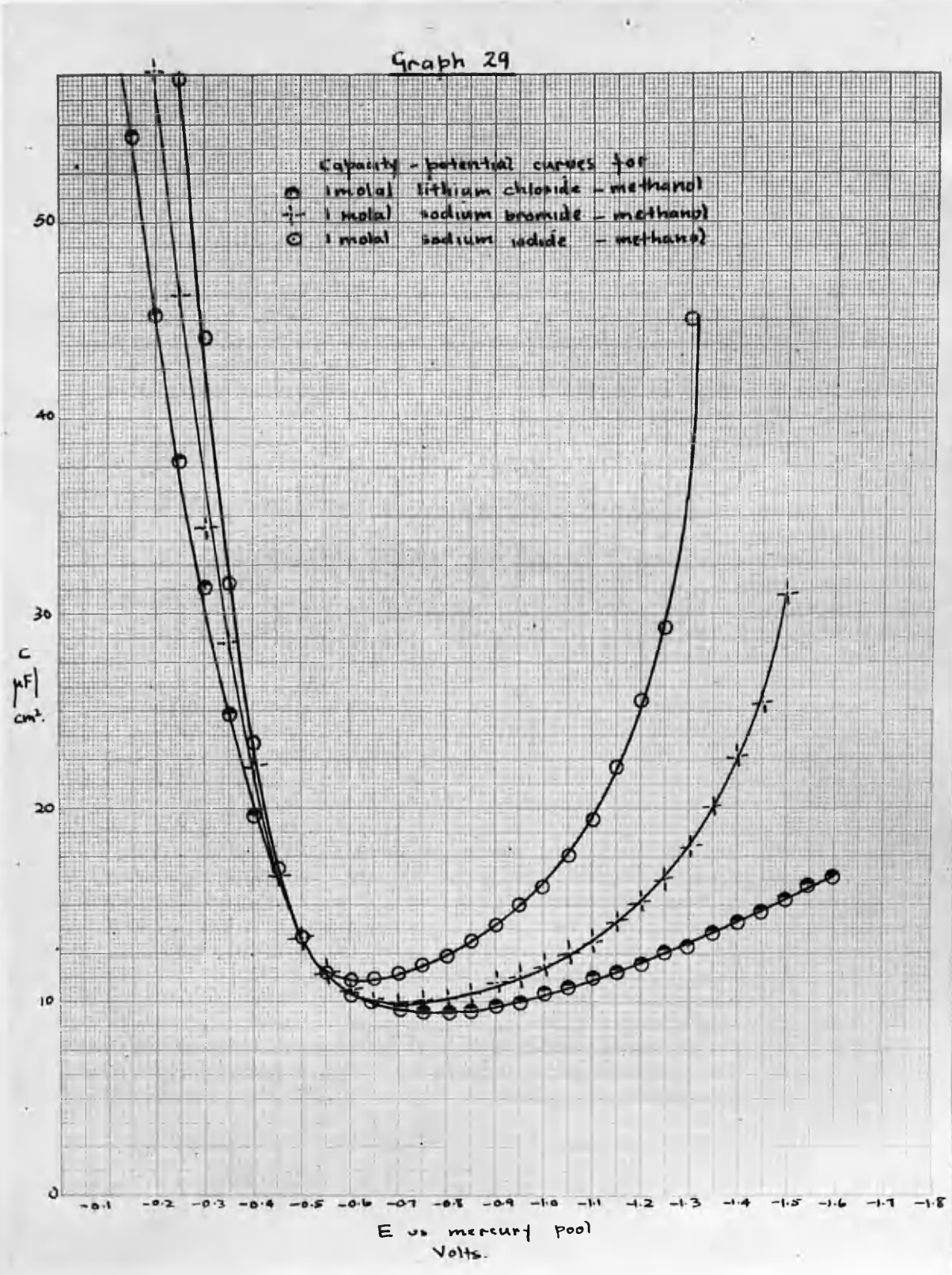
Graph 29
Capacity - potential curves for
1 molal lithium chloride - methanol
1 molal sodium bromide - methanol
1 molal sodium iodide - methanol
C
μF
cm².
50
40
30
20
10
0
-0.1 -0.2 -0.3 -0.4 -0.5 -0.6 -0.7 -0.8 -0.9 -1.0 -1.1 -1.2 -1.3 -1.4 -1.5 -1.6 -1.7 -1.8
E vs mercury pool
Volts.

A double layer capacity determination of the system Cu/Cu" by two different methods.

Introduction.

Several of the transition elements, e.g., iron, cobalt and nickel, exhibit an over-potential in solutions of simple salts of their own ions. Using an oscillographic technique, Hickling (29) has determined the double layer capacity at a nickel cathode in a buffered solution of nickel sulphate. This was achieved by examining the slope of the charging curve obtained during the attainment of the over-voltage and prior to cathodic electrolysis. The value reported was 430-470 $\mu F/cm^2$. Copper, in a solution of cupric ions, also exhibits an over-potential of the same type. It is, however, smaller in magnitude, i.e., about 100 m.v. at a current density of 20 milliamps/cm^2. compared with 0.5 volt for nickel. A number of workers (76-80) have investigated polarisation effects at copper surfaces, and so it was thought to be of interest to examine the double layer behaviour of such an interface since both the A.C. bridge and oscillographic techniques could be applied.

Method 1. The A.C. bridge.

Experimental.

The bridge arrangement was almost the same as that described previously in connection with the dropping

mercury measurements. It was, however, found necessary to incorporate a small additional circuit, consisting of an accumulator in series with a variable resistor and milli-ammeter, to enable a steady current to be passed between the cathode under examination and the relatively large copper anode. This cathodic electrolysis could be effected either during or prior to a bridge reading. Since capacity measurements were being made at a static surface, ear-phones were reverted to, and bridge balance was indicated by a null point.

Cell description.

With the exception of the limb supporting the cathode, the cell was made entirely of Pyrex glass, and a diagram illustrates the essentials of its construction. The cathode was a small length of copper wire sealed into and supported by the central glass limb. Further details of this are given shortly. The anode consisted of a cylinder of high grade copper foil held symmetrically around the cathode by the central cylindrical part of the cell. Electrical connection to the anode was made by the platinum wire contact indicated in the diagram. B7 cones and sockets at the top of the cell enabled a reference electrode and a gas inlet tube to be inserted.

The reference electrode.

This took the form of a mercury - mercurous sulphate electrode with the cell solution as electrolyte. Liquid junction potentials were thus avoided.

Preparation and pretreatment of the cathode.

The cathode was prepared by sealing a small length of borated copper wire 0.6 mm. in diameter into its soda glass support, electrical connection being made by a mercury seal. Prior to the taking of capacity readings and the introduction of the cathode into the cell, the following procedure for obtaining a reproducible surface was adopted (80). The surface was degreased in benzene, and cleaned in a hot sodium cyanide solution. It was then subjected to anodic polishing in phosphoric acid solution at a current density of 10 m.a/cm^2, washed in water, immersed in 10% sulphuric acid to remove the phosphate, rinsed once more in water and mounted in the cell immediately afterwards. The surface area of the electrode was usually about 0.1 cm^2., its dimensions being measured by a travelling microscope.

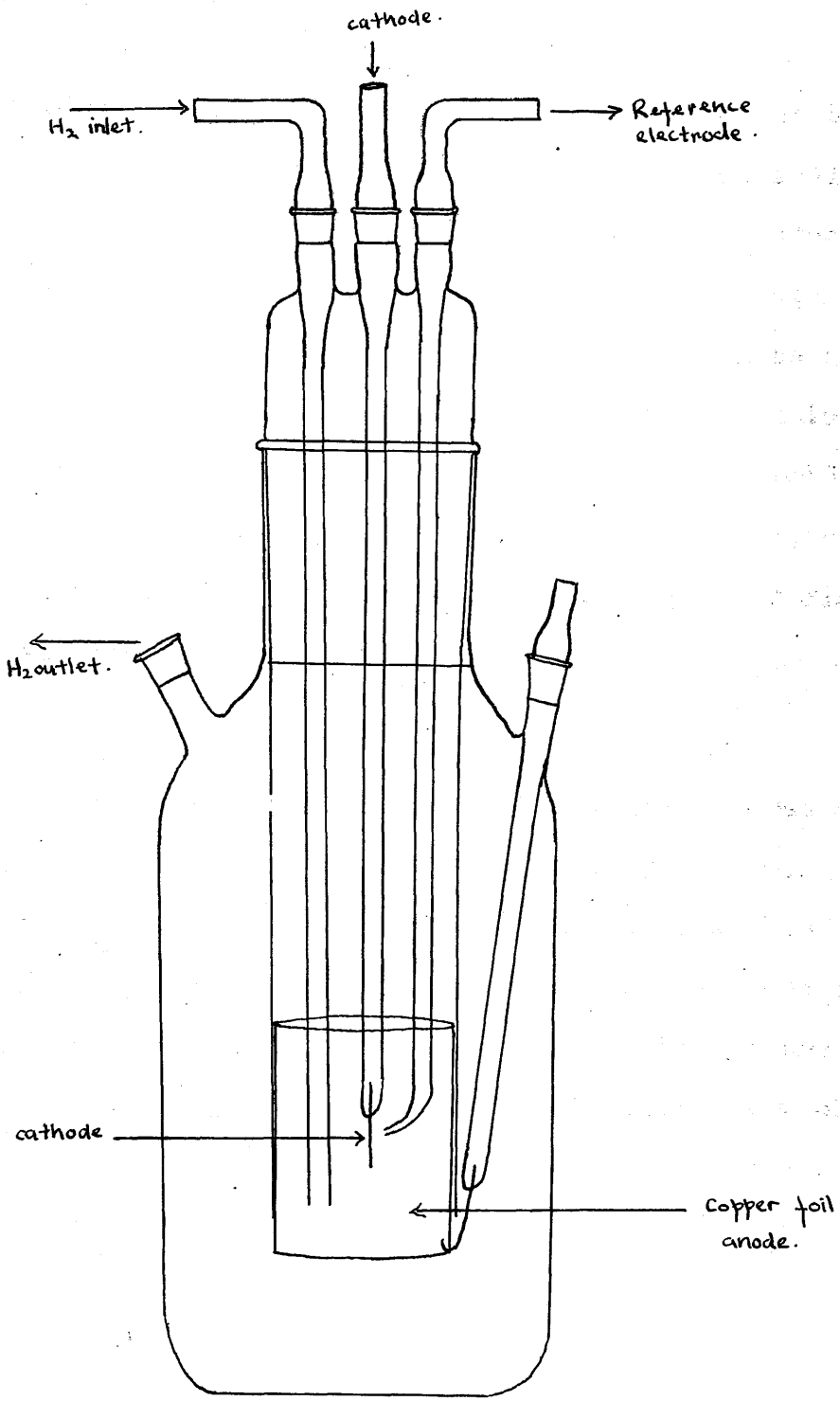

Cell for the double layer capacity determination of copper.

Purification of materials and preparation of solution.

The solution was prepared by the method of Shreir (80). Analar hydrated cupric sulphate was twice recrystallised from conductivity water to which a little concentrated sulphuric acid had been added. Conductivity water was further distilled from potassium permanganate and sodium hydroxide, and the purified copper sulphate dissolved therein immediately afterwards. The solution prepared was 0.5 M copper sulphate - 1 N sulphuric acid, analar acid being used. The solution was boiled, cooled in a stream of nitrogen, and stored in a quickfit flask under an atmosphere of the same gas.

General run procedure.

The technique of capacity measurement was similar to that described for the dropping mercury system. The solution having been introduced to the cell, a brief further dearation followed by bubbling nitrogen or hydrogen for a few minutes. The cathode was then subjected to the treatment already described, and immediately thereafter placed in the cell. The static potential of the cathode relative to the reference electrode was fixed and a capacity reading taken as quickly as possible.

Results and discussion.

In the first instance, the results obtained were neither steady nor reproducible, and this was particularly so if less rigid purification than that described above were adopted. After experiment, however, it was found that capacities could be reproduced if, immediately before a bridge reading, the cathode were subjected to a brief steady electrolysis. The additional circuit already described enabled this to be done, the current density being adjusted to 20 milliamps./cm^2. It was necessary to take a reading as soon as possible after switching off the steady current, since a capacity drift was almost always in evidence. In general the drift was predictable, there being an immediate fall followed by a steady rise to a fairly high value. This rise is presumably due to the adsorption of anions at the copper surface. However, irrespective of the extent of the drift, the original capacity could be reverted to by a few seconds pre-electrolysis followed immediately by a bridge reading.

Little capacity change was observable on altering the applied static potential of the cathode. This was also the case when readings were taken during steady electrolysis.

The results were found to be frequency dependent, a minimum value of about 55 $\mu F/cm^2$. being recorded at 10,000 cycles per second. Between this frequency and about 1000 c.p.s., capacity rose gradually, after which there was a sharp rise as the frequency tended to zero. The results are shown on Graph 30, on which the solution resistance variation with frequency is also illustrated. These variations are consistent with the measurements of Shaw and Remick (81) who determined capacities at a platinum electrode in sulphuric acid, by a similar method.

The effects of gelatin and thiourea.

It was known that these reagents had a profound effect upon the surface characteristics and upon the overpotential of copper. Their effects on double layer capacity at a fixed potential and frequency are indicated on Graph 31. Again, as in the case of the dropping mercury electrode, capacity is progressively lowered with increasing concentration of the addition reagent, until the value is about half that originally recorded. Thereafter, there is no further capacity change, indicating that maximum adsorption has occurred.

Method 2. The cathode ray oscillograph.

The apparatus designed by Hickling (29) for the production of charging curves was constructed. The diagram illustrates the essentials of the circuitry. However, a hard cathode ray tube (VCR 97) was used in place of the soft tube (4050 B.B.) in the original design. This necessitated the building of a 2000 volt power unit to supply the VCR 97. The stability obtained was entirely satisfactory provided adequate screening precautions were observed. A brief explanation of the circuit follows. The cathodic double layer is in series with a standard condenser C, both of which are linearly charged through a constant current pentode, V 1. Discharge of the system is effected by a thyratron V 2 which strikes when the potential difference between anode and cathode is at a value determined by the grid - cathode potential and destrikes when the condensers have discharged sufficiently. Adjustment of this potential affords a frequency control, and variation of the screen grid potential of V 1 provides a method of adjusting current density. The linear potential drop across the layer is amplified by the triode V 3 and fed to the Y plates of the C.R.T., while the voltage across condenser C, which is proportional to the double layer charge, is fed to the X plates. The slope of the resultant curve, i.e., dq/dv,

will therefore give the desired capacity. Since the oscillogram is effectively a graph of surface charge density as a function of potential, it is therefore equivalent to an integrated differential capacity curve of the type previously encountered.

After suitable calibration, the capacity of the nickel - nickel sulphate system was determined and the results agreed substantially with those of Hickling. The copper - copper sulphate electrode was then reverted to, using the same solution as before. Since, however, the over-potential is about 100 m.v., and since the height of the oscillogram is representative of this value, difficulty was experienced in producing the desired curve. Further amplification was indicated, and so the A 1 amplifier of a Cossor double beam oscilloscope was incorporated in series with, and after V 2, thus providing a variable gain stage. Even then, no charging curve was observable until a critical current density of 20 m.a./cm^2. was attained. The diagram indicates the general shape of a typical oscillogram which is similar to those previously obtained by Hickling. The curve was exactly linear until the onset of electrolysis, when it began to flatten. The slope, however, was highly susceptible to frequency and to current density. As in the A.C. bridge method, capacity rose on

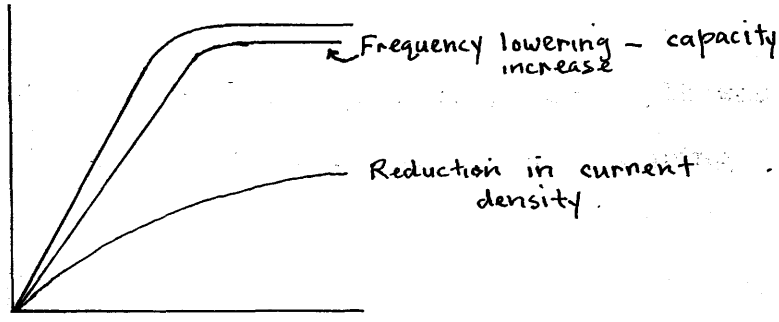

lowering the frequency. A small readjustment of the current density control was, however, capable of destroying the entire curve. The repetition frequency of the charging curve was measured by means of a Cossor oscilloscope, and a few capacities measured at spot frequencies, and at a current density of 20 m.a./cm^2. The results were within about 10% of the values recorded by the A.C. bridge method. It was concluded, however, that, although it was possible to produce an oscillogram, because of the low over-potential and the high susceptibility of the curve slope to current density and to frequency, copper did not adequatly lend itself to accurate capacity measurement by a charging curve method.

The effect on the oscillogram of small traces of thiourea was noted. The copper cathode turned black and the oscillogram was entirely inhibited. If copper be made anodic in copper sulphate solution and in the presence of thiourea, the surface becomes blackened presumably owing to

oxidation and the formation of copper sulphide. It was concluded, therefore, that the discharge cycle, during which current is reversed through the cell and the cathode becomes effectively an anode, was responsible for the surface blackening and curve inhibition.

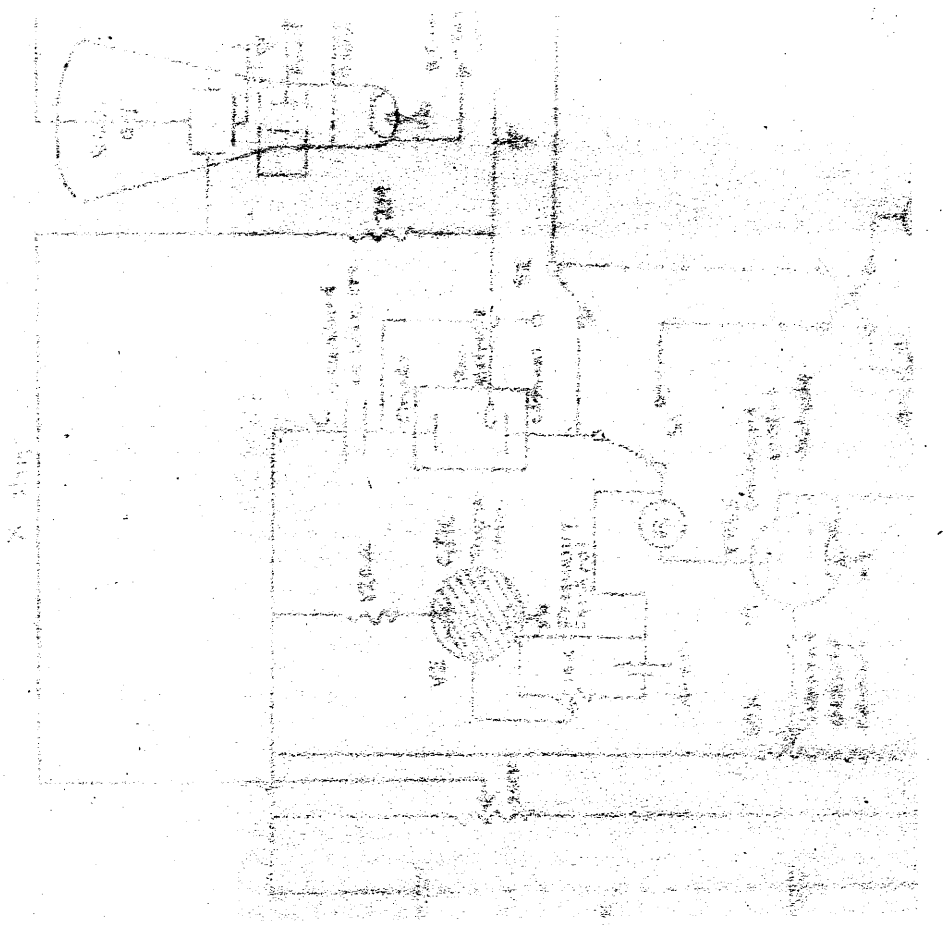

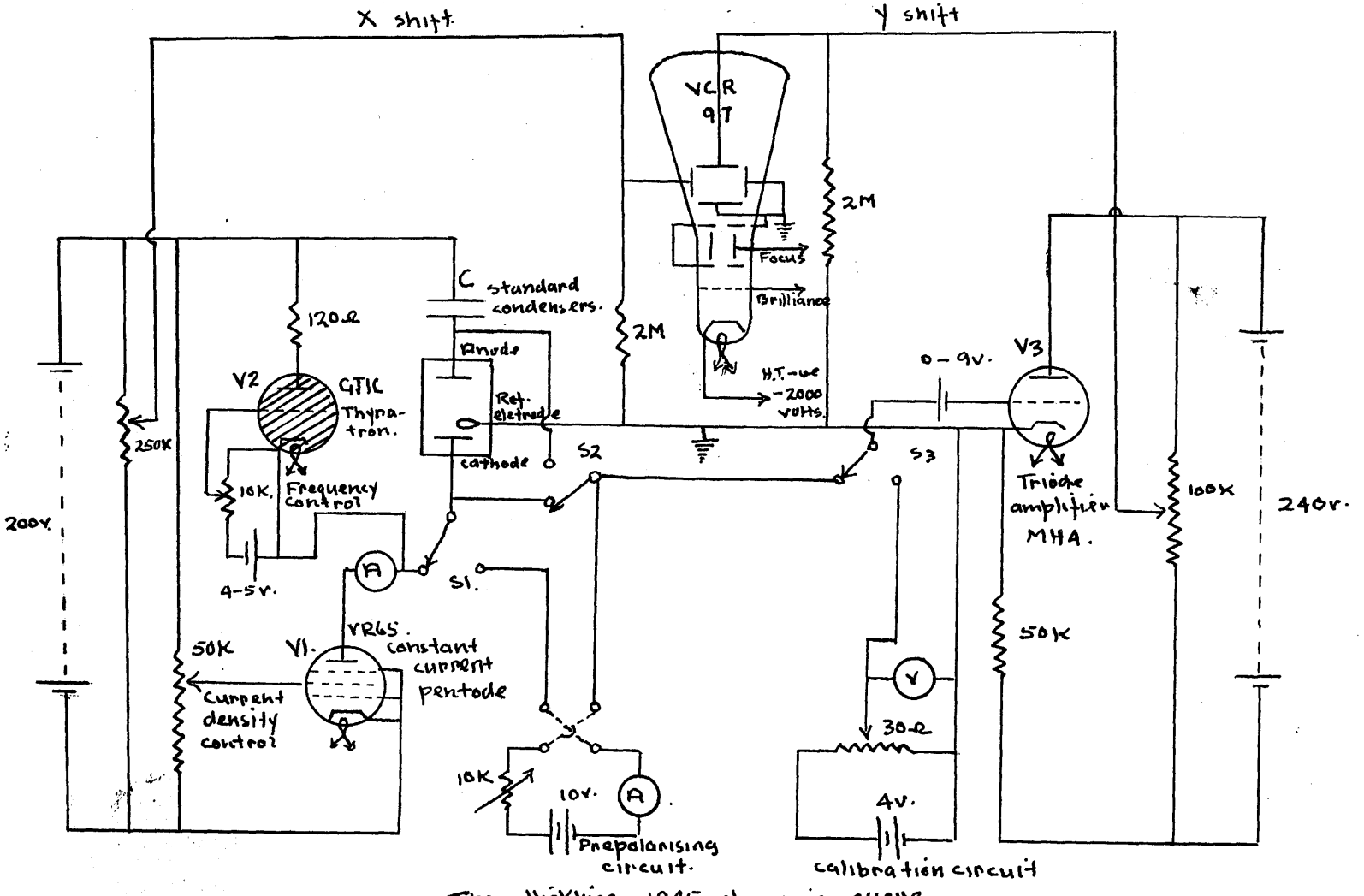

The Hickling 1945 charging curve circuit modified for cathodic working by the inclusion of S.2. Additional amplification after V3 was introduced for copper measurements.

Graph 30

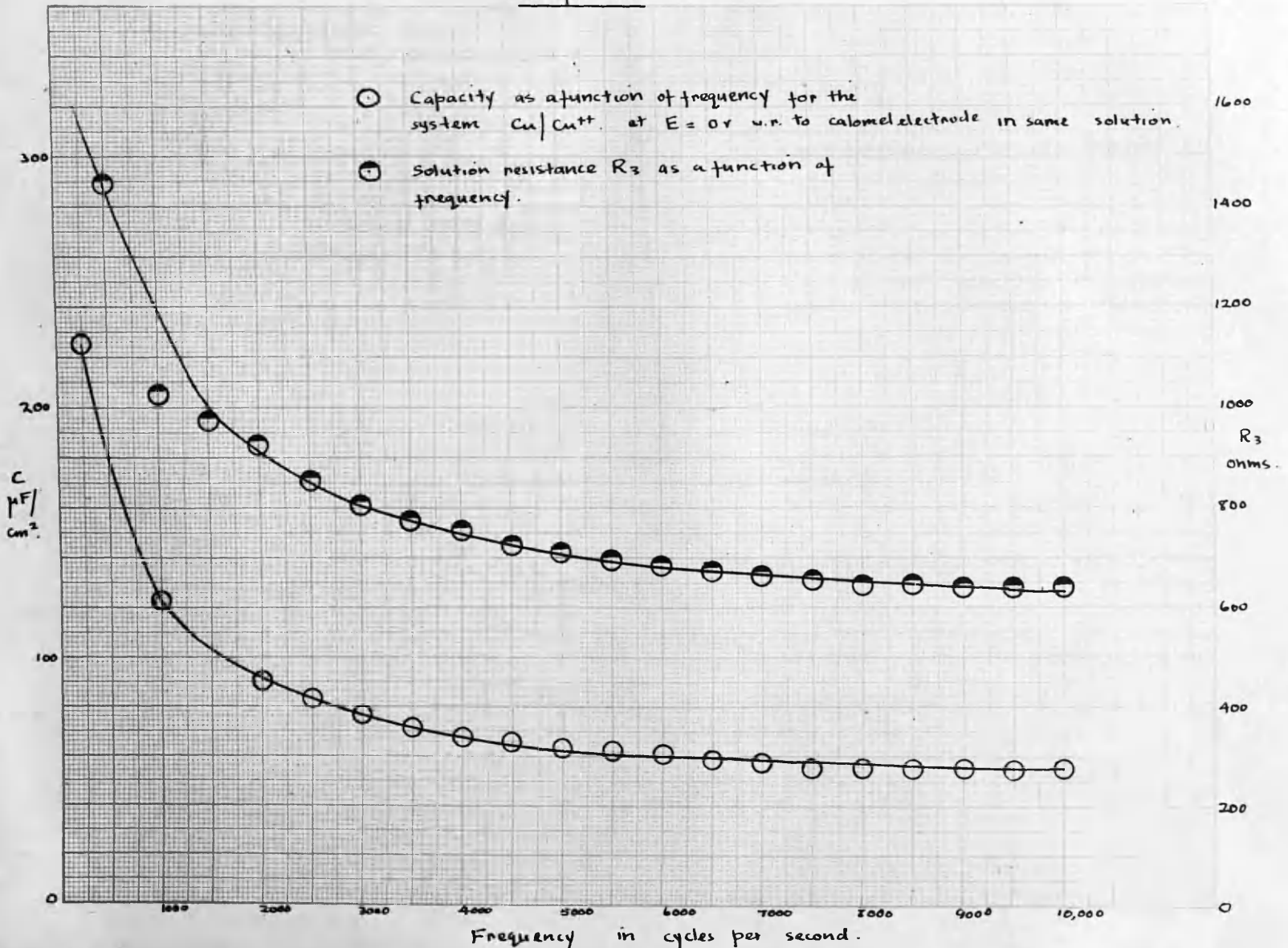
Capacity as a function of frequency for the system Cu | Cu++ at E = 0 v. w.r. to calomel electrode in same solution.
Solution resistance R3 as a function of frequency.
C μF/cm².
R3 ohms.
300
200
100
0
1600
1400
1200
1000
800
600
400
200
0
1000
2000
3000
4000
5000
6000
7000
8000
9000
10,000
Frequency in cycles per second.

Graph 31

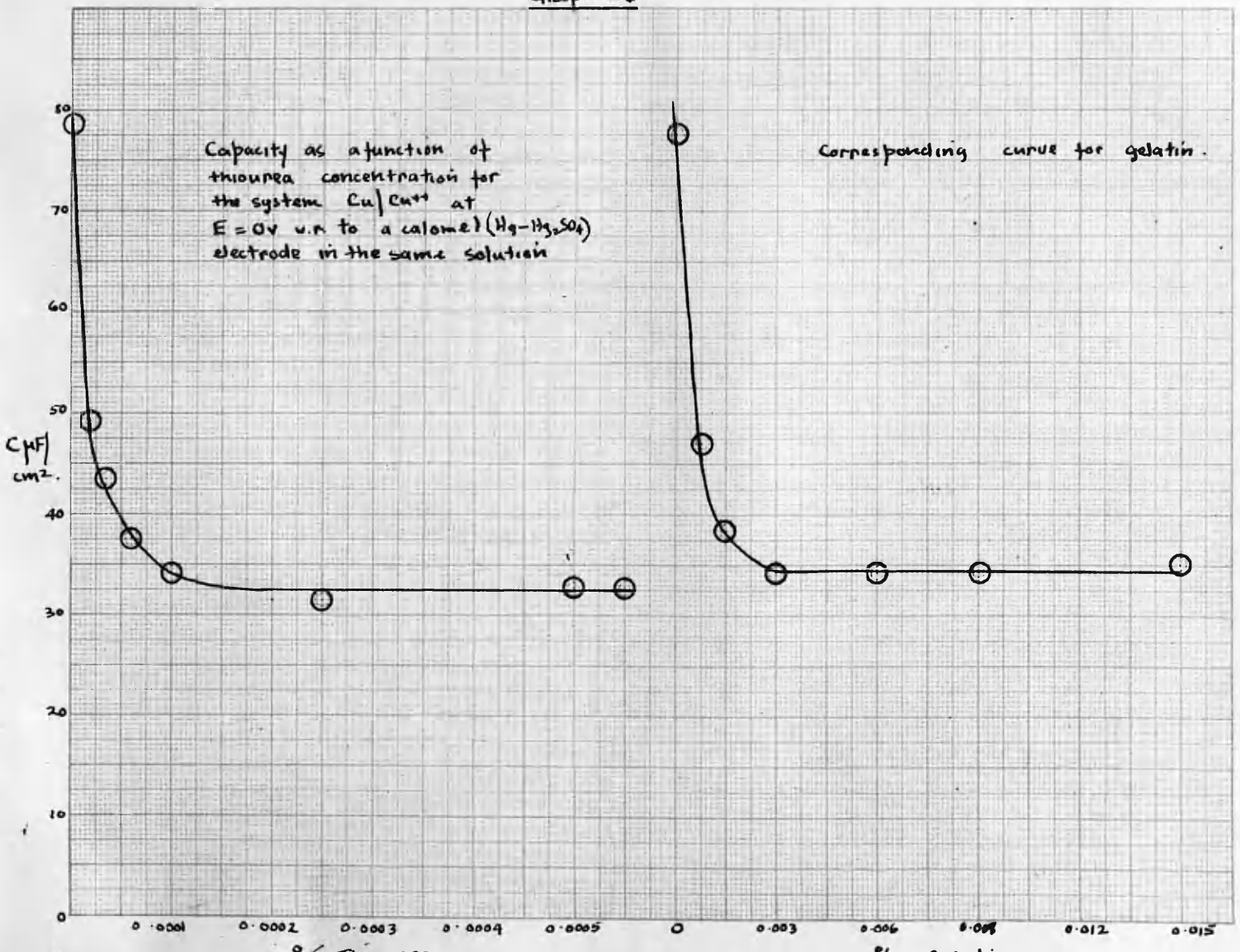
Capacity as a function of thiourea concentration for the system Cu | Cu++ at E = 0V w.r. to a calomel (Hg-Hg2SO4) electrode in the same solution
Corresponding curve for gelatin.
C μF / cm2.
80
70
60
50
40
30
20
10
0
0·0001
0·0002
0·0003
0·0004
0·0005
0
0·003
0·006
0·009
0·012
0·015
% Thiourea
% Gelatin

Ion Association in Aqueous Solutions of Metal Dicarboxylates.

The work in this section is of a different nature from that previously described. It was done in collaboration with the late Dr. J.C. James, and the accompanying reprint gives the details. The ion association which occurs in aqueous solutions between the cations Ba", Cu", La"', $Co(NH_3)_6$"', and the anions afforded by the series of dicarboxylic acids, oxalic, malonic, succinic, glutaric and adipic acids, was studied by conductometric, potentiometric and spectrophotometric methods. Less detailed measurements for maleic, fumaric and phthalic acid were also obtained and dissociation constants for all of these complexes were evaluated. It is concluded that, in general, the stability of the products of association in the dicarboxylate series increases with ring size. This is particularly true of the transition type element, there being a 500 fold increase in dissociation constant (K) on passing from zinc oxalate to glutarate, whereas there is only a 2 fold increase for the corresponding barium salts. Since it seems probable that the magnitude of the dissociation constant is mainly dependent upon two factors, the hydration energy of the cation and the energy of interaction of the associating ions, it would appear that with cations such as magnesium, barium, lanthanum and hexammino-cobalt, little chelation occurs and the interaction energy is

largely of an electrostatic nature. Stronger chelation tendencies are displayed by transition type elements, and consequently greater changes in K values are observable. Maleates and fumarates show differences in K to be expected on steric grounds, while phthalates occupy a position intermediate in strength between malonates and succinates.

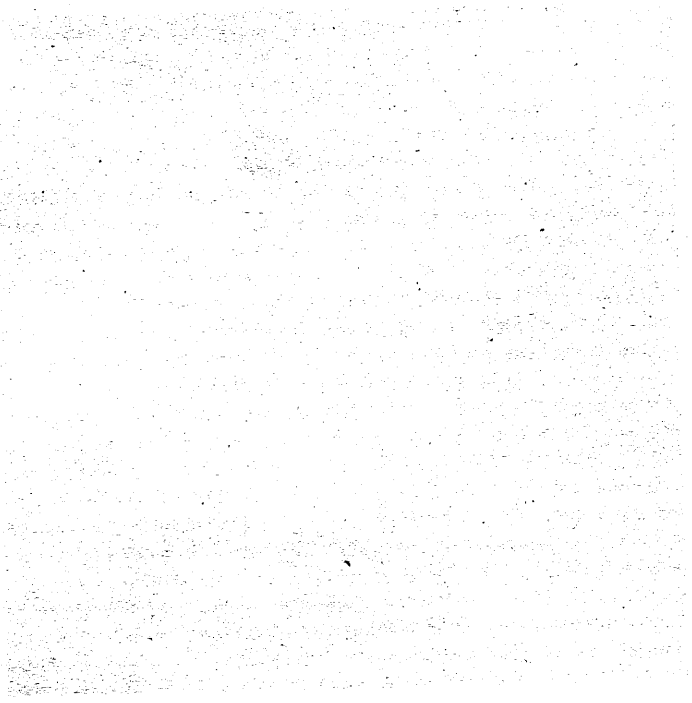

References.

1). Quincke: Pogg.Ann., 1861, 113, 513.

2). Helmholtz: Wied.Ann., 1879, 7, 337.

3). Craxford: Trans.Faraday Soc., 1940, 36, 86.

4). Gouy: Annales de phys., 1917, 7, 129.

5). Chapman: Phil.Mag., 1913, 25, 475.

6). Bikerman: ibid., 1942, 33, 384.

7). Stern: Z.electrochem., 1924, 30, 508.

8). Grahame: Chem.Rev., 1947, 41, 441;
Technical Report No.6 to the Office of Naval Research, May 25, 1951.

9). Whitney and Grahame: J.Chem.Phys., 1941, 9, 827.

10). Lippmann: Pogg.Ann., 1878, 149, 547;
Ann.Chim.Phys., 1875, 5, 494;
ibid., 1877, 12, 265.

11). Lippmann: J.Phys.Radium, 1883, 2, 116.

12). Gibbs: Collected Works, 1928, 1, 336.

13). Parsons and Devanathan: Trans.Faraday Soc., 1953, 49, 404.

14). Gouy: Ann.Chim.Phys., 1903, 29, 145:
ibid., 1906, 8, 291.

15). Koenig: Z.physikal.Chem., 1931, 154, 454.

16). Hansen and Williams: J.Physical Chem., 1935, 39, 439.

17). Craxford and McKay: ibid., 1935, 39, 545.

18). Frumkin and Gorodetzkaya: Z.physikal.Chem., 1928, 136, 451.

19). Karpachov and Strombergi: J.Physical Chem., U.S.S.R., 1937, 10, 739.

20). Frumkin: "Couche Double", Act.Scient., 1936, 373, Paris.

21). Rehbinder and Wenstrem: Acta Physicochim., 1944, 19, 36:
Doklady Akad.Nauk., 1949, 68, 329.

22). Bockris and Parry-Jones: Nature, 1953, 171, 929.

23). Philpot: Phil.Mag., 1932, 13, 775.

24). Frumkin: Z.physical Chem., 1923, 103, 55.

25). Ilkovic: Coll.Czech.Chem.Comm., 1936, 8, 170.

26). Bowden and Rideal: Proc.Roy.Soc., 1928, 120,

27). Erdey-Grúz and Kromrey: Z.physikal.Chem., 1931, 157A, 213.

28). Barclay and Butler: Trans.Faraday Soc., 1940, 36, 128.

29). Hickling: ibid., 1940, 36, 364:
ibid., 1945, 41, 333.

30). Loveland and Elving: J.Physical Chem., 1952, 56, 250:
ibid., 1952, 56, 255.

31). Loveland and Elving: Chem.Rev., 1952, 51, 67.

32). Jones and Christian: J.Amer.Chem.Soc., 1935, 57, 272:
Wien: Ann.Physik., 1902, 8, 373.

33). Robertson: J.Electrochem.Soc., 1953, 100, 194.

34). Kruger: Z.physikal.Chem., 1903, 45, 1.

35). Proskurnin and Frumkin: Trans.Faraday Soc., 1935, 31, 110.

36). Borrisova and Proskurnin: Acta.Physicochim., U.R.S.S., 1936, 4, 819.

37). Grahame: J.Amer.Chem.Soc., 1941, 63, 1207:
ibid., 1946, 68, 301;
ibid., 1949, 71, 2975.

38). Ockrent: J.Physical Chem., 1931, 35, 3354.

39). Hickling: Trans.Faraday Soc., 1937, 33, 1540.

40). Smith: Trans.Faraday Soc., 1951, 47, 63.

41). Gouy: Ann.Chim.Phys., 1906, 9, 75.

42). Ksenofontov, Proskurnin and Gorodetskaya: Acta Physicochim. U.R.S.S., 1938, 9, 39.

43). Gorodetskaya: ibid., 1940, 12, 309.

44). Doss and Kalyanasundram: Proc.Indian Acad.Sci., 1952, 35A, 27.

45). Wiesner: Coll.Czech.Chem.Comm., 1947, 12, 594.

46). Meites and Meites: J.Amer.Chem.Soc., 1951, 73, 177.

47). Kaye and Stonehill: J.Chem.Soc., 1951, 1, 27.

48). Heyrovský, Šorm and Forejt: Coll.Czech.Chem.Comm., 1947, 12, 11.

49). Randles: Discuss.Faraday Soc., 1947, 1, 11.

50). Ershler: ibid., 1947, 1, 269.

51). Breyer and Gutmann: ibid., 1947, 1, 19.

52). Heyrovský: ibid., 1947, 1, 212; Coll.Czech.Chem.Comm., 1953, 16, 455.

53). Brand, James and Rutherford: J.Chem.Phys., 1952, 20, 530.

54). Sdělení: Chemické Listy, 1951, 45, 365.

55). Vlček: Coll.Czech.Chem.Comm., 1951, 16, 230: Chemické Listy, 1951, 45, 377.

56). James: Trans.Faraday Soc., 1951, 47, 1240.

57). Bergman and James: ibid., 1952, 48, 956.

58). Arthur and Lyons: Analyt.Chem., 1952, 24, 1422.

59). Grahame, Larsen and Poth: J.Amer.Chem.Soc., 1949, 71, 2978.

60). Parsons and Devanathan: Trans.Faraday Soc., 1953, 49, 673: Gouy: Ann.Chim.Phys., 1903, 29, 145.

61). Gouy: Ann.Physik., 1916, 6, 5.

62). Brand: J.Chem.Soc., 1946, 585.

63). Orton and Bradfield: ibid., 1927, 983.

64). Davidson and McAllister: J.Amer.Chem.Soc., 1930, 52, 519.

65). Bachman and Astle: ibid., 1942, 64, 1303.

66). Bachman and Astle: ibid., 1942, 64, 2177.

67). Craxford: Trans.Faraday Soc., 1940, 36, 101.

68). Bennewitz and Delijannis: Z.physikal.Chem., 1927, A125, 144.
Bennewitz and Küchler: ibid., 1931, A153, 443.

69). Bowden and Grew: Discuss.Faraday Soc., 1947, 1, 91.

70). Lund and Bjerrum: Ber., 1931, 64, 210.

71). Mahan and Bailey: J.Amer.Chem.Soc., 1937, 59, 2449.

72). Frumkin: Z.physikal.Chem., 1923, A103, 43;
Ergebn.exakt.Naturwiss., 1928, 7, 235.

73). Grahame: J.Electrochem.Soc., 1951, 98, 343.

74). Grahame: Technical Report No.1 to the Office of Naval Research, March 9, 1950.

75). Grahame: J.Amer.Chem.Soc., 1952, 74, 17.

76). Fink and Philippi: Trans.Electrochem.Soc., 1926, 50, 267.

77). Graham: ibid., 1927, 52, 157.

78). Haring: ibid., 1926, 49, 417.

79). Kern and Rowen: ibid., 1929, 56, 399.

80). Shreir and Smith: ibid., 1951, 98, 193.

81). Shaw and Remick: J.Electrochem.Soc., 1950, 97, 324.